Università degli studi di Roma

"Sapienza"

Dottorato in Scienze Chimiche

XXIV Ciclo

Self-Assembled Monolayers of aromatic thiols on gold and copper in aqueous environment: an electrochemical and spectroscopic study

Dr. Fabrizio Caprioli

Supervisore:

Prof. Franco Decker

Coordinatore:

Prof. Camillo La Mesa

Acknowledgements

I want to sincerely thank my tutors Prof. Franco Decker and Prof. Valeria Di Castro, not only for the scientific guide they gave me during these three years but mainly for the respect and the trust they always demonstrated toward me and my work.

I want to thank Prof. Robertino Zanoni, Prof. Delia Gazzoli, Prof. Andrea Martinelli, Dott. Andrea Marrani, Dott. Alice Boccia, Dott. Paolo Bucci and Mr. Marcello Inversi, because with their competence and their helpfulness made possible the realization of this work.

I want to thank my family, because if I am finally grown up I owe it to all their lessons.

I want to thank all my friends and colleagues, who filled my life during these three years.

Finally, I want to thank Anna, because although it was very difficult bear me during the last months, she did it with all the love of the world, as well as in the last seven years.

With all my gratitude,

Fabrizio Caprioli

Abstract

Thiolate Self-Assembled Monolayers (SAMs) offer the unique opportunity to tailor surface properties of noble and coinage metal in extremely fine way through a simple bottom-up approach, making them very attractive in a wide range of technological applications. On copper surfaces, n-alkanethiolate monolayers have been extensively studied as corrosion inhibitors in aqueous solutions revealing excellent performances but relatively poor stability, a problem affecting SAMs in many of them applications. On the other hand, very few studies have been performed on SAMs constituted by simple aromatic thiols and none of them assessed their long term stability, although the relatively strong ring interaction should in principle positively affect the layer durability.

In the present work the protective properties and the long term stability in strongly acidic solution (H_2SO_4 0.5 M) of two aromatic SAMs, namely Benzenethiol (BT) and 2-Naphthalenethiol (2-NT) was compared to that of one long-chain n-alkylic SAM, the 1-Undecanethiol (1-UT) by means of XPS, Raman spectroscopy, DCA and electrochemical techniques. The results not only demonstrated the aromatic SAMs to be remarkably stable, but also highlighted a favourable influence of the aqueous environments on the layers structures, resulting in a durable enhancement of their protective properties.

Subsequently, the effect of different p-substituent groups (-F, -CH_3, -OH, -COOH, -$NHCOCH_3$) on the performance and the stability of the aromatic SAMs was investigated. All such molecules, similarly to BT, showed a steep increase of their inhibition efficiency upon ageing. The rate and the durability of the enhancement resulted mainly dependent from the polar effect of the tail group; moreover, the hydrophobicity seems to influence the protective properties of the layers as well.

Finally SAMs of BT and 1-UT on gold, both freshly prepared and aged in ultrapure water, were characterized electrochemically. Again BT layers showed an improvement of their structural order following the exposure to aqueous environments, indirectly supporting the hypothesis of a direct involvement of water molecules in this process. In addition, a new method to prepare high quality aromatic SAMs on gold has been proposed.

List of abbreviations

AA – 4-Acetamidothiophenol

AFM – Atomic Force Microscopy

BE – Binding Energy

BT – Benzenethiol

CPE – Constant Phase Element

CV – Cyclic Voltammetry

DCA – Dynamic Contact Angle

e.g. – exempli gratia

EIS – Electrochemical Impedance Spectroscopy

et al. – et alii

FBT – 4-Fluorobenzenethiol

HREELS – High Resolution Electron Energy Loss Spectroscopy

i.e. – id est

IPE – Ideal Polarizable Electrode

ITO – Indium Tin Oxide

KE – Kinetic Energy

LEED – Low Energy Electron Diffraction

MBA – 4-Mercaptobenzoic acid

MBT – 4-Methylbenzenethiol

MF – 4-Mercaptophenol

NEXAFS – Near Incidence X-ray Absorption Fine Structure

OCP – Open Circuit Potential

PVD – Physical Vapour Deposition

RAIRS – Reflection Adsorption Infra Red Spectroscopy

SAM – Self Assembled Monolayer

SPM – Scanning Probe Microscopy

STM - Scanning Tunneling Microscopy

TDS – Thermal Desorption Spectroscopy

UHV – Ultra High Vacuum

UPD – Under Potential Deposition

XPS – X-ray Photoelectron Spectroscopy

Table of contents

Chapter 1: Introduction

1.1 Self-Assembled Monolayers (SAMs): how to model a surface

1.1.1 Surface chemistry and Self-Assembled Monolayers

As recognized by the classical science, the matter essentially exists in three aggregation states: solid, liquid and gaseous. Nevertheless is known that the atoms and the molecules situated at the interfaces behave in markedly different way from those in the bulk phase[1-3]. This happens because the surface atoms experience a different environment and different forces respect to those in the bulk and thus have different free energy, electronic state, reactivity, mobility and structure[3]. Therefore, in a sense, surfaces can be considered as a fourth state of matter[4].

Although the study of the solid surface can boast a very long history it is still extremely topical, being a key element of modern technology in numerous field. The chemical and physical properties of surfaces are responsible, for example, of heterogeneous catalysis (*e.g.* industrial ammonia synthesis) and gas separation (as in the extraction of oxygen and nitrogen from air); mechanical surface properties give rise to adhesion, friction and slide; magnetic surfaces are used for information storage and their electrical behavior often give rise to surface charge build up which is used in electron transfer in integrated circuit[3]. Therefore is easy to comprehend the importance to finely modulate the properties of a surface in order to make it suitable for every specific need. Bare surfaces of metals and metal oxides tend to readily adsorb adventitious materials lowering the free energy of the interface between the substrate and the environment[3]. These adsorbates may alter the interfacial properties and have a significant influence on the stability of nanostructures of metals and

metal oxides: for example they can act as a physical or electrostatic barrier against aggregation, decrease the reactivity of the surface atoms, or act as an electrically insulating film. Surfaces coated with adventitious materials are, however, not well defined: they do not present specific chemical functionalities and do not have reproducible physical properties (*e.g.*, conductivity, wettability, or corrosion resistance)[4]. Self-Assembled Monolayers (SAMs), on the contrary, provide a convenient, flexible, and simple system to tailor the interfacial properties of metals, metal oxides, and semiconductors. SAMs are assemblies formed by the adsorption of organic molecules from solution or from gas phase onto the surface of solids or in regular arrays on the surface of liquids (in the case of mercury and probably other liquid metals and alloys) where the adsorbates organize spontaneously into crystalline (or semicrystalline) structures. Their stability, arising from the strong covalent interaction between the organic molecules and the substrate, their reproducibility and their ease of preparation make them a perfect tool to tune the surface properties, allowing to directly correlate the structure of the molecules constituting the SAM with macroscopic properties like wettability, friction, adhesion, etc.[5]. In addition such molecules often exhibit optical, electrical, optoelectronic, mechanical, chemical, or spectroscopic properties resulting interesting from an applicative point of view in many different areas. Considering the several million of organic compounds known, and the correspondent wide variety of molecular properties, it is easy to realize the huge versatility of these systems, which represent the key for their success.

1.1.2 Historical outline

For the reasons mentioned above, deposition of organic films has always attracted considerable attention by the scientists over the years. Already in the 19th century, Pockels prepared organic monolayers at the air-water interface[6-9]. Later, monolayers of amphiphilic molecules on the water surface where studied by Langmuir[10,11], whereas Blodgett carried out the firsts studies on the deposition of long-chain carboxylic acids on solid substrates (Langmuir-Blodgett films)[12,13]. The story of Self-Assembled Monolayers started *de facto* in

1946, when Zisman *et al*. described the adsorption of amines and alkanoic acids on glass surfaces from an alcoholic solution[14]. Nevertheless the potentialities of the SAMs were not immediately understood. In fact, an intense research activity on SAMs began only in the early '80 thanks to the pioneer works of Sagiv[15-18], who investigated the self-assembly process of trichlorosilanes on glass and silicon oxide; and, especially, of Nuzzo and Allara[19,20], who for the first time described the adsorption of organic disulfides on a gold surface from solution obtaining self-organized, highly ordered and reproducible monolayers. This finding represented a considerable improvement with respect to the Langmuir-Blodgett deposition method, where only physisorbed, thermally unstable mono/multilayer films were obtained[21] (Fig 1.1). Gold revealed to be an excellent choice to investigate the chemical-physical properties of SAMs, and it is still today the most popular substrate for thiols adsorption[4]. The success of gold is due to several reasons: it is easy to obtain as thin film by various method (Physical Vapour Deposition, sputtering, electrodeposition); it is an inert metal which does not oxidize at temperature lower than its melting point and does not react with most chemicals; and it binds thiols with high affinity, giving rise to quite stable system. An important contribution to the comprehension of the structural basis of thiolate Self-Assembled Monolayers on gold is due to the studies carried out at the end of the '80 by Bain and Whitesides[22-31], which led to the determination of packing arrangement, layer thickness, tilt angle, adsorption kinetic and intermolecular interaction of SAMs with different chain length and terminal group.

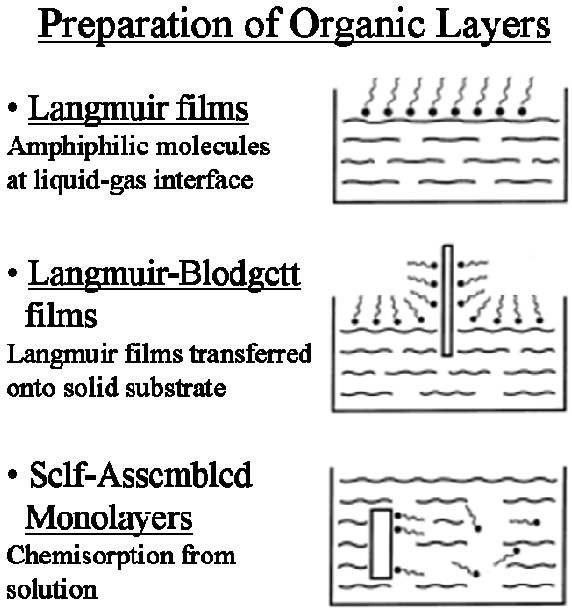

Figure 1.1: Schematic overview of some preparation methods for organic thin films. The figure has been elaborated from reference 5

From the beginning of the nineties the research on SAMs received further propulsion by the introduction of new types of substrates: the thiolic function, in fact, revealed to be a suitable ligand not only for gold but also for others noble and coinage metals. So thiolate Self-

Assembled Monolayers on surfaces of silver[32,24], copper[32,34], platinum[35], palladium[36] and their alloys[37] were gradually prepared and characterized. Moreover the functionalization of surfaces of semiconductors and/or metal oxides of scientific interest has been successfully performed both by thiols and by other classes of organic molecules. To cite some example, organosilicons and alkenes have been used to functionalize, respectively, oxidised[38,39] and hydrogenated[40] silicon; fatty acids are able to self-assemble on oxidized metal surface such as Al_2O_3[41-43] and AgO[44] whereas TiO_2, as well as the Indium Tin Oxide (ITO), showed a good affinity for the phosphonic group[45,46]. Molecular monolayers have been formed even on organic surfaces, like polymers[47], and highly dense liquids, like mercury[48]. Furthermore the development of evermore advanced methods for the surface analysis, such as the various Scanning Probe Microscopes (SPM) techniques[49], not only provided information about layers structure almost at atomic level[50], but also made possible to pattern the SAMs at the same resolution[39,51], allowing to modulate the surface properties in an extremely fine way and stirring up, if it were needed, the interest for functionalized surfaces.

In the last decade the rapid development of nanoscience[52] opened new perspective for the investigation about SAMs, allowing to apply the concept of self-assembly to nanostructured materials. The availability of new types of nanostructures with well defined shape and size both on planar support (metal structure on silicon wafers or glass slides) and in solution (nanoparticles, templated structures) has stimulated wide application of SAMs for stabilizing these new structures of metallic (and others) nanoscale materials and/or manipulating their interfacial properties. To comprehend the strong synergy between nanostructures and SAMs, it suffices to consider that more than half of the atoms constituting nanoparticles smaller than 2nm, are situated at the surface. Furthermore, in the last years, diffraction methods began to play a very important role for an even deeper comprehension of three-dimensional structure of SAMs, highlighting, for example, the role of gold adatoms on the assembly process of thiolates on Au (111) surfaces[53]. In sum, although they are a rather well known system with a rather long history behind them, Self-Assembled Monolayers are still today an extremely topical investigation field, which already find use in a wide range of areas and which have, potentially, almost unlimited applications. The great vitality of this sector is clearly evidenced by the trend of published papers concerning SAMs in the last twenty years

(Fig. 1.2), which point out how, after more than twenty-five years from the pioneer work of Nuzzo and Allara, around two thousands papers about SAMs are published every year on international scientific journals, more or less the double amount than ten years ago.

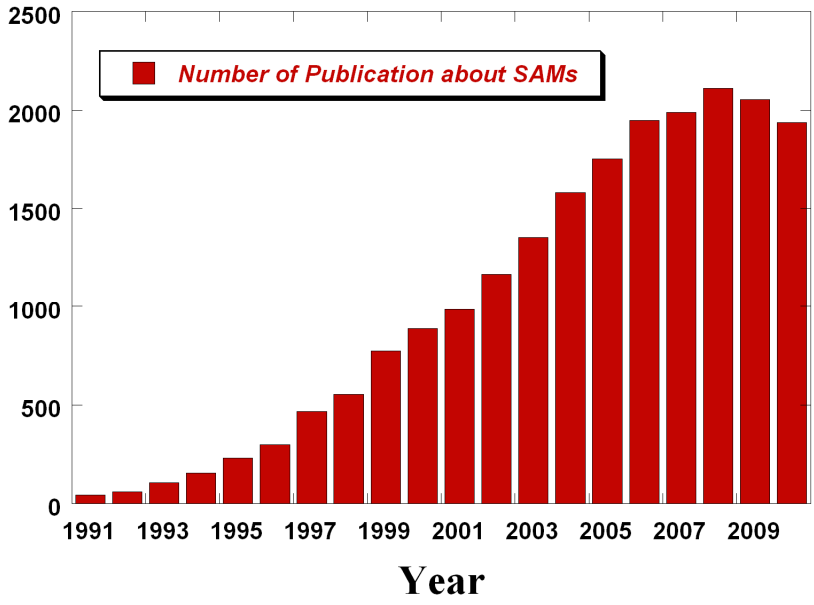

Figure 1.2: Number of paper per year concerning SAMs published on international scientific journal from 1991 to 2010. Source: Scifinder scholar 2007 edition.

Nevertheless, much remains to be done. In fact, still today, our knowledge about the chemistry of the thiolate–metal bond is, at least, incomplete, as well as the detailed comprehension of the structure at the adsorbate/substrate interface for the most important ordered lattices (both low- and high-coverage). Another key point is the control of the quality of the SAMs: the ‘‘perfect’’ Self-Assembled Monolayer is far from reality, existing different types of defects which seriously limit their applications[54]. Finally, the search for strategies to increase the oxidation resistance of SAMs becomes crucial for their use in ambient conditions and/or in aqueous solutions[54]. Succeed in these challenges would not mean only to solve an academic problem, but also take an important step toward a wider application of these systems.

1.2 Self-Assembled Monolayers on copper and gold surfaces

1.2.1 General properties and structural components

Although the expression Self-Assembled Monolayers indicates a very wide and variegated number of systems, it is possible to identify three basic structural components that are common to all SAMs: a headgroup, a spacer chain and a tail group (Fig. 1.3). The headgroup (or linking group) is an organic function with high affinity for the substrate, which guides the self-assembling process linking the organic molecules to the surface through a strong covalent bond. In many systems, the strong headgroup-substrate interactions can overcome the pre-adsorbed molecules, displacing them from the surface. As previously said, in the case of gold, copper and other noble and coinage metals, the headgroup coincide with the thiolic function.

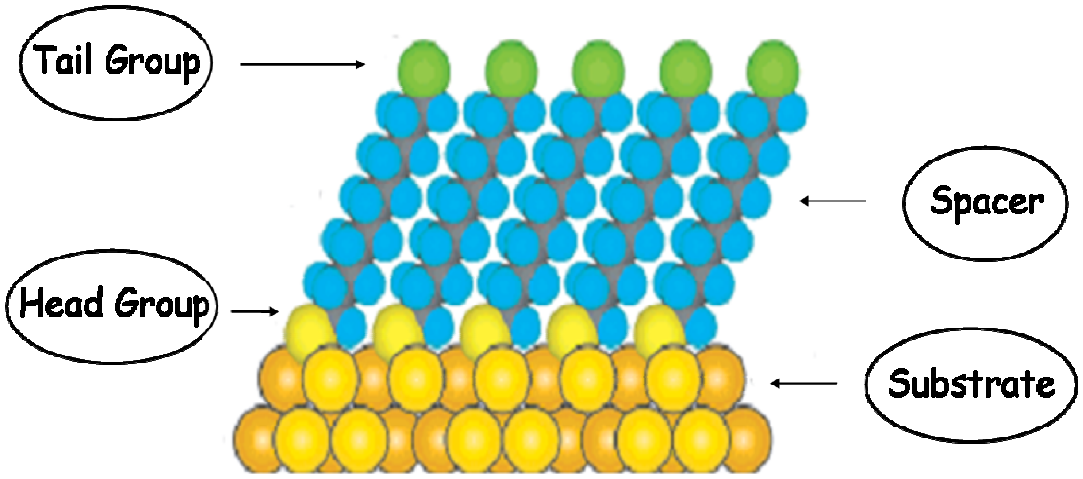

Figure 1.3: Schematic representation of an n-alkanethiol SAMs supported on a metal surface. The basic structural components are highlighted. The figure was elaborated from reference 4

The spacer, usually a hydrocarbon chain of variable length, is set between the head and the tail group. Its function is not only to determine the thickness of the organic layer, and consequently affecting several properties like, for example, the charge-transfer resistance through the SAMs[55-57]. Numerous studies, in fact, pointed out how the interactions among

backbone hydrocarbon chains, involving Van der Waals and hydrophobic forces, favour a more efficient packing of the monolayer, giving an important contribution in the stabilization of structures with increasing chain length[27,32,54].

The tail (or terminal) group practically represents the new surface exposed to the external environment, and thus play the primary role in the modification of the physical and chemical properties of the substrates[4,54]. Thus, $–CH_3$ and $–CF_3$ terminal groups make the surface of the SAM hydrophobic, metallophobic and highly anti-adherent[58], while –COOH, $–NH_2$ or –OH groups yield hydrophilic surfaces with good metal ion and protein binding properties[4,59]. Another extremely interesting class of SAMs are dithiols, which can be regarded as –SH-terminated layers, and are very useful to bind metallic ions and nanoparticles to the surface[60,61] or to study charge-transfer through metal-molecule-metal junction[62]. In addition, if the tail group is able to establish an intermolecular hydrogen bond (e.g.: -OH, -COOH, -NHCO) it may contribute in relevant way to the correct arrangement and to the stabilization of the SAM[63,64].

The energy related to each part of the organic molecules has very different values: for the bond between the sulphur atom and the metal substrate it is typically around 50 kcal mol^{-1} [4,54], for a possible intermolecular hydrogen bond between terminal group it can reach 5-7 kcal mol^{-1} [64], whereas the energy for the Van der Waals interaction between hydrocarbon chain has been estimated around 1-2 kcal mol^{-1} per methylene unit[54]. However, all three parts of the molecule play an important role to determine the structure and the chemical-physical properties of the SAMs.

1.2.2 Preparation and mechanism of assembly

1.2.2.1 Choice and pretreatment of the substrates

The adsorption of a thiolate SAMs on a metal surface, both from gas phase and from solution, is a complex process which can be affected by several parameters. The first issue to consider in the preparation of SAMs is related to the choice and the preparation of the

substrate. Some kinds of studies, such as a deep investigation of the mechanism of electron-transfer through the organic molecules or a very refined structural characterization, necessarily require single crystal surfaces. Nevertheless very less expensive polycrystalline substrates are more than enough for most of the applications of the SAMs on planar surfaces. For economic reasons the most common polycrystalline gold substrate for SAMs adsorption are thin film (50 nm – 200 nm) supported on silicon wafer, glass or mica. In particular, freshly cleaved mica supporting a thin film of gold is commonly used as a pseudo-"single crystal" substrate for microscopic studies by scanning tunneling microscopy (STM) or atomic force microscopy (AFM)[65,66]. In fact, gold films grow epitaxially with a strongly oriented (111) texture on the (100) surface of mica. Physical Vapor Deposition (PVD)[67] and electrodeposition[68] methods can be used to easily prepare thin films of a wide range of metals and alloys[4]. Nevertheless, in the case of relatively cheap material such copper or silver work directly on a metal plate is often preferred. A crucial parameter to check, in order to obtain highly ordered and reproducible SAMs, is the cleanliness of the substrate. The presence of adsorbed adventitious material, which might be hard to displace by the thiols, can seriously affect the structures and the number of defects of the SAMs. Common methods to remove contaminants from gold surfaces are the treatment with strongly oxidizing chemicals such as hot "piranha" solution (3:1 concentrated H_2SO_4: 30% H_2O_2 at 90 °C)[4,69] or electrochemical polish in acidic ambient[4,70]. These treatments not only remove impurities, making the surface suitable for the correct adsorption of the thiols, but also favour the formation of flat surfaces with an enhanced (111) texture[4]. The polishing of less noble metal substrates like copper is usually performed by a chemical etching in a strongly acidic and oxidizing solution like concentrated HNO_3, leading a fresh, reactive and oxide-free surface[71-74]. In fact, even if has been proved that thiols are able to displace (or reduce) small quantities of copper oxide during the adsorption process[75-76], the initial presence of a significant amount of Cu_2O or CuO represent an impediment to the growth of high quality, reproducible and stable SAMs[4,32,76].

1.2.2.2 Adsorption of the thiols

As previously said, there are essentially two methods to achieve the adsorption of organic thiols onto a metal surface: from gas phase and from solution. Requiring an UHV apparatus, deposition from gas phase is an impractical and relatively expensive way to prepare thiolate SAMs, becoming preferable only for some specific studies. For example, coupled with the use of single crystal substrates, this deposition method allows for deep structural characterizations[77-81] and provides a useful tool for studying the early stage dynamics of assembly[4], which seem to be similar to that from solution[4,5] although with different kinetic.

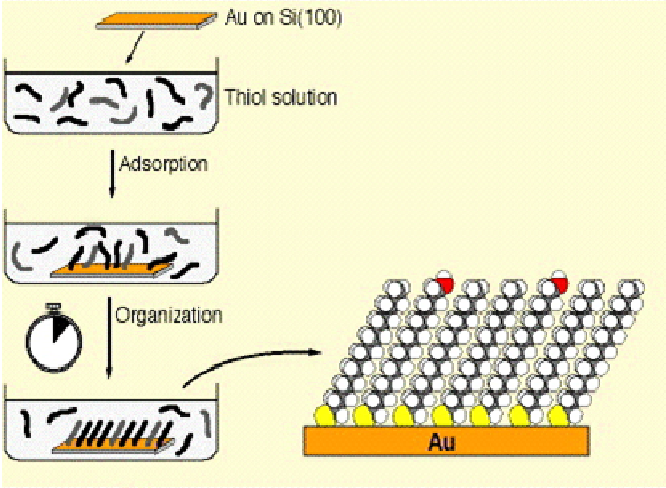

Figure 1.4: Schematic representation of the adsorption from solution of a thiolate SAMs on a metal surface.

The most common protocol for preparing SAMs on gold and copper (and other noble and coinage metals) is the immersion of a freshly clean substrate into a dilute (0.1 – 10 mM) solution of the appropriate thiol for several hours (generally 12 – 24 h) at room temperature. As firstly observed by Bain *et al.*[27], the growth of SAMs from solution involves at least two stages: a first rapid adsorption step leading to ~ 90% coverage after few minutes (at the usual millimolar concentration), followed by a slow reorganization process requiring times in the order of hours (or days) to maximize the density of molecules and minimize the defects in the SAM (Fig. 1.4). This result was subsequently confirmed by several authors[82-85].

The mechanism of the reaction leading to the chemisorption of thiols both on gold and copper is still debated[4,54]. In the case of gold, in particular, the fate of hydrogen atom is not clear, even if its elimination as H_2 molecule, involving the oxidation of Au(0) to Au (I) appear the most probable hypothesis[4,86]:

$$2\ RS - H + 2\ Au(0) \rightarrow 2\ RS - Au(I) + H_2 \uparrow$$

This reaction would occur through two steps: an oxidative addition of the S-H bond to the gold surface followed by the reductive elimination of hydrogen[87]. Alternatively a mechanism involving an electron transfer step has been proposed[88]:

$$RS - H + Au(0) \rightarrow RS - Au(I) + H^+ + e^- (Au)$$

In the instance of copper, which is more reactive than gold toward oxygen and other environmental contaminants (*e.g.* CO_2), the oxidation of the surface atoms is not required. Even a carefully cleanliness of the substrate performed in air, in fact, give rise to a slightly oxidized copper surface. As previously discussed, thiols are able to bind the substrate displacing the small amount of Cu_2O and eliminating the hydrogen as a stable water molecule following the reaction[76,89]:

$$2RS - H + Cu_2O \rightarrow 2RS - Cu(I) + H_2O$$

The adsorption rate (as well as the final structures and properties of the SAMs) may be affected by numerous parameters, even if the effect of many of these is still not completely understood. As might be expected, concentration of the thiols and immersion time are inversely related parameters: low concentrated solutions require longer immersion times[27,90]. However, although the concentration considerably influences the initial growth rate[27,82,85,91], performing the deposition in low concentrated solution for long time seems to lead to a more ordered and less defective structure[92]. Anyway, concentration lower than 1 μM should be avoided [4,27].

Several common organic solvents (tetrahydrofuran, dimethylformamide, acetonitrile, cyclooctane, toluene, ethanol, n-hexane, acetone, etc.) have been tested for preparing SAMs. Among them, ethanol is by far the most widely used. There are at least four factors contributing to the diffusion of ethanol: it solvates a variety of thiols with varying degrees of polar character and chain length; it is inexpensive; it is available in high purity; and it has low toxicity[4]. The effects of the choice of the solvent on the assembling process are still not completely clear[4]. Some properties of SAMs on gold, such as limiting mass coverage and wettability, seem to be not significantly affected by the nature of the solvent used[27]. On the other hand, although kinetic studies suggested the growth to be faster in non-polar solvent

rather than ethanol[83,93], electrochemical and STM measurements pointed out that the use polar liquids, which are relatively poor solvents for thiols, seem to reduce the quantity of some types of defects found in SAMs (conformational arrangements, regions of missing adsorbates, etc.) and to promote densely packed monolayers[94-97]. The low solubility of thiols in such solvents probably leads to a segregation of the thiols at the metal surface and thus more efficiently drive the assembly processes involving them. In the instance of deposition on copper surfaces, Rubinstein *et al.* demonstrated that the use of toluene instead of ethanol, allows to obtain more organized and less defective SAMs[89]. This result was attributed to the reactivity of ethanol towards copper surfaces, leading the solvent to compete with the thiols for the binding sites. Nevertheless, the differences in the layer quality did not resulted so significant to balance the advantages of ethanol, which remains widely the most common used solvent also with copper substrates.

The control of the temperature, finally, is often an undervalue factor. The preparation of SAMs is conventionally performed at room temperature, although some studies suggested that working at slightly higher temperature favors the desorption of adventitious materials and physisorbed solvent molecules, improving the kinetics of formation and reducing the number of defects in the layer[98,99]. Yamada and co-workers, in particular, suggested that the effect of temperature is particularly relevant during the first few minutes of immersion, when most of the adsorption process is taking place[99].

1.2.3 Structure and defects

1.2.3.1 High coverage phase structure on gold and copper

The huge amount of studies performed in the last twenty years in order to determine the structure of SAMs on coinage metal led today to a fair, but still incomplete, comprehension of the nature of the metal-thiolate interface[4,5,54,86,87,100]. For SAMs formed of n-alkanethiols on gold and copper (as well as on silver, palladium, mercury, platinum, and other materials) the alkane chains adopt a quasicrystalline structure where the chains are fully extended in a

nearly all-trans conformation[4]. The orientation of the organic molecules constituting an ordered SAMs can be described by two parameters: the angle of tilt (α) for the backbone of the molecule away from the surface normal and the angle of rotation (β) about the long axis of the molecule[4] (Fig. 1.5). Many investigations[32,33,101], performed using many different techniques (NEXAFS, RAIRS, Raman spectroscopy, etc.) indicates for alkylic thiols on Au (111) a tilt angle of around 30° and an average rotational angle of around 50°, with small deviation due to the influence of the chain length and/or the terminal group[31,102]. Although in a very less extent, also the structure of aromatic thiols on gold, especially of the Benzenethiol (BT), has been investigated and deduced. In spite of their possibility to establish relatively strong intermolecular interaction, simple aromatic SAMs on gold appear relatively poorly defined[103]. Several studies, in fact, agree indicating BT molecules on gold to be more canted than long-chain alkylic thiols, with an average tilt angle close to 50°[104-106]. Moreover, recently Käfer *et al.* established that they assume a low density packing arrangement (Fig. 1.7), with all the rings oriented in the same direction and a relatively high area per molecules (~39.7 Å^2 per molecule vs ~21.5 Å^2 per molecule of

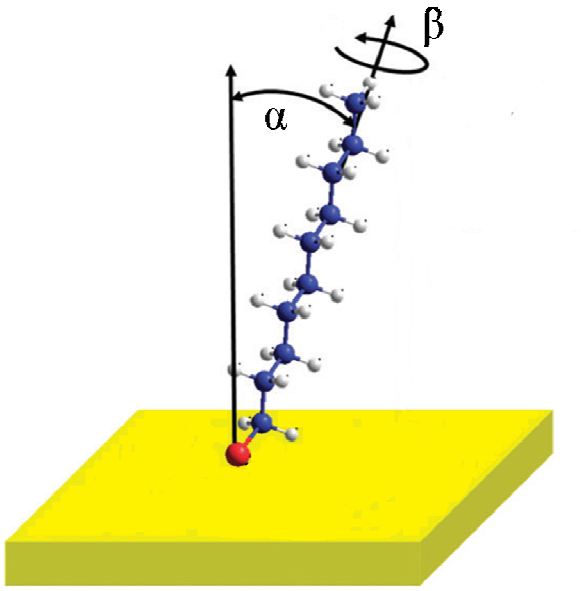

Figure 1.5: Representation of an alkylic thiol adsorbed on a metal surface. The angles determining the molecule orientation are highlighted. The figure was elaborated from reference 54

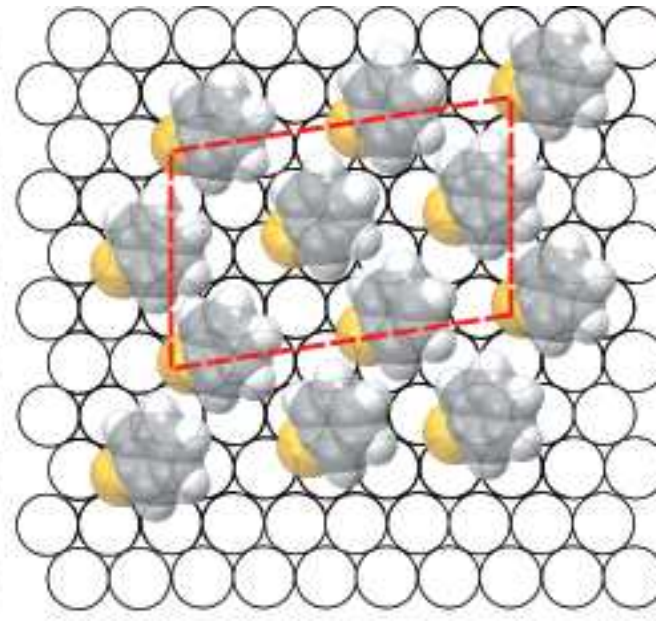

Figure 1.6: Representation of the packing arrangement recently proposed for BT SAMs on Au (111) surfaces. The figure was elaborated from reference 106

an alkylic thiol). On the contrary molecules containing more than a ring seem to prefer a standing-up configuration, probably driven by π-π interactions[107,108], and a highly ordered herringbone motif structure[109,110].

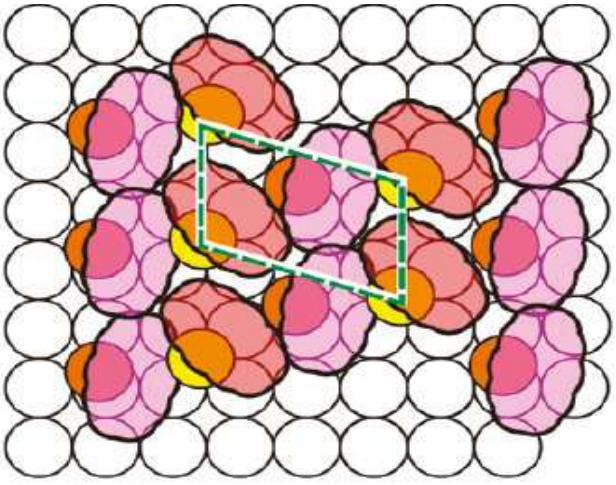

Figure 1.7: Representation of the packing arrangement proposed for BT SAMs on Cu (100) surfaces. The figure was elaborated from reference 81

Although considerably less studied, the structure of SAMs on copper surface is, from some points of view, more clear than that on gold. Long chain alkanethiols adsorb on copper with a higher packing density than on gold[4,32] (~ 19 $Å^2$ for chain on copper vs ~ 21.5 $Å^2$ for chain on gold, depending by the chain length) and, at full coverage, show highly ordered and quasi-crystalline structures[4,32]. Several studies pointed out that the hydrocarbon chains are less tilted (~ 12°)[32,111-113] respect to SAMs on gold, whereas the rotational angle β was estimated to be ~ 45°[4]. The difference in orientation resulted to be considerably higher in the case of aromatic SAMs, especially for the simpler ones. Recent NEXAFS measurements attributed to BT molecules on Cu (100) a tilt angle of ~ 20° respect to the normal at the surface[81,114] revealing a total up-right configuration, in contrast with what seen on Au (111). Moreover, by means of LEED and STM, simple aromatic thiols on Cu (100) have been found to give rise, at saturation coverage, to a highly ordered structure, presenting a herringbone motif package[81,115] (Fig. 1.7). In addition, TDS and XPS experiments suggested a higher surface coverage for BT SAM respect to long chain alkylic layers[116]. A possible explanation for the noticeable difference in structural order between aromatic SAMs on gold and copper is the different distance between the binding sites, which could allow in the latter instance to take more advantage from the intermolecular ring interaction.

1.2.3.2 Defects and stability of the SAMs

In literature SAMs on metal substrates are often described as perfect coats, with all the molecules in a closed packed configuration. Although these systems typically exhibit a highly ordered structure, this idea is far from reality. In fact, both alkanethiol and arenethiol SAMs contain several types of defects that can have an important influence on their efficiency in some of their applications[4,54]. Some of these imperfections arise from external factors, such as the cleanliness of the substrate and the purity of the thiolic solution, which can lead to the adsorption of adventitious material on the surface, causing a discontinuity in the layer. Obviously this type of defects can be avoided, or at least minimized, adopting an appropriate adsorption protocol. Nevertheless, some defects characterizing the SAMs are intrinsic of the layer structure and it is impossible remove them completely. At the origin of this imperfection there are several causes. Some of them are related to the structure of the metal surface: the use of polycrystalline substrates (which have been chosen for the most of investigations about SAMs), typically characterized by a high density of intergrain boundaries and other gross structural irregularities, clearly lead to a dramatic increase of SAMs defects but even on single crystal surfaces misalignments or defects at step edges (Fig. 1.8a) are rather common. Other defects, probably arising from the surface reconstruction following the thiols adsorption[4,54], are the so called vacancy island (Fig. 1.8b), a sort of "holes" in the metal surface typically with a diameter of few nanometers and a monoathomic or diathomic (~ 2.4 Å / ~ 4.8 Å for gold) depth. Although both STM and AFM images demonstrated that the bases of these vacancies are covered by thiols[87,117,118], the interfacial properties of coated metals, and in particular their electrochemical behaviour[119,120], result to be quite sensitive to the density of these "holes". Some intrinsic defects of the SAMs, on the other hand, do not trace the substrate imperfections, but directly arise from the adsorption mechanism. This category of defects includes: boundary between domains formed by different nucleation center and having different orientation (Fig. 1.8c); missing of small number of molecules (or "pinholes defects", Fig. 1.8d) or regions with molecules whose spacers lie parallel to the surface (also called collapsed sites, Fig. 1.8e). Finally there are defects that are related to the dynamic of the organic components of the

SAMs. An example is the presence of gauche conformers in n-alkanethiolate SAMs. To these intrinsic flaws, those arising from the temporal degradation of the SAMs must be added. The chemical stability of thiolate SAMs is maybe the most serious problem for their large scale applications[54]. Although they are considered kinetically stable systems, in contact with air or aerated solutions they undergo severe damage, seriously affecting their properties, in a range of time which can vary between hours or days. The rate and the mechanism of the degradation process depend by several parameters like ageing ambient (air, solution or even vacuum), presence of oxidative agents (like oxygen or ozone), exposure to UV radiation, pH, applied potential and temperature. The declension rate results generally to be inversely proportional to the layer thickness[34,120,121] and to the density of the imperfection of the surface[123]. Nevertheless, interestingly, Vericat *et al.* recently demonstrated that monolayers prepared on nanostructured Au surfaces are more stable than that adsorbed on flat supports[124]. Also the presence of relatively strong lateral interactions, like intermolecular hydrogen bonds, positively affects the stability of the SAMs[63,64,125].

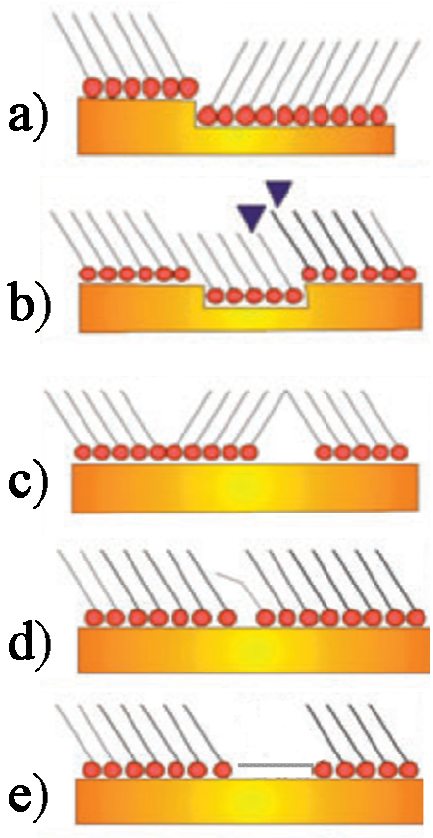

Figure 1.8: Representation of some kind of defects affecting the SAMs. The figure was elaborated from reference 54

There are essentially two way by which the desorption of the organic layer may occur. It can involve the oxidation of the thiolic function to disulfide or sulfonate, which being less strongly bonded to the metal substrate respect to the thiolate are more easily prone to desorption or, alternatively, it may occur through S-C bond cleavage, leading to desorption of the hydrocarbon chain and leaving the sulfur atom on the surface as Me_2S.

The stability of SAMs on gold and copper has been tested in various liquid media, including ethanol, hexane, water and THF[126]. The desorption rate of the organic molecules seems to be strictly related to their solubility in the ageing solvent. Nevertheless, also the exposure to

aqueous solutions strongly influences the chemistry of the thiolic group leading to the formation of highly defective areas (collapsed sites, pinholes defects, presence of physisorbed material, disordered domains, etc.) which can seriously affect the layer properties. For monolayers growth on gold, a considerable amount of studies verified that in the latter instance (but also for other solvents) the declension of n-alkanethiols proceeds through the formation of both disulphide and sulphonate[126,127], depending by the ageing conditions, whereas the stability of simple aromatic SAMs in liquid media has never been closely investigated. The layers display a fair durability (several days) in closely neutral solutions (phosphate buffer)[128,129], but they are poorly stable in aggressive environments, especially at strongly alkaline pH[130].

On the other hand, even if some studies on the stability of n-alkanethiolate SAMs on copper showed a quite rapid degradation, especially in aggressive environments[74,131-133], the mechanism of damage has still never been deeply investigated. Presumptively, it should be quite similar to that observed for gold, but a partial disruption of S-C bond cannot be excluded. In the case of copper the pH dependence of the degradation rate is related to the formation of insoluble oxidation products for pH > 3. The growth of copper oxide on the surface, in fact, hampers the correct package of the molecules, seriously affecting the structural order of the SAMs[134]. Also for copper substrates, studies aimed to verify the stability of simple aromatic thiols in aqueous solutions have never been carried out.

1.3 Applications of SAMs on copper and gold

The applications of SAMs are many and involve very different areas of expertise. Their utilization may be finalized either to control macroscopic interfacial properties, such as wetting[23,135], adhesion[136] and tribology[137]; as well as in nanotechnology[4], thus ranging between the quite big to the extremely small. As previously said, their success is mainly related to three reasons: the preparation protocol is very simple and gives reproducible results; they are inexpensive and, most of all, they are extremely versatile systems. A field in which such versatility is clearly visible is the micro and nanofabrication: the utilization of

physical tools capable of selectively positioning or damaging the organic molecules enables the fabrication of surfaces with well-defined patterns of SAMs in the plane of the surface with lateral features ranging from 10 nm to 10 cm[4,138]. This, together with the huge number of combination available between spacers and tail group, allows designing surfaces suitable for almost every specific necessity.

Several interesting application of the SAMs are related to their electrochemical behaviour. Thiolate monolayers are very popular tools to modify electrodes and have been widely employed to investigate charge-transfer processes[139]. SAMs of alkanethiols are essentially dielectric layers[140] able to prevent the diffusion of electroactive species to the metal surfaces, allowing in this way to define the distance between donor and acceptor at subnanometric level[139]. In addition, the use of molecules terminating with a redox group (*e.g.* ferrocene or ruthenium pentaamine) allows to eliminate the effects of diffusion in the measured current response[57,141,142]. Among of the charge-transfer phenomena studied by SAM-modified electrodes there are: response to the variation of the parameters affecting electron transfer (distance from the surface, electrolyte, temperature, metal) through alkane chains[143,144] and through unsaturated chains (e.g., polyphenylene vinylene, polyphenylene ethynylene)[145]; coupled electron-proton-transfer reactions[146]; the effect of solvatation of electroactive species in hydrophobic environments on redox reactions[147], the effect of counterion motion on the rates of electron transfer[148].

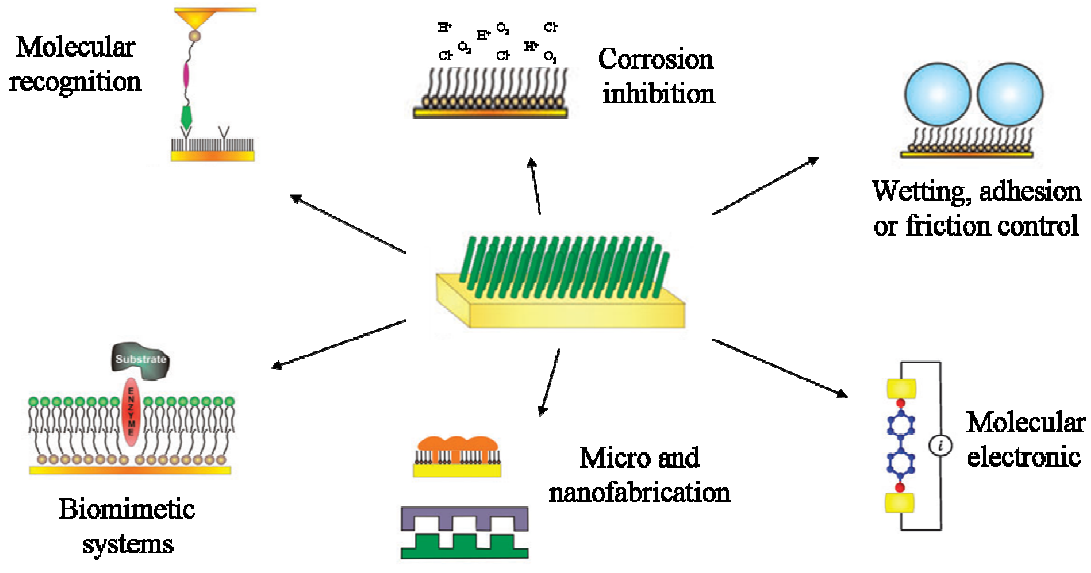

Figure 1.9: Some popular applications for thiolate Self-Assembled Monolayers. The figure was elaborated from reference 54

Some of these studies laid the foundation for molecular electronics, a branch of nanoscience that has received considerable attention in both scientific and popular literature over the past fifteen years, which aims to the development of electronics devices where the active components are constituted by single molecules rather than traditional semiconductors[149]. The state of molecular electronics in this decade evolved rapidly, also thanks to the development of scanning probe methods, which have made possible to achieve with relative facility a number of metal-molecule-metal junction[4].

SAMs may also be designed in order to achieve the immobilization of macromolecules (both covalently and non-covalently) such as proteins or fragment of nucleic acids[150,151] or, more in general, to generate model biological systems[4,54]. This ability allows, for example, to investigate electron transfer rate and mechanism of redox active enzymes[152] (or their mutant), as well as to perform studies about molecular recognition[153] or the charge transfer through bilayer lipid membranes[154]. In addition, it makes SAMs particularly suitable for biosensing applications[155,156], a field where their flexibility is extremely useful. SAMs find also applications in biomedicine, where are used as linkers or protective groups for biomolecule carriers (*e.g.* drug delivery)[157] or to functionalize the surface of medical devices such as gold stents[158]; and as template for oriented crystallization of both proteins[159] and inorganic salts[160]. Moreover, thiolate SAMs are also important in the synthesis of metal nanoparticles, which in turn are found to have plenty of applications[52]. Their role is not limited to the stabilization of the nanostructures against aggregation and to the control of the cluster size by tuning the hydrocarbon chain length, but also includes the functionalization of the nanoparticles in order to make them suitable for several uses[4,52,54].

Mainly owing to its inert nature, gold is the most often used substrates for SAMs in most of their applications. The principal application of SAMs on copper is mainly related to the inhibition of the corrosion process. Thanks to its favourable thermal, mechanical and electric properties[161], in fact, copper is today an irreplaceable material in many fields, ranging from electrical engineering to buildings, from industrial machinery to computer and integrated circuit manufacture, where it is increasingly replacing aluminium owing to its larger electrical conductivity and heat dissipation capacity. Unfortunately copper is subject to

corrosion when exposed to air or to other oxidizing environments, seriously affecting its performance in most of its applications, especially in electronic, and making necessary the protection of the surface. Thus, especially in some branch of modern technology, such as microelectronic and micromechanic, the availability of high efficiency nanometric scale corrosion inhibitors is very desirable. Since Laibinis and Whitesides demonstrated that n-alkanethiolates are able to self-assemble on a copper surface[32] protecting it from air oxidation[34], the effectiveness of the SAMs as corrosion inhibitors was object of various investigations, that showed how these systems provide excellent performance either in acidic,[74,131,162] alkaline,[71,133,163-165] closely neutral[166-170] and chloride containing solutions [71,73,163-165,171]. This is mainly related to the good stability of the S-Cu bond and to the closed packed structure of the SAMs, which act as a barrier against oxidizing agent preventing them to reach the metal surface, conferring to the coat high passivating properties. The superiority of SAMs of 1-dodecanethiol over benzotriazole, currently the most widely used corrosion inhibitor for copper, has been recently demonstrated in various environments[71,166,172]. Several studies pointed out a direct relationship between the protective properties of the SAMs with their thickness. Both in air[34] and in aqueous solution[169,173] with increasing chain length, SAMs showed higher performance and higher durability. This behaviour is referable to two reasons. First, as demonstrated either experimentally[169] and theoretically[174], a thicker layer hampers in a greater extent the diffusion of oxidative agents (e.g. O_2) and/or aggressive anions (e.g. Cl^- or OH^-) toward the metal surface, slowing down not only the corrosion process of the substrate but also the declension of the protective coat (oxidation of the thiolic function, breakage of the S-C bond). Second, a longer hydrocarbon chain allow for stronger intermolecular Van der Waals interactions conferring to the layer a less defective and quasi crystalline structure, which strongly affect the blocking behaviour of the SAMs[170]. In addition, in aqueous environments, also the wettability degree seems to play a key role in the determination of the protective properties of the SAMs: layers having highly hydrophobic terminal groups showed considerably better performance than hydrophilic terminated ones[72,169]. These findings oriented the investigations mainly toward long-chain alkylic thiols (CH_3-(CH_2)n-SH with $n \geq 10$) and their synthetically favourable derivates allowing to form relatively thick (3-6 nm) protective films or to achieve highly hydrophobic surfaces. For

example, Aramaki *et al*. have been extensively studied the modification of 11-mercapto-1-undecanol SAMs by alkylchlorosilanes[175-180] and more recently Laibinis et al. tested the efficiency of long chain ω-alcoxy-n-alkanethiols[181,182]. Also highly hydrophobic perfluorinated SAMs received in the last years considerable attention[163,183,184], not only for their protective behaviour, but also for their excellent lubricant properties.

Many of these studies demonstrated that SAMs on copper can reach and exceed the 99% of corrosion inhibition efficiency. Their principal limitation from an applicative point of view is represented by their relative poor durability, especially in aggressive aqueous solutions. In fact, EIS measurements revealed that in such harsh conditions their charge-transfer resistance can decrease even of 80% - 90% already after 12 h – 24 h ageing, even if they continue to keep significant protective properties for days[74,131,181]. Thus, the research of new strategies to improve the stability of these systems represents a very topical challenge for the modern surface science.

1.4 Why study aromatic SAMs? Aim and organization of this work

In comparison with the huge amount of investigations dedicated to the characterization of SAMs constituted by alkylic molecules adsorbed on coinage metal, monolayers obtained by the adsorption of aromatic thiols have been considerably less studied. However in the recent past the attention of the scientific community focused on these systems, because of several attractive properties directly related to their molecular structure. First of all, they are able to establish relatively strong intermolecular π-π ring interaction which, in principle, should contribute in a greater extent to the stabilization of the monolayer[185] compared with alkylic backbone of comparable length. In addition, both theoretical studies[186] and experimental evidences[187] pointed out that the S-C bond is significantly stronger when the carbon atoms belong to an aromatic ring (~ 86 kcal mol^{-1} for Benzenethiol vs. ~ 73 kcal mol^{-1} for n-alkylic thiols). Furthermore, owing to their rigid structure, aromatic SAMs present a higher

conformational order than corresponding alkylic layer, because they are not affected by gauche defects. Accordingly, higher thermal stability for arenethiols respect to the corresponding n-alkanethiols has been reported either on gold[188] and copper[116].

A very interesting characteristic of oligo-phenyl thiols is related to the possibility of promoting lateral cross-linking by exposure to electron beam[107] or UV radiation[189]. The cross-linked SAMs exhibit a strongly enhanced etching resistance[190] and thermal stability[191], besides a high mechanical strength allowing separating them from the substrate as a free-standing nanosheets[192].The combination of these properties makes cross-linked aromatic SAMs a very attractive material for applications in nanotechnology and nanopatterning[193].

Aromatic highly conjugated molecules play a primary role also in the emerging field of the molecular electronic, where their high conductivity makes them particularly attractive as molecular wires[194,195], but also other devices such as molecular switches[196] or molecular transistors[197]. Recently many studies have been performed in order to achieve a higher control on the structure of these layers, which seems to be a crucial parameter to control in order to tune their electronic properties[109,198,199].

On copper, some investigation allowed to determine the structure of simple aromatic thiols (mainly Benzenethiol) on single crystal surfaces[81,114,115,200]. On the other hand, because of their limited thickness, very few studies have been performed on aromatic thiols as copper corrosion inhibitors[72,133,201] even if, in theory, the presence of relatively strong lateral ring interactions could confer to this SAMs a more closely packed and more stable arrangement. Zamborini *et al.* reported aromatic thiols to be more effective than alkylic thiols of comparable length in the protection of UPD copper surfaces[201]. More recently Tan *et al.* studied the ability of several *p*-substituted simple aromatic thiols to inhibit the copper corrosion in strong acidic solutions[72]. They concluded that these systems are fairly effective in passivating the underlying copper, accordingly with their thickness and with the hydrophobicity degree of the terminal group; thus in agreement with the previous literature. Nevertheless, to the best of my knowledge, investigations aimed to determine the durability of simple aromatic layers in aqueous solutions has never been performed neither on copper nor on gold.

The aim of the present work is the spectroscopic and electrochemical characterization of monolayers constituted by simple aromatic thiols adsorbed on polycrystalline copper and, to lesser extent, gold surfaces; with particular attention to their long-term stability in aqueous solutions. Toward that aim, many experimental techniques have been employed: several electrochemical methods such as Electrochemical Impedance Spectroscopy (EIS), Cyclic Voltammetry (CV) and linear polarization have been used to assess the passivation properties of the various SAMs; XP spectroscopy allowed us to check the surface composition and the stability of the thiolic group as a function of the ageing time, whereas the changes in the structural order of the layers were followed by means of Raman spectroscopy and Dynamic Contact Angle (DCA) measurements.

In the next section (Chapter 2) all the experimental details pertaining to this investigation will be illustrated. The presentation and the discussion of the experimental results, instead, have been divided in three parts. In Chapter 3 the corrosion inhibition efficiency and the stability up to a week in a strongly acidic environment (aerated H_2SO_4 0.5 M) of two aromatic thiols with different length, namely Benzenethiol (BT) and 2-Napthalenethiol (2-NT), and one long-chain alkylic thiol, *i.e.* 1-Undecanethiol (1-UT), is compared. The acidic ambient has been chosen in order to avoid the growth of insoluble oxidation products on the surface, since in this condition the copper corrosion proceeds accordingly to the reaction:

$$2\ Cu(0) + O_2 + 4\ H^+ \rightarrow 2\ Cu^{2+} + 2\ H_2O$$

In the following Chapter the effect of several p-substituent group (-CH_3, -OH, -COOH, -F, -$NHCOCH_3$) on the stability of the aromatic SAMs has been investigated. Again, the ageing process has been performed in aerated H_2SO_4 0.5 M up to a week, in order to get a direct comparison with the BT performances. Finally, in Chapter 5, are illustrated preliminaries results about the effect of prolonged exposure to ultrapure water on SAMs of BT and 1-UT adsorbed on polycrystalline gold. The quality of the layers as a function of the ageing time has been investigated by means of EIS and CV.

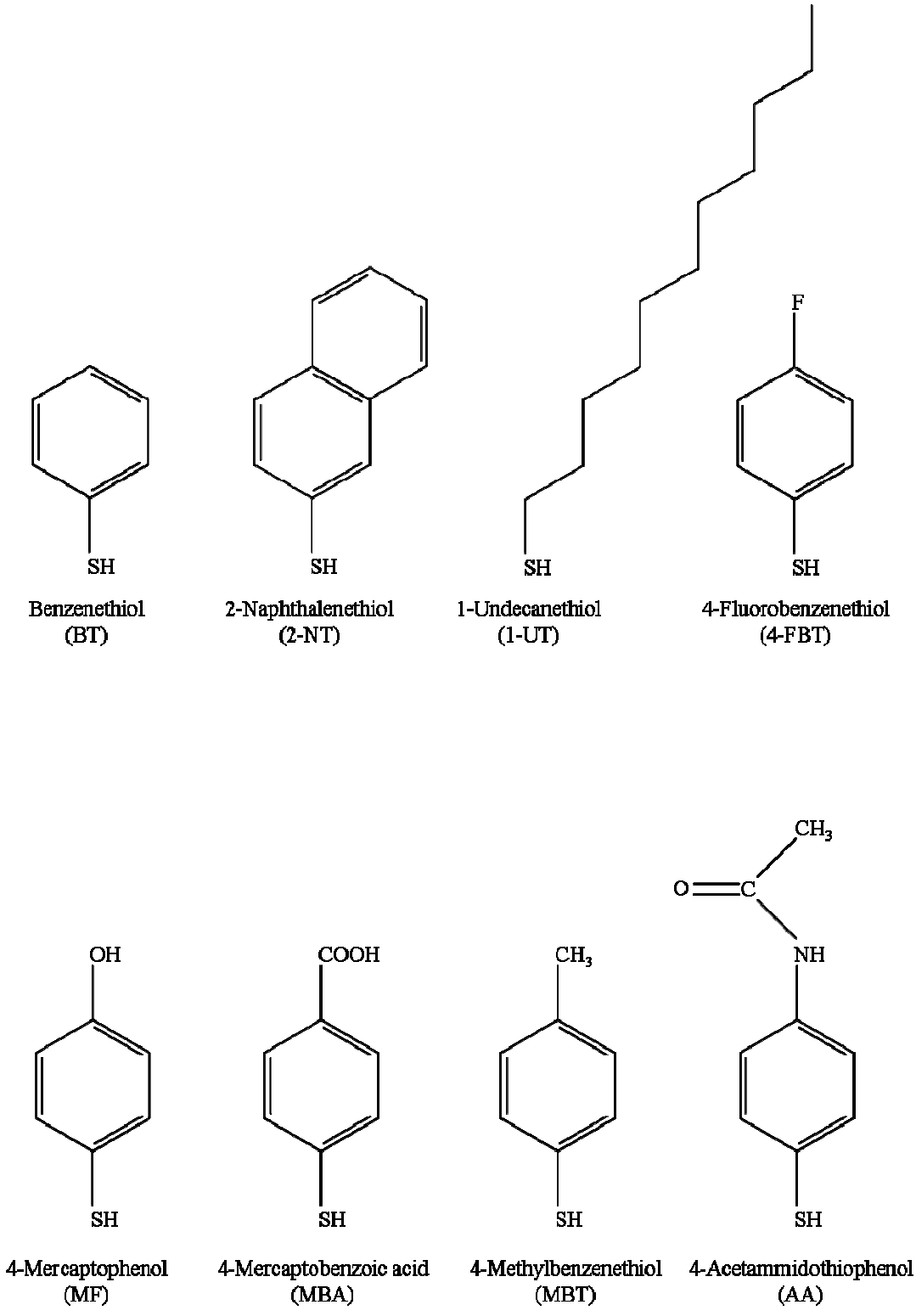

Figure 1.10: Schematic representation of the various molecules studied in this work

Chapter 2: Experimental details

2.1 Samples preparation

2.1.1 Preparation of samples on copper substrates

Pure copper (≥ 99.95 % purity) used as substrate for thiols adsorption was purchased by Goodfellow Ltd. For electrochemical measurements, XPS and Raman experiments, copper plates (Fig. 2.1) with dimension 18 × 15 × 1 mm were used as received, whereas for dynamic contact angle measurements little rectangles with dimension 20 x 10 x 0.25 mm were cut by a pure copper foil and made flat by means of a hydraulic press. In order to remove previously adsorbed thiols, or other kinds of impurities, the copper plates were initially physically scratched with different abrasive papers with decreasing grain size. Subsequently they were immersed in acetone and kept in an ultrasonic bath for 15 min, to remove possible organic physisorbed molecules and traces of copper dust arising from the scratching. Then, accordingly with several literature reports[71-74], the substrates were treated for 20 sec with concentrated (32.5 %) HNO_3 which removed the upper layers of the metal leading fresh, reactive and oxide free surfaces. The substrates were rapidly rinsed in distilled water, and then submitted to a second acidic etching, this time by diluted (3.7 %) HCl for 7 min, followed by a copious rinse in distilled water. At the end of this polishing procedure, samples used as standard copper have been rapidly dried under nitrogen flow and immediately characterized. The adsorption of the monolayers, instead, was carried out by a 24 h immersion of the polished substrate in 0.75 mM solutions of the suitable thiol, obtained from direct dissolution of Benzenethiol (BT, ≥ 99%, Sigma – Aldrich), 2-Naphtalenethiol (2-NT, 99 %, Acros Organics), 1-Undecanethiol (1-UT, 98 %, Sigma - Aldrich), 4-Fluorobenzenethiol (FBT, 98 %, Sigma - Aldrich), 4-Mercaptobenzoic acid (MBA, 90 %,

Sigma - Aldrich), 4-Mercaptophenol (MF, 97 %, Sigma - Aldrich), 4-Acetoamidethiophenol (AA, 95 %, Acros Organics) and 4-Methylbenzenethiol (MBT, 98 %, Sigma - Aldrich) in technical ethanol (96 % Carlo Erba reagents). The thiolic solution, in the first stage of the adsorption process (1 – 2 h), was slightly heated in order to favour the desorption of adventitious material[99]. After 24 h the samples were copiously rinsed with ethanol, to eliminate possibly physisorbed molecules, dried under nitrogen flow and finally characterized. No experiments aimed to assess the roughness of the polished substrates have been performed. Before each measurement, except for electrochemical experiments which are carried out directly in the acidic solution, aged samples were profusely rinsed firstly with distilled and then with ultrapure water, dried under nitrogen flow and immediately characterized.

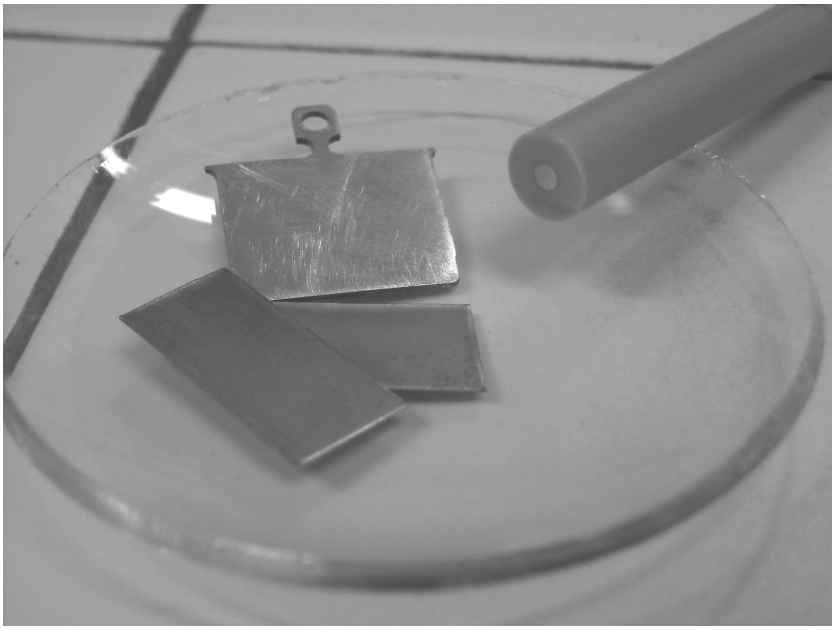

Figure 2.1: Picture of the different substrates used.

2.1.2 Preparation of samples on gold substrates

SAMs of BT and 1-UT were deposited on a polycrystalline Au – electrode – tip purchased from Metrohm Srl (Fig 2.1). The electrode has circular shape with a diameter of 2 mm, and hence an apparent surface area of about 0.0314 cm^2. The protocol followed to polish the gold

surface in order to make it suitable for the thiols adsorption is very similar to that recently reported by Tkac *et al.*[70]. The first step consisted in the complete removal of traces of adsorbates arising from previous experiment by reductive desorption in alkaline solution, accordingly with the well known reaction[202,203]:

$$RS - Au(I) + e^- \rightarrow RS^- + Au(0)$$

performed keeping the potential at the fixed value of – 1.55 V vs Ag/AgCl for around 1 min in deaerated NaOH 1 M. Subsequently, the electrode has been submitted to electrochemical polishing (Fig. 2.2a), performed by 20 successive CV scan between - 0.13 V and + 1.67 V vs Ag/AgCl in H_2SO_4 0.1 M at the scan rate of 100 mVs^{-1}, immediately followed by electrochemical oxide stripping (Fig. 2.2b), carried out by 15 successive CV scan between + 0.17 V and + 0.72 V Vs Ag/AgCl, in the same electrolyte and with the same scan rate.

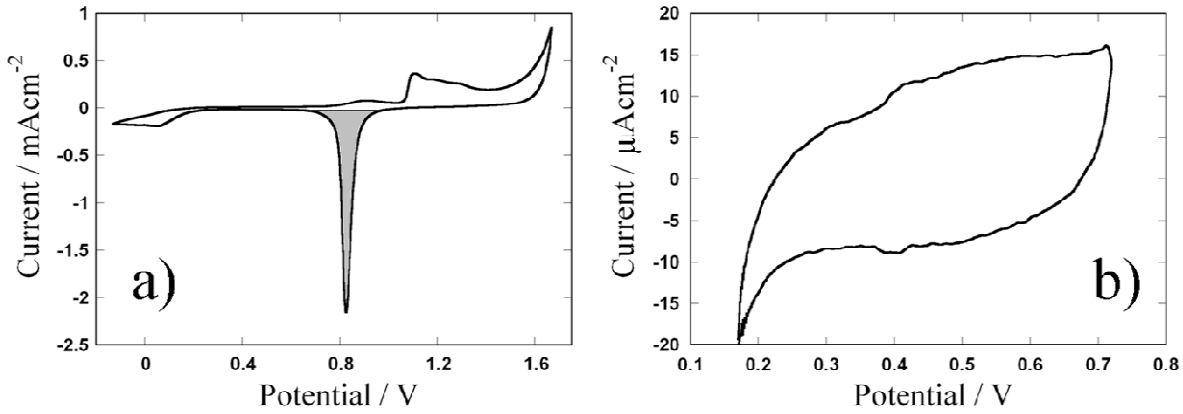

Figure 2.2: Voltammogram relative to the two step of the electropolish procedure adopted for gold electrodes: a) typical response obtained by the "polish" step. The cathodic peak highlighted in grey, relative to the reduction of gold oxide, was used to assess the roughness coefficient. b) typical response obtained by the "stripping" step. Both experiment were carried out in aerated H_2SO_4 0.1 M at the scan rate of 0.1 Vs^{-1}

Then, the substrates were kept for 15 – 20 min in ethanol, to achieve a full reduction of the gold oxide. In fact, is well known that ethanol can reduce gold oxide through oxidation to acetaldehyde[70,204]. Finally the electrode was immersed in the suitable thiolic solution for 24 h (see previous section), copiously rinsed in ethanol and immediately characterized. In Fig 2.2a the typical voltammogram of the last scan of the electrochemical polish is reported. The sharp cathodic peak at around 0.82 V (in grey in the figure) is related to the reduction of gold

oxide and was used to assess the roughness of the surface. In fact, oxygen is assumed to be chemisorbed on gold in a monoatomic layer prior to O_2 evolution with a one-to-one correspondence with surface metal atoms[205], so the area of the reductive peak can be directly related to the real electrode surface. Considering for perfectly flat polycrystalline gold surface a value of 390 ± 10 μCcm^{-2} [205], we calculated for our electrodes a roughness coefficient of 3.2 ± 0.2.

2.2 Experimental setup

2.2.1 Electrochemical measurements

All the electrochemical experiments were performed by means of a computer-controlled Autolab Electrochemical Analyzer (model PGSTAT 12, Eco Chemie BV, The Netherlands). The acquisition program employed for DC and AC measurements were respectively GPES 4.6 version and FRA 4.6 version. All the experiment were carried out at room temperature (23 ± 2 °C) using a conventional three electrode cell, where the counter electrode was a platinum wire and the reference electrode was an Ag /AgCl / Sat. KCl electrode (+ 0.197 V vs. SHE) to which are referred all the potentials reported in this work. All the electrolytic solutions employed were prepared for direct dissolution in (or dilution with) ultrapure water (Water Plus, Carlo Erba Reagenti, conductivity ≤ 0.1 $\mu S\ cm^{-1}$). For the characterization of copper samples, a Teflon cell with the approximate volume of 15 ml was used (Fig 2.3). The design of the cell allowed to fix the position of counter and reference electrode, whereas the flat copper working electrode was pressed against an O-ring sealing a small aperture opened in the

Figure 2.3: Electrochemical cell used for the characterization of copper samples.

lateral wall of the cell, defining exactly the area exposed to the electrolyte (0.33 cm^2). A little window allowed to verify the correct position of the electrodes, as well as to exclude the presence of air bubble on the surface of the sample. The electrochemical impedance spectra (EIS) were recorded at the open circuit potential in a frequency range included between 30 kHz and 50 mHz, with modulation amplitude of 0.01 V. The measurements has been repeated on the same samples at different ageing time (5 min, 1 h, 6 h, 24 h, and then at regular intervals of 24 h up to a week). To extrapolate the parameters of the equivalent circuit the data were fitted using ZSimpwin 3.21 software. The linear polarization measurements were carried out in anodic direction starting from - 0.3 V up to + 0.3 V, at the scan rate of 1 mVs^{-1} both on freshly prepared and 24 h aged samples. The data were analyzed by GPES 4.6 version, allowing the calculation of the exchange current.

The measurements aimed to determine the blocking properties of BT and 1-UT monolayers on gold, instead, were carried out in a solution containing $[Fe(CN)_6]^{3-/4-}$ both in 5 mM concentration, whereas $NaClO_4$ 0.1 M was used as supporting electrolyte. CV experiments were performed between – 0.25 V and + 0.65 V at the scan rate of 100 mVs^{-1}, whereas EIS measurements were conducted at the rest potential (around + 0.19 V) in a frequency range comprised between 30 kHz and 50 mHz, applying a potential perturbation of 0.01 V. Both characterization methods were performed both on freshly deposited and on aged samples (2 h, 4 h, 6 h, 8 h and 24 h). The ageing was carried out in ultrapure water.

2.2.2 XPS measurements

The systematic employment of XP spectroscopy allowed us to constantly check the surface composition of the copper samples after different ageing time. The measurements were performed using a modified Omicron MXPS system with a dual anode X-ray source (Omicron DAR 400) and an Omicron EA-125 energy analyzer (Fig. 2.4), using Mg K_α photons ($h\nu$ = 1253.6 eV) generated operating the anode at 14-15 kV, 10-20 mA. All the reported XP spectra were acquired using analyzer pass energy of 20 eV and a take-off angle of 11° with respect to the surface normal. All the measurements were carried out at room

temperature with a pressure in the analyzer chamber lower than $2 \cdot 10^{-9}$ mbar during the spectra detection. No sign of sample degradation or charging effects, such as broadening or progressive shift, under the X-rays were observed during acquisition times (about 1 h for each sample). The binding energy (BE) of the Cu $2p_{3/2}$ line at 932.7 eV was used as internal standard reference. The experimental spectra were theoretically reconstructed by fitting with symmetric Voigt functions with a Gaussian - Lorentzian ratio let free to vary between 50% and 100%. To quantify the adlayer atomic composition, XPS atomic ratios were estimated from experimentally determined area ratios of the relevant core lines corrected for the corresponding Scofield cross sections[206]. For the quantitative analysis a default error of 10 - 15 % should be considered[207]. For all the SAMs measurements on freshly prepared samples and 24 h, 72 h, 120 h and 170 h aged plates were performed; for BT, 2-NT and 1-UT additional spectra after 1 h, 6 h and 48 h in the acidic solution were recorded.

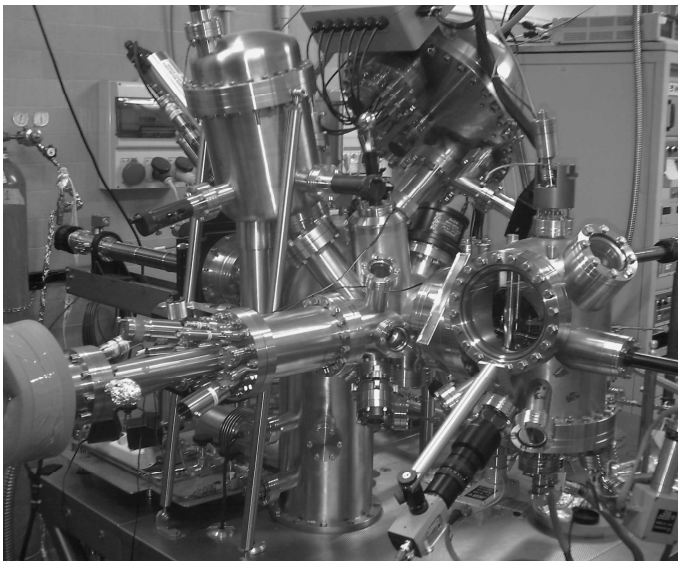

Figure 2.4: Experimental apparatus employed to perform XPS measurements.

2.2.3 Raman Spectroscopy

Raman spectroscopy, in ordinary and Surface-enhanced Raman Scattering (SERS) detection set-up, can provide convenient tools for investigating the changes of aliphatic and aromatic adsorbed thiols in terms of interaction, preferential orientation and conformation with increasing ageing time (0 h, 24 h, 72 h, 170 h). Raman spectra were collected in the back-scattering geometry with an inVia Renishaw spectrometer equipped with an air-cooled CCD detector and a super-Notch filter (Fig 2.5a). The 785.0 nm emission line from a diode laser was focused on the sample under a Leica DLML microscope using a 20x objective. The

spectral resolution was 2 cm^{-1} and the spectra were calibrated using the 520.5 cm^{-1} line of a silicon wafer. Repeated (10-20) 10 s scans were accumulated for each experimental run to provide better signal-to-noise ratios with a power of the incident beam on the sample of about 5 mW. Multiple spot analyses were carried out on different regions of the same sample to check for spectral reproducibility. Data analysis included base line removal and curve fitting using a Gauss-Lorentz cross-product function by Peakfit 4.12 software (Jandel, AISN Software).

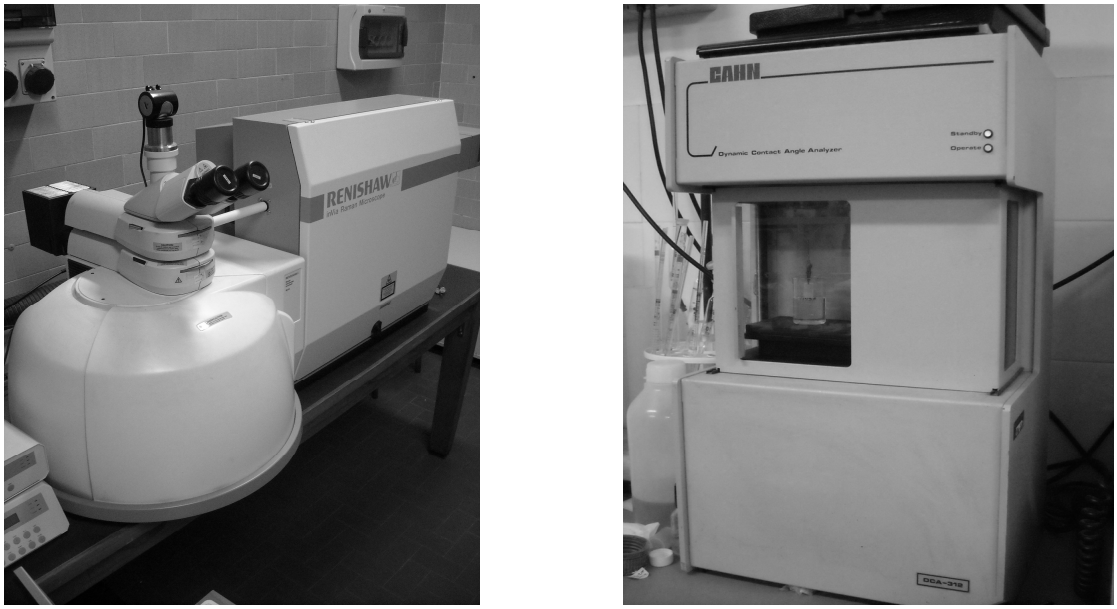

Figure 2.5: Experimental apparatus employed to perform measurements of Raman spectroscopy (left) and dynamic contact angle (right).

2.2.4 Dynamic Contact Angle measurements

Contact angles provide a very sensitive probe for the characterization of the outermost few angstroms of the sample surface. When water is used as wetting medium, the contact angle is primarily a measure of the surface polarity. The changing in the wetting behaviour of SAM-modified copper plates, following the ageing in H_2SO_4 0.5 M, was evaluated by employing a dynamic contact angle analyzer (DCA-322, Chan, CA) based on the tensiometric Wilhelmy method (Fig 2.5b). Dynamic advancing and receding contact angles were measured at room temperature in immersion and withdrawal cycle using deionized water (Water Plus, Carlo

Erba, γ_w = 72.6 mN m^{-1}) as wetting medium and a stage speed of 100 μm s^{-1}. In order to check any possible contamination during DCA analysis, the water surface tension was controlled after each measurement by using a standard platinum Wilhelmy plate. No γ_w change was recorded.

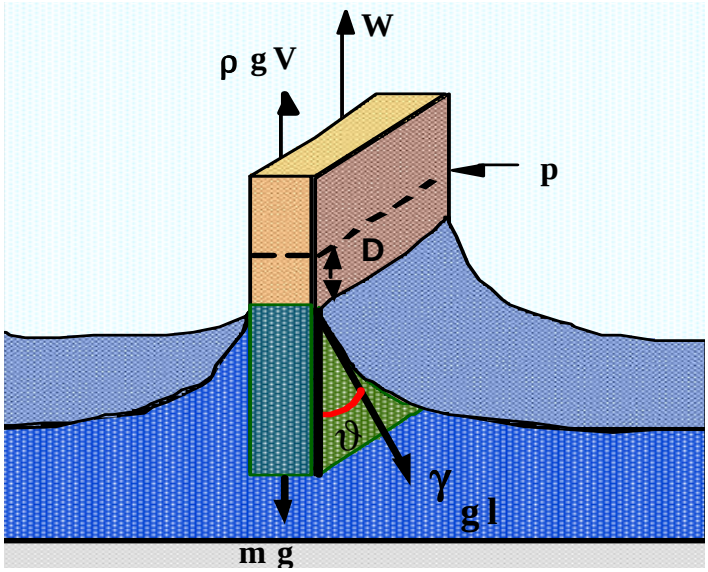

Figure 2.6: Schematic representation of a DCA experiment. The forces considered in the extrapolation of the contact angle are illustrated: mg = gravity; ρgV = buoyancy; p = perimeter of the sample; γ_{gl} = gas-liquid surface tension; D = sample position; W = force of meniscus; Θ = contact angle.

Chapter 3: aromatic *vs* alkylic SAMs on copper: protective properties and long term stability in acidic solution

3.1 Brief introduction to the chapter

Among their numerous applications, Self-Assembled Monolayers of thiols revealed to be excellent inhibitors of copper corrosion process showing performance that exceed by far those of benzotriazole[71,166,172], nowadays the most popular system to protect copper surfaces. Nevertheless, their employment is still curbed by their limited durability[54]. Several studies pointed out that the effectiveness and the durability of n-alkanethiols SAMs are strictly related to the layer thickness[169.173], addressing the subsequent investigations toward molecules allowing the formation of relatively thick protective films. On the other hand, very few studies concerning shorter simple aromatic thiols have been performed[72,133,200] and none of them assessed the durability of such systems in harsh conditions, even if the relatively strong intermolecular ring interaction could limits the number of the defect as well as improve the layer stability. In this chapter a direct comparison of the evolution of protective properties up to a week in strong acidic environment (H_2SO_4 0.5 M) of two aromatic thiols (BT and 2-NT) vs a long-chain alkylic thiol (1-UT) adsorbed on a polycrystalline copper surface is reported. The selected systems diverge not only in the molecular structure but also in the layer thickness: geometrical calculation performed using bond lengths and tilt angles reported in literature[114,173] attributes a layer thickness of around 0.65 nm for BT, 0.90 nm for 2-NT and 1.60 nm for 1-UT. In order to obtain a complete picture of the examined systems, a multi-technique approach has been applied: EIS and linear polarization were employed to verify the changes of the protective properties of the various samples following the ageing, whereas the evolution of surface composition,

molecular structure and wettability as functions of the immersion time were assessed through the systematic application of XPS, Raman spectroscopy and DCA measurements respectively.

3.2 Characterization of freshly prepared samples

The quality of SAMs of BT, 1-UT and 2-NT was assessed by XP spectroscopy, Raman spectroscopy and DCA measurements. In figure 3.1a, b and c the XP spectra relative to the S2p region of the three SAMs are reported. The analysis of the peaks revealed, for all the samples, the presence of a main spin-orbit doublet (1.2 eV shift, 2:1 ratio) with maximum at 162.35 ± 0.1 eV. This signal, characteristic of S-Cu covalent bond[34,73,133,163,164], confirms the effective chemisorption of the thiols on the copper surface. In the case of BT and 1-UT no other components were observed, indicating the absence of detectable quantity of physisorbed molecules or sulfur oxidation products. On the contrary, spectrum of 2-NT showed two minor components, with maximum at 163.4 ± 0.1 eV and 167.7 ± 0.2 eV, which were ascribed to traces of physisorbed molecules[208,209] and sulfonates[34,71], respectively. Nevertheless the main component due to the chemisorbed thiolate represented almost the 95 % of the total sulfur also in the instance of 2-NT, which means that the most of the molecules are covalently bonded to the metal substrate.

The C1s spectra (Fig 3.2 a, b and c) revealed the presence of two components for all samples. The main signal (in green in the figure), ascribed to the molecules backbone, was found for BT and 2-NT at 284.1 ± 0.1 eV and for 1-UT at 285.0 ± 0.1 eV, *i.e.* in positions characteristic for aromatic and alkylic carbons, respectively[69,105,210,211]. The peaks are enlarged by a minor component (in red in the figure) at slightly higher binding energy (around 0.7 ± 0.2 eV higher respect to the main signal) ascribed to the carbon atom bonded to the sulfur. The best fit performed, perfectly reflects the molecular structures (C-C/C-S ratio: 5:1 for BT, 9:1 for 2-NT, 10:1 for 1-UT). Together with the values calculated for the C/S atomic ratios (5.7 for BT, 11.7 for 1-UT and 9.7 for 2.NT), which are in excellent

agreement with the theoretical values, this demonstrates the absence of significant amount of organic impurities.

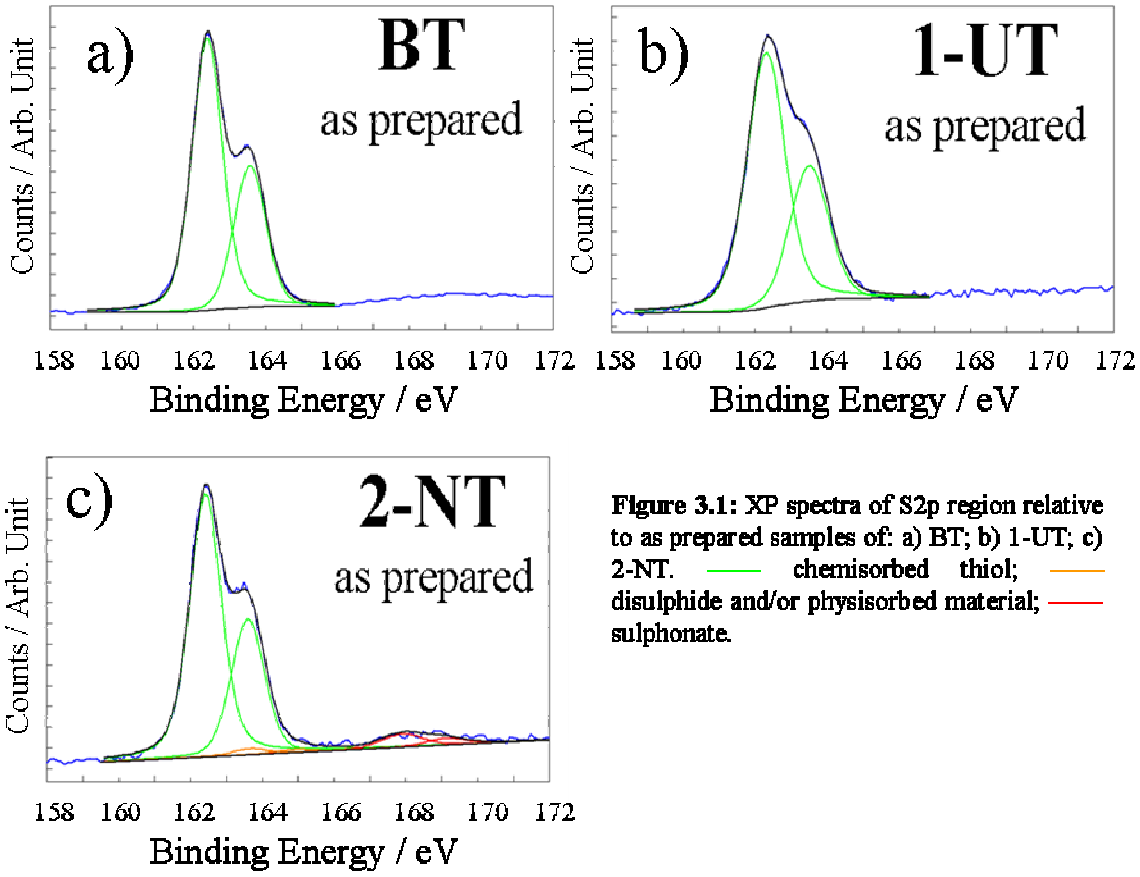

Figure 3.1: XP spectra of S2p region relative to as prepared samples of: a) BT; b) 1-UT; c) 2-NT. —— chemisorbed thiol; —— disulphide and/or physisorbed material; —— sulphonate.

The surface coverage was estimated by the S/Cu atomic ratio value and the analysis of the CuLMM Auger spectra (Fig. 3.3). All the samples shows a S/Cu ratio in line with the highest values reported in literature for similar systems[163,212] (0.50 for BT, 0.55 for1-UT, 0.57 for 2-NT), indicating a complete coverage of the substrate.

The Auger CuLMM spectra (Fig. 3.3) allowed to distinguish between Cu(I) and Cu(0), which is impossible to do by the analysis of Cu2p spectrum where the two components fall at the same binding energy[213-215]. All the layers showed a main component at 916.1 ± 0.1 eV, typical of the thiolate-bonded Cu(I)[163], and a shoulder lying at 918.7 ± 0.1 eV, assigned to the bulk atoms[164,216]. The clear difference of intensities between the two components confirms the quantitative analysis, suggesting a full surface coverage. In the case of the spectrum of the bare copper, added for comparison, the larger component is clearly that due

to the bulk atoms, whereas the minor peak at 916.5 ± 0.1 eV is related to the presence of cuprous oxide[217]. In no case the presence of signals ascribable to Cu(II) was observed, as also confirmed by the Cu2p spectrum (data not shown).

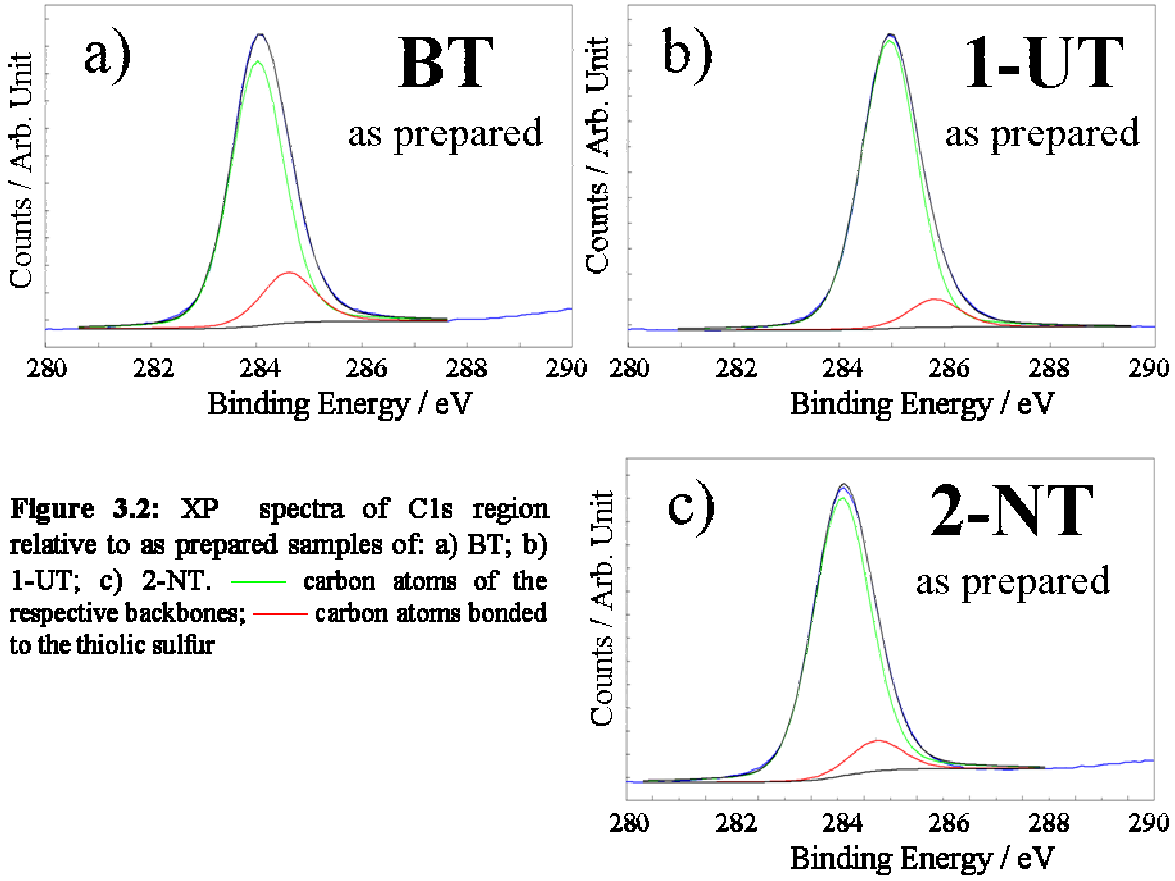

Figure 3.2: XP spectra of C1s region relative to as prepared samples of: a) BT; b) 1-UT; c) 2-NT. —— carbon atoms of the respective backbones; —— carbon atoms bonded to the thiolic sulfur

The small quantities of oxygen detected (O/Cu atomic ratio: 0.05 for BT, 0.15 for 1-UT and 0.14 for 2-NT) are probably related to the presence of some solvent molecules kept trapped in the organic layers, but could be also due to the presence of little quantities of cuprous sub-oxide. However the low values of the O/Cu ratio and the peak position (531.5 ± 0.1 eV, whereas the crystalline Cu_2O is expected at 530.3 ± 0.1 eV)[218,219] suggests that the copper oxide possibly present on the copper surface has been mostly displaced during the thiolate adsorption. In no coated samples traces of chlorine arising from the polishing procedure have been detected.

Raman spectra of as prepared BT, 1-UT and 2-NT SAMs are displayed in figure 3.4a-c. For our thiols adsorbed on copper the use of the 785 nm laser line in ordinary Raman setup is expected to yield an enhancement of the molecular layer very close to the metal surface[220].

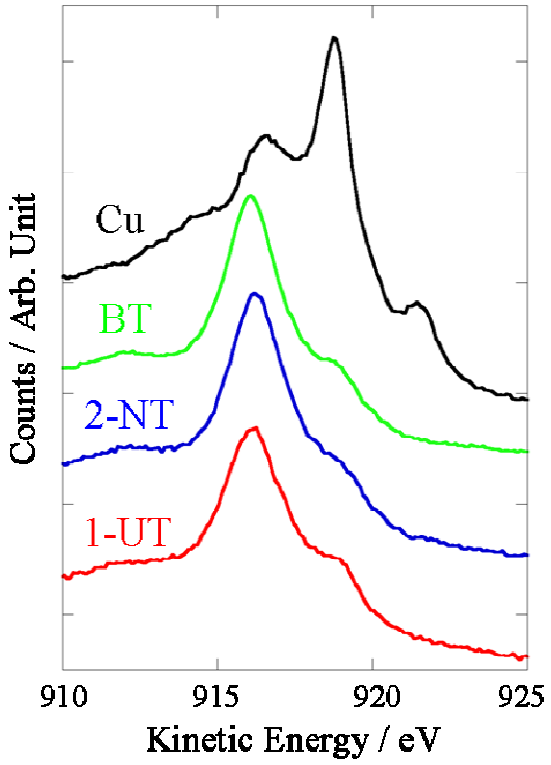

Figure 3.3: Auger CuLMM spectra relative to as prepared samples of: —— Cu bare; —— BT; —— 1-UT; —— 2-NT

Theoretical calculations predict three groups of bands for neat aromatic thiols, associated with Me–S stretching vibrations, displacement of S atom within the ring and benzene ring vibrations[221]. The most prominent benzene ring vibrations (υ12, υ18a, υ1 and υ8a C-C modes) are expected at 1000, 1021, 1064 and 1572 cm^{-1} respectively, whereas bands at 417, 701, 917, and 2561 cm^{-1} are related to the ν_{7a} and ν_{6a} ring modes with contributions from the C-S stretching vibration (νCS), the CSH deformation (δCSH) and the S-H stretching (νSH), respectively. The measured spectrum of BT freshly adsorbed on copper (Fig. 3.4a) showed distinct bands at about 406, 993, 1015, 1074 and 1574 cm^{-1} and a broad feature containing contribution at about 486, 534, 581, 612, 695 cm^{-1}. The first set of bands corresponds to C-H out-of-plane bending and C-S stretching, ring out-of-plane deformation, ring in-plane deformation and C-C symmetric stretching with C-S contribution, respectively[220-222]. Further bands in the range 480-590 cm^{-1} resulted from the superimposition of C-S out of plane bending and vibrations of the surface oxide layer, probably formed following the air exposure during the measurements. On the other hand, the band at about 612 and 695 cm^{-1} can be attributed to the ring in-plane deformation with contributions from the C-S stretching vibrations (νCS). The ν(Cu–S) stretching vibration is expected in the range 200–280 cm^{-1}, a region not clearly seen in our experimental set up. The absence of the S-H stretching mode (νS-H) at about 2586 cm^{-1} and of the S-H in-plane bending at about 915 cm^{-1} and the lowering in the band positions with respect to those of non-adsorbed BT molecules clearly indicate that it adsorbed dissociatively as benzenethiolate, forming a copper-sulfur bond[222]. The spectrum of the freshly prepared 1-UT (Fig. 3.4b) on copper were poorly defined and dominated by the strong feature in the range

400-800 cm^{-1}, where the oxide vibration and the ν(C-S) stretching mode occur. In the Raman spectra of alkanethiol monolayers, usually in SERS configuration, the most prominent bands occur in the 600-750 cm^{-1} range for the ν(C-S) stretching mode and in the 1000-1100 cm^{-1} range for the ν(C-C) stretching vibrations. The n(C–H) vibrations, including symmetric and antisymmetric stretching and deformation modes yield complex structures occur in the range 2800-2950 cm^{-1} and 1410-1480 cm^{-1}, respectively. Rocking and wagging (CH_2) modes are in the range 708 - 905 cm^{-1} and 1270-1370 cm^{-1}, respectively. The ν(C-S) region can provide conformational information about C-C bonds adjacent to the C-S bond. In the range 600-750 cm^{-1} adsorbed alkanethiol molecules give two bands assigned to gauche (G) conformation, $\nu(C–S)_G$, at about 655 cm^{-1} and to trans (T) conformation, $\nu(C–S)_T$, at about 730 cm^{-1} [33]. Comparing their intensities with those for the respective molecules in the liquid phase, the (G) conformation indicates disorder[4] and therefore it is absent in the solid phase. Thus, the prominent band at about 725 cm^{-1} indicates that the adsorbed molecules were preferentially in (T) conformation, suggesting for 1-UT SAMs a highly ordered structure. The measured spectra of 2-NT adsorbed on copper (Fig. 3.4c) showed the strongest molecular bands at about 770, 1066, 1379, 1425, 1430, 1574 and 1625 cm^{-1} and a broad feature in the range 450 – 650 cm^{-1} containing distinct peaks at about 515, 595 and 646 cm^{-1}. The absence of the S-H

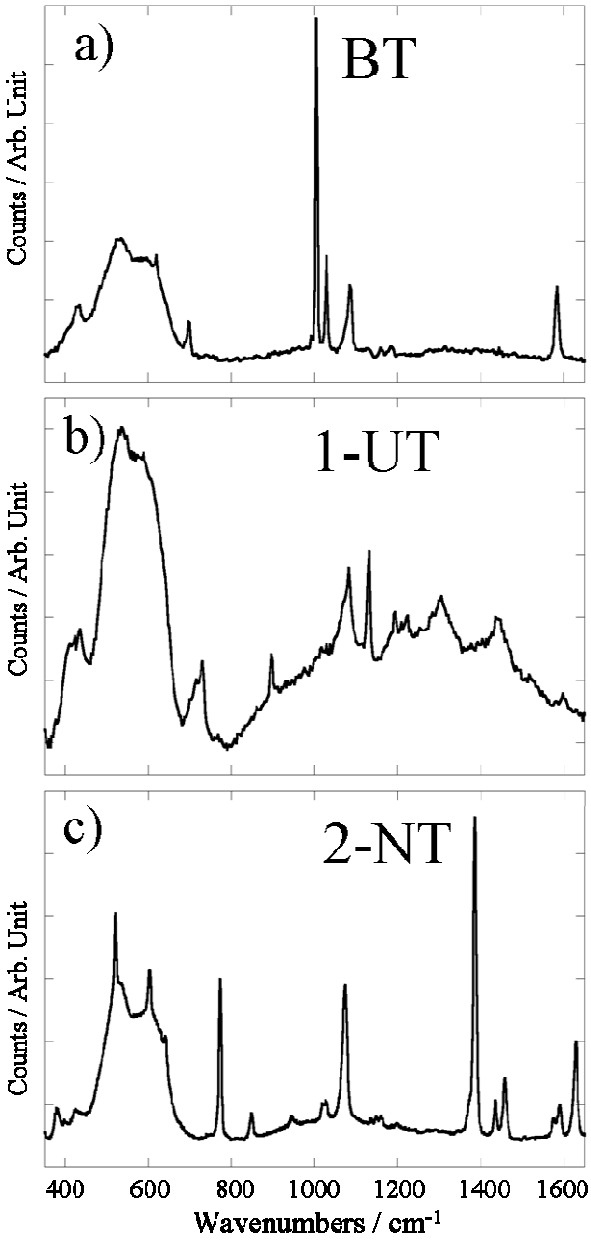

Figure 3.4: Raman spectra of as prepared: a) BT; b) 1-UT; c) 2-NT, in the region 350-1650 cm^{-1}

stretching vibration bands at about 2650 cm^{-1} (not shown in the plot) confirmed the cleavage of the S-H bond with ensuing formation of thiolate structures. The significant vibrations for 2-NT in the region 200–1000 cm^{-1} are assigned to the in-plane deformation of the ring with C–S contribution, and the two in-plane ring breathing modes, respectively, the strongest band being at about 765 cm^{-1} (in-plane bending mode)[223]. Other relevant bands due to in-plane vibrational frequencies appear at 1080 cm^{-1} (C-H bending) and at 1378, 1430, 1567 and 1620 cm^{-1} (ring stretching modes). The slight decrease in the band positions with respect to the unsupported 2-NT confirmed the interaction with the support.

The surface free energy variations of copper surface after the reaction with various thiols can be easily studied by water wetting experiments. The average value ($n \geq 3$) of advancing (ϑ_{adv}) and receding (ϑ_{rec}) contact angle that bare copper and freshly prepared SAMs form with ultrapure water are reported in figure 3.5. The clean copper surface resulted highly wettable, with $\vartheta_{adv} = 44°$ and $\vartheta_{rec} = 11°$. Working with not perfectly homogeneous surfaces like our systems, the advancing contact angle may be associated with the wetting behavior of the low-energy surface fraction whereas the receding contact angle to that of the high-energy areas, *i.e.*, in experiments carried out in water, with the hydrophobic and hydrophilic components, respectively[224]. Accordingly, for high quality SAMs containing a hydrophobic terminal group such as a methylene unit or a phenyl ring a high value of the advancing contact angle is expected. Thus the noticeable increase in advancing contact angles upon reaction with thiols is a further confirmation of the formation of the organic layers with a high order degree[32]. Nevertheless, our experimental results were pretty far from literature reports for similar systems on gold (data on copper obtained with similar experimental set up were not available). In fact all the samples, and in particular the aromatic ones, showed higher ϑ_{adv} and higher hysteresis (ϑ_{adv} - ϑ_{rec}) than expected[69,225], probably because of the elevated surface roughness of our substrates. The morphology of the surface has a great influence on wettability experiments: for example Wang *et al.* recently revealed that highly rough copper surfaces provide an amplification effect for both hydrophobic and hydrophilic behaviour[226]. Furthermore both Abe *et al.*[227] and Yang *et al.*[228] reported that higher roughness and smaller gold grain size lead to higher advancing angle and higher hysteresis, in agreement with our interpretation. Accordingly with the higher hydrophobic character of

the alkylic chain, which debars the interaction and the surface adsorption of water molecules during the immersion cycle, 1-UT sample showed the higher advancing and, especially, receding contact angle.

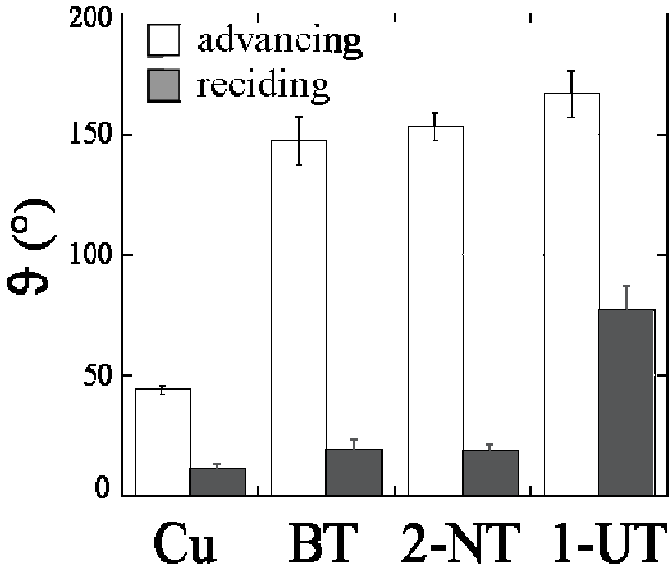

Figure 3.5: Average values obtained for advancing (white) and receding (grey) contact angle of as prepared samples.

Since several investigations pointed out a relationship between the chain length and the wettability of the SAMs[226,229], this result is also coherent with the greater thickness of the monolayer. This behaviour has been ascribed to the combination of two factors: one hand the chain-length dependent changes in the structure of SAMs[27,32], such as enhancement of order and packing density with increasing chain length; the other the possible Van der Waals interactions of liquids with metallic substrates supporting the organic layer[32,229].

On the other hand, no significant differences between the contact angles of BT and 2-NT have been observed, in spite of their thickness gap. This could mean that the layer thickness are close enough to not cause appreciable difference in the wetting behaviour, even if this could be due to a slightly better organization of BT with respect to 2-NT. The latter hypothesis is also supported by XPS data, which detected in 2-NT samples small amounts of sulfonates and physisorbed molecules.

3.3 Ageing in aerated H_2SO_4 0.5 M

3.3.1 Electrochemical characterization

The purpose of this work was to check the variation in protective properties, structure and composition of different SAMs when they are exposed to a strongly acidic solution. Toward that aim EIS provided a very powerful tool, firstly because it allowed to easily extrapolating important parameters of the system like the charge-transfer resistance or the double layer capacitance, secondly because it is a non destructive technique, allowing us to perform many different measurements on the same sample after different immersion times in the electrolyte. In figure 3.6a-b, the equivalent circuits used to fit the data respectively for uncoated and protected copper are illustrated.

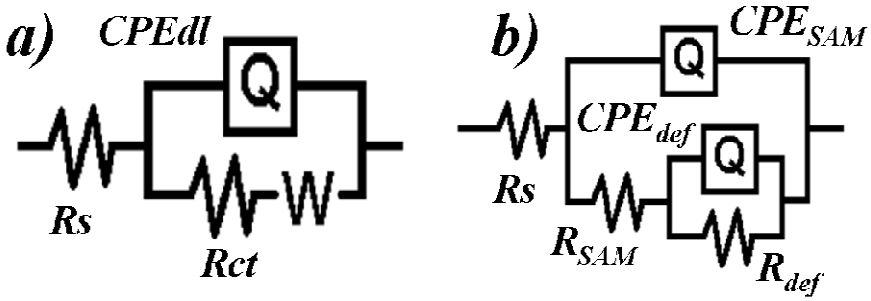

Figure 3.6: Representation of the equivalent circuit used to analyze the EIS data relative to: a) bare copper; b) protected copper

In circuit a) Rs represent the solution resistance, Rct and CPEdl describe respectively the charge-transfer resistance and the double layer capacitance at the electrode-solution interface whereas the Warburg element describes the diffusion of corrosion products and dissolved oxygen occurring at low frequencies[74]. The circuit b) has been recently adopted to describe the behaviour of a defective SAM where the mass transport contribution may be neglected[73,74,213,230-232]. The model consists, in addition to the electrolyte resistance Rs, in two resistive-capacitive loop referred to the charge transfer process respectively through the organic layer (R_{SAM} and CPE_{SAM}) and at the metal-solution interface in correspondence with the defects of the SAMs (R_{def} and CPE_{def}). In both circuits capacitors were substituted by

constant phase element, taking in account the roughness of the copper surface and the non homogeneous distribution of the corrosion current density. In order to evaluate the properties of the various SAMs three parameters were considered: i) the overall charge-transfer resistance R_{tot}, arising by the sum of R_{SAM} and R_{def} ; ii) the value of the Open Circuit Potential (OCP); iii) and the value of the frequency independent parameter Y_0 associated to the constant phase element CPE_{SAM}. The admittance of a constant phase element is given by $Y = Y_0 (j\omega)^n$, where closer is n value to 1, closer is the CPE to an ideal capacitor (and Y_0 to the "real" double layer capacitance). Since in our experiments n_{SAM} always keep a value higher than 0.9 we conclude that the value of Y_0 is representative of the SAMs capacitance, giving us precious information about the quality of the layer and its permeability to the electrolyte. In fact, SAMs may be assimilated to a dielectric set between the plates of a planar capacitor[173]. Thus, the double layer capacitance is given by:

$$C_{dl} = \varepsilon_0 \varepsilon_r A d^{-1}$$

where ε_0 and ε_r are the permittivities, d is the layer thickness and A is the surface area. The formation of defects in the layer (desorption of molecules upon oxidation or formation of collapsed sites) would lead up to a penetration of the electrolyte, with increase of the relative permittivity, and to a decrease in the average film thickness. This would involve an increase of the capacitance value, which for this reason is a crucial parameter to check the quality and the durability of these systems. Also the Y_0 value associated with the CPE_{def} should provide informations about the permeability of the SAMs to the electrolyte and generally its trend qualitatively followed that of CPE_{SAM} but with considerable higher values. Nevertheless, its marked deviations from an ideal capacitor[231,232] (n values are usually included between 0.52 and 0.70) makes very difficult to directly correlate the Y_0 values with the real capacitance and renders the data quite hard to interpret, so that they are usually omitted.

In figure 3.7a and impedance spectra of polished bare copper is displayed. The uncoated copper shows a kinetic controlled high frequency domain, where the little semi-circle associated to the charge transfer process is clearly visible, and a diffusion controlled low frequency domain. The data fitting revealed, as expected, high double layer capacitance (Y_0 = 1060 ± 120 $\mu S s^n cm^{-2}$ with n = 0.70) and low charge transfer resistance (115 ± 22 Ωcm^2).

The measurements performed on the freshly prepared samples (Fig. 3.7b-d, black circles) shows that the charge transfer resistance of the protected samples at t = 0 scale up with the thickness of the monolayers.

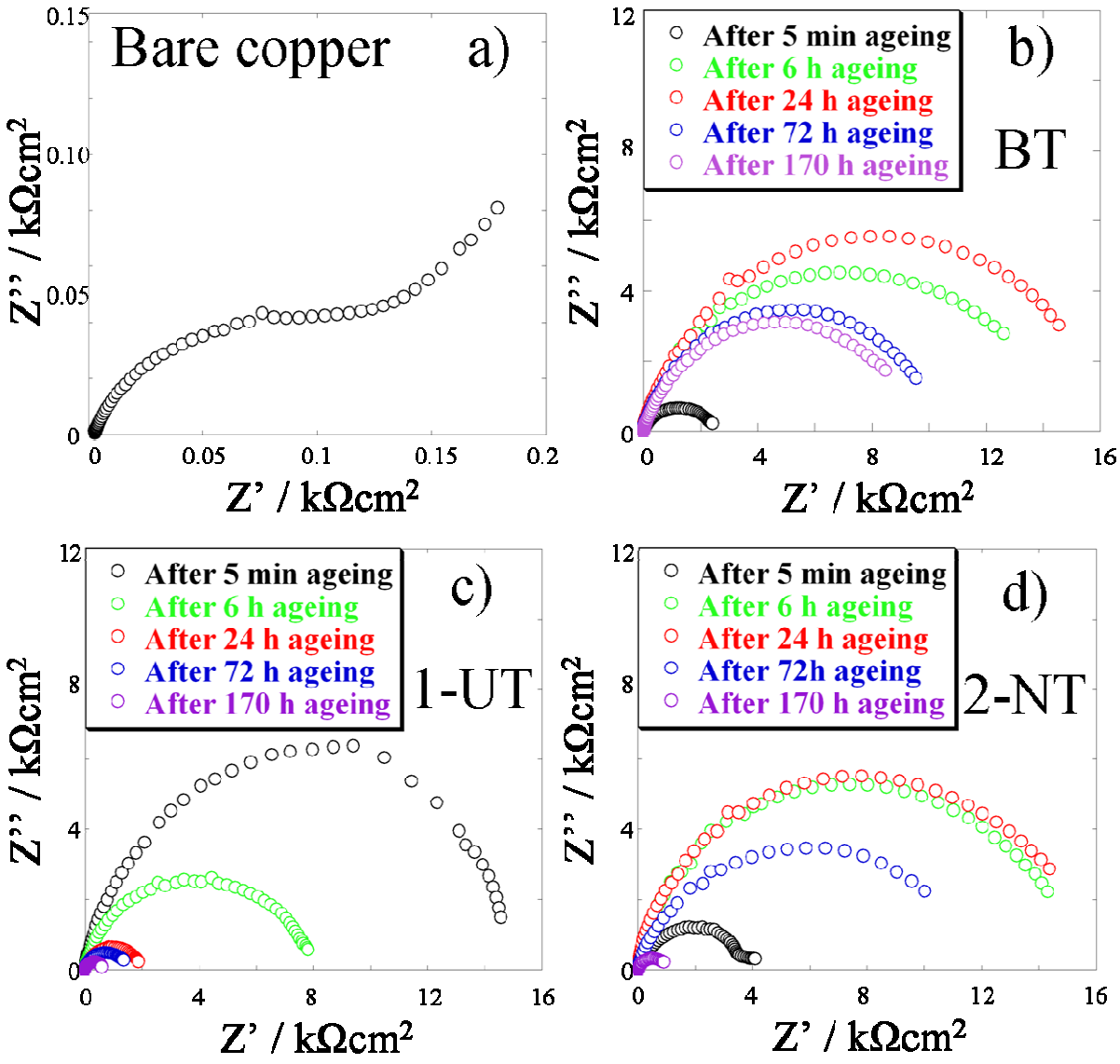

Figure 3.7: Impedance spectra collected on: a) freshly polished bare copper; b) BT; c) 1-UT; d) 2-NT after different ageing times in aerated H_2SO_4 0.5 M

Even if BT provided a good protection of the underlying copper, the EIS data clearly show that the resistance of the thicker 2-NT was roughly twice, and that of 1-UT notably much larger than that of 2-NT. The freshly prepared 1-UT SAM presented in fact excellent protective properties, with a R_{tot} around 15 kΩcm^2, *i. e.* more than two orders of magnitude higher than that of uncoated copper. It is worth noticing that the values of the parameters

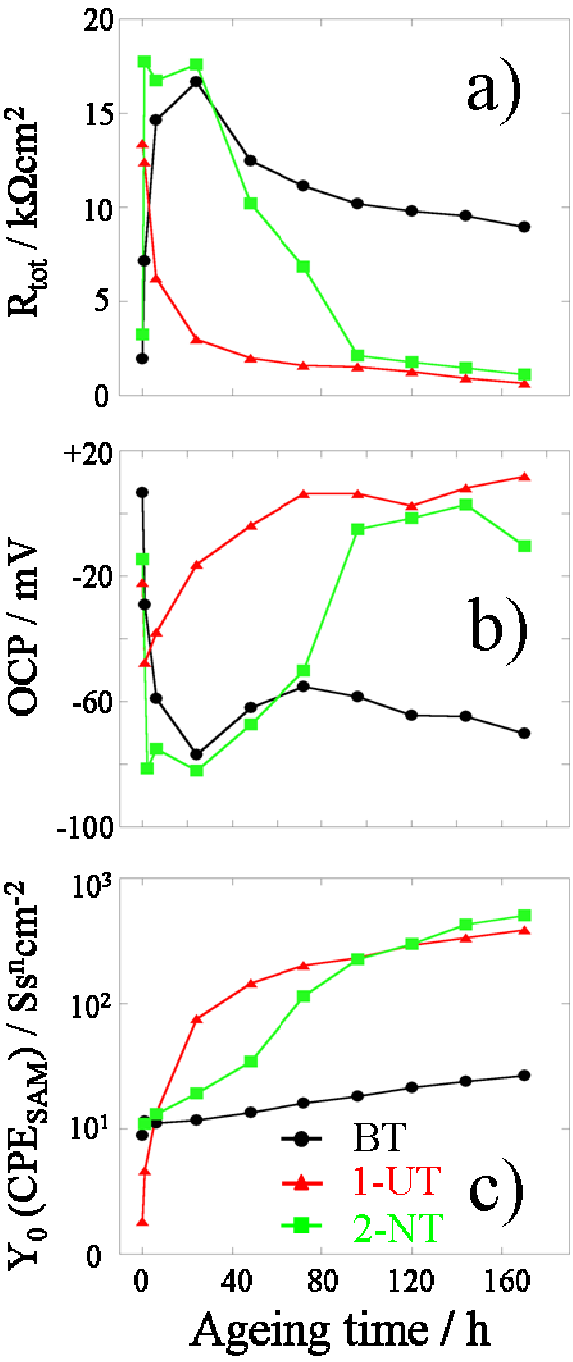

Figure 3.8: average trend (n≥3) of the parameters extracted from the EIS measurements as a function of the ageing time. A maximum error of 25% was found

associated with the layer capacitance correctly reflect the differences in the molecular structure of the various samples. The thicker and less polarizable 1-UT SAMs showed the lower capacitance (1.9 ± 0.5 μSs^ncm^{-2} with n_{SAM} ~ 0.95), followed by 2-NT (5.0 ± 1.1 μSs^ncm^{-2} with n_{SAM} ~ 0.94) and by the thinnest BT (8.7 ± 1.3 μSs^ncm^{-2} with n_{SAM} ~ 0.95). On the whole, the data are indicative of the good quality of the adsorbed layer.

The measurements performed on aged samples denoted for 1-UT a rapid decrease in the protective properties: in the course of exposure to acidic solution, their charge-transfer resistance became half of the initial value already after 6h, and further on decreased up to 20 % after 24h and to 5 % after one week. This dramatic loss in the inhibition efficiency of long-chain alkylic SAMs subsequent to their exposure to an aggressive environment has been already described by several authors[74,131,181]. On the other hand, the SAMs of aromatic thiols, surprisingly, followed exactly the opposite trend. Both BT and 2-NT samples, in fact, during the first 24 h exposure to the acidic solution showed a steep increase of their charge-transfer resistance, reaching values exceeding that of the freshly prepared 1-UT (Fig. 3.7b and d, Fig 3.8a). To the best of our knowledge this attractive phenomenon has never been described before in literature. Is

interesting to note that this behavior of BT and 2-NT went along with a shift of their open circuit potential in the negative direction (from ~ -10 mV to ~ -70 mV, Fig. 3.8b), suggesting the growth of their protective properties to be mainly related to the inhibition of the cathodic reaction of the corrosion process, *i. e.* the reduction of dissolved oxygen. Furthermore, aromatic SAMs appeared considerably more stable respect to the alkylic layer. BT samples, in particular, showed an exceptional durability: as evidenced in figure 3.8a, their charge-transfer resistance reached a maximum during the first 24 h of ageing and then decreased slightly and linearly, but yet after one week ageing its inhibition efficiency was still clearly higher than that of freshly prepared samples. On the contrary 2-NT SAMs after around three days in the ageing conditions underwent a sudden breakdown, with a collapse of the overall charge-transfer resistance accompanied by a concomitant increase of the OCP. After about 100 h ageing there was almost no difference in the performance of 1-UT and 2-NT. The changes in the layer capacitance values, extracted from the fitting of EIS data, traced out that of the charge transfer resistance. All the modified electrodes made record an increase with time, but with very different slopes (Fig. 3.8c).

How previously discussed, the raising trend can be attributed to the progressive formation of defects in the layers during immersion and to the consequent penetration of the electrolyte in the SAM, with increase of its relative permittivity and diminution of the average film thickness. The steepest increase in electrode capacitance has been detected for 1-UT confirming that this sample rapidly undergoes serious damages when in contact with acidic electrolyte. The lowest slope is clearly that of the BT-coated electrode, that appears to be the most stable among the three samples. The electrode capacitance for the 2-NT-coated sample was close to that of BT in the first part of the ageing, but gradually increased and approached the same values as for the 1-UT electrode, in agreement with the other EIS parameters.

The trend observed in EIS experiments was also confirmed by linear polarization measurements, illustrated in the Tafel plots in figure 3.9a, b and c. Comparing the Tafel curve relative to the naked Cu plates with those recorded on the coated electrodes, is evident that all the three SAMs provide a clear inhibition effect on the copper corrosion. The extrapolation of the exchange currents (see Table I) clearly shows that the freshly prepared 1-UT samples assured the best protection to the underlying substrate, with a decrease of

almost two orders of magnitude with respect to the value obtained for the uncoated copper; but is equally clear that these layers degraded very rapidly, so that after 24 h ageing the measured corrosion current was raised by more than ten times. One the contrary, aromatic SAMs exhibited an evident decrease of the corrosion current and a negative shift (by ~ 70 mV) of the corrosion potential, approaching the inhibition efficiency of the freshly prepared 1-UT, perfectly in agreement with the impedance data.

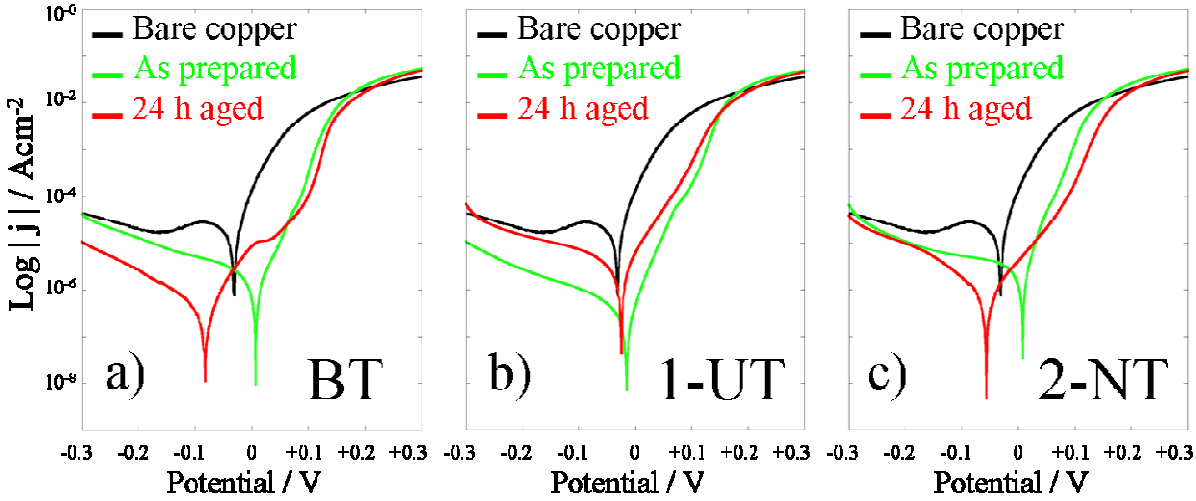

Figure 3.9: Tafel plot relative to: a) BT; b) 1-UT and c) 2-NT as prepared (green line) and after 24 h ageing (red line). The curve relative to the freshly prepared bare copper (black line) was added for comparison. Measurements was carried out in aerated H_2SO_4 solution at the scan rate of $1mVs^{-1}$

	Ageing time hours	Jcorr μAcm^{-2}	Ecorr mV
Cu	0	28.5 ± 8	- 40 ± 5
BT	0	1.80 ± 0.6	13 ± 9
	24	0.69 ± 0.2	- 65 ± 15
1-UT	0	0.31 ± 0.07	- 42 ± 4
	24	4.56 ± 2	- 31 ± 5
2-NT	0	1.68 ± 0.7	1 ± 7
	24	0.88 ± 0.3	- 66 ± 11

Table I: Average values (n≥3) of exchange current and corrosion potential deduced by linear polarization measurements.

3.3.2 Spectroscopic characterization and wetting behaviour

XPS measurements carried out on aged samples allowed us to check the evolution of the adsorbed layer exposed to the acidic solution. The trend of the S/Cu ratio (Fig 3.10a) demonstrated that in all the samples the thiols resist on the copper surface even in these aggressive conditions. The slight increase observed is probably related to a weakening of the $Cu2p_{3/2}$ signal, which was used in the calculation of the atomic ratio, due to the absorption of some impurities following the ageing process. The presence of impurities on the surface was also supported by the progressive increase of the C/S ratio (3.10b). No significative changes in the shape of Cu2p and CuLMM signal have been observed (data not shown). The evolution of O/S atomic ratio, reported in Fig. 3.10c, showed a growing trend for all the samples. The increase of the oxygen content in the aged samples can be attributed to the formation of copper oxide, to the oxidation of some thiols to sulfonates or to the presence of some electrolyte molecules trapped in the organic layer or adsorbed on the metal surface. So, following the oxygen abundance on a sample allows to roughly estimating its permeability to the electrolyte and its tendency to the oxidation. As highlighted in the plot BT samples constantly showed values considerably smaller than 2-NT and 1-UT suggesting being the less permeable and the less prone to oxidation, thus the most effective in the substrate protection, in spite of its lower thickness and in agreement with the electrochemical data.

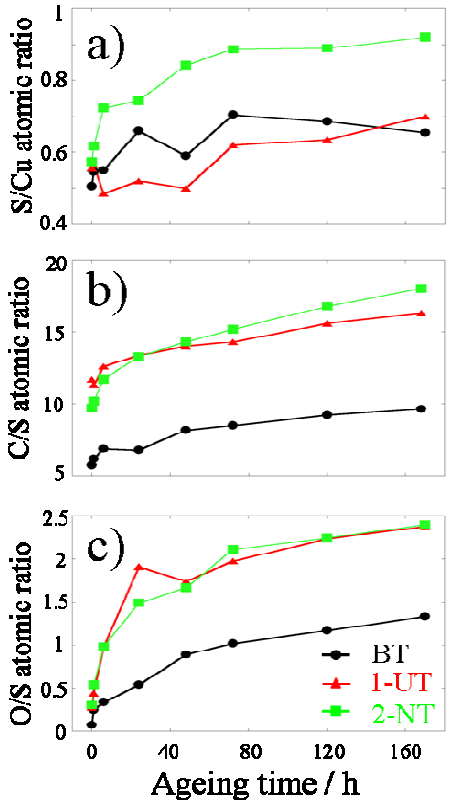

Figure 3.10: Average trend (n≥3) of atomic ratios obtained by XPS measurements for various samples. An error of 10% should be considered.

The evolution of the S2p region resulted very significative, providing precious information not only on the stability of the different films, but also on the degradation mechanism. The

best fits carried out on the spectra relative to aged samples are consistent with the surprising electrochemical response, denoting a noticeable difference of stability between the SAMs of aromatic thiols and the 1-UT samples. In fact, as shown in Fig. 3.11a, b, c, g, i, and h; even after several days in H_2SO_4 0.5 M the majority of the aromatic thiols remained steadily chemisorbed to the copper surface. SAMs made of BT (Fig. 3.11a, b, c), in particular, demonstrated again to be extremely stable, so that even after one week of ageing the component of the S2p spectra ascribable to the sulphur covalently bonded to the substrate (maximum at 162.35 ± 0.1 eV, green line in the figure) represents around the 85% of the total (Fig. 3.12).

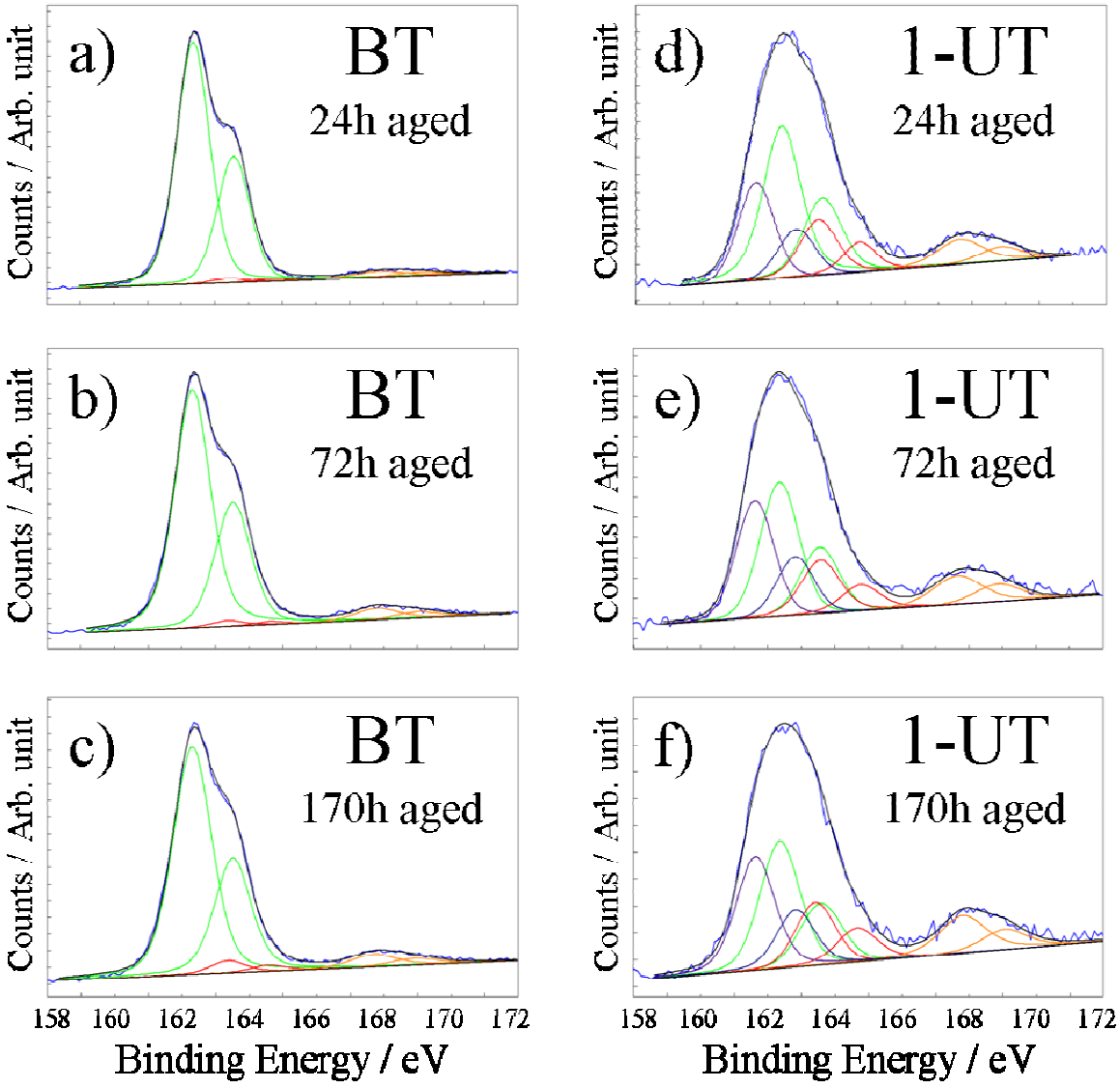

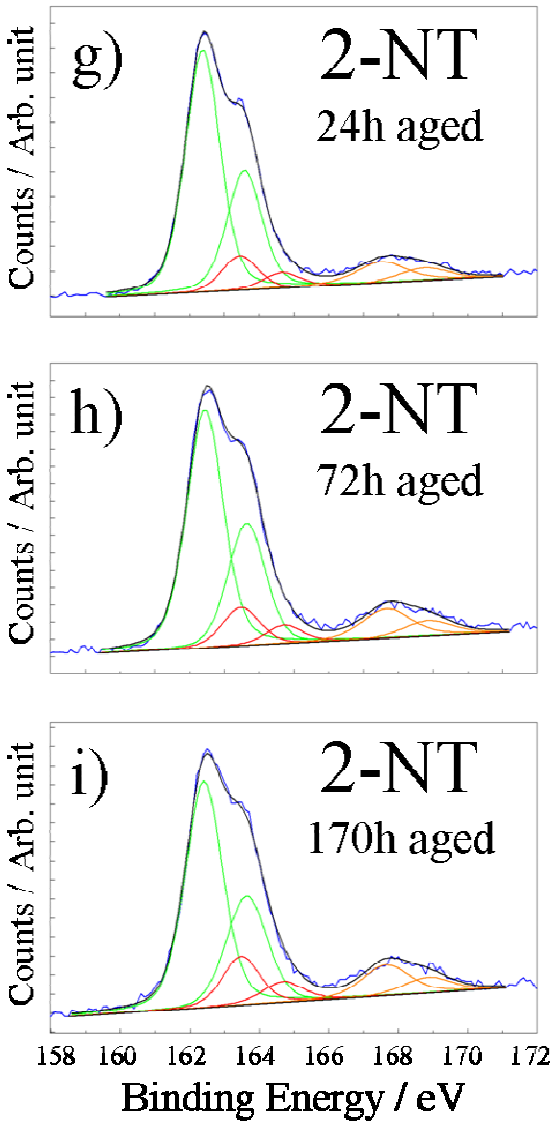

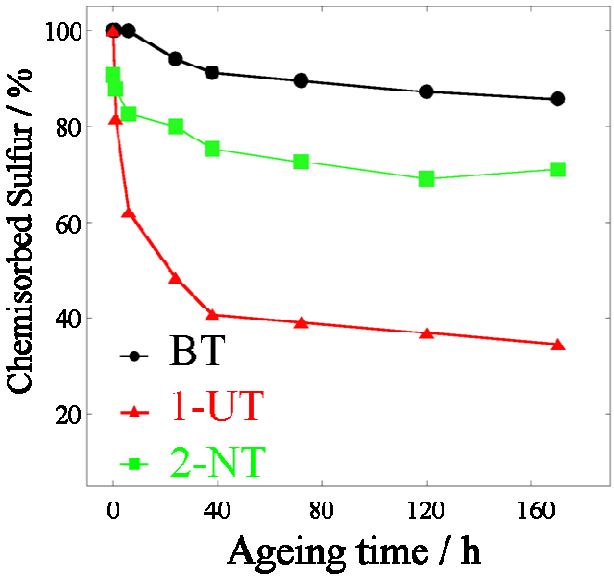

Figure 3.11: XP spectra of S2p region of: a), b) and c) BT; d), e) and f) 1-UT; g), h) and i) 2-NT, after different ageing time in aerated H_2SO_4 0.5 M. The fit component have been assigned to: —— chemisorbed thiol; —— disulphide; —— sulphonate; —— Cu_2S

Figure 3.12: Ratio between chemisorbed thiol and total sulfur as a function of the ageing time for various samples. Values were obtained from the best fit performed on S2p spectra.

The remaining signal was quite equally distributed between two minor doublets with maximum at 163.4 ± 0.1 eV (red line in the figure) and 167.7 ± 0.2 eV (yellow line in the figure), assigned to trace of disulfide (or free thiols) and sulfonates, respectively.

Although it appeared to be less stable than BT, 2-NT samples showed a good durability in the ageing condition as well. None experimental evidence that could be associated to the sharp performance decrease pointed out by EIS have been detected. The fits of the S2p peaks (Fig.3.11g, h, i) highlighted that, after 7 days, around the 70% of molecules were still covalently bonded to the surface, whereas the percentage of both disulfide (or free thiols) and sulfonates was roughly twice than that observed for BT (Fig. 3.12). 1-UT SAMs (Fig 3.11d, e, f), on the contrary, seemed to undergo serious damage after few hours of exposure to the acidic solution already. In fact after only 24 h ageing in H_2SO_4 the percentage of

chemisorbed thiol becomes less than 50 % and as low as 35 % after a week (Fig 3.12). Furthermore, in addition to the peaks ascribable to disulfide and sulfonate formation, which resulted to be more than the double compared with aged BT samples, a new large component, lying at 161.6 ± 0.1 eV (purple line in the figure), appeared in the S2p spectra relative to the aged 1-UT samples. This signal, indicative of the presence of Cu_2S on the surface[233], demonstrates that under these aggressive environments the S-C bonds in the alkylic SAMs are prone to breakage, whereas this does not happen in the aromatic layers. Moreover, the great intensity of this component suggested that, in these conditions, the cleavage of the S-C bond is the principal degradation way for alkylic SAMs.

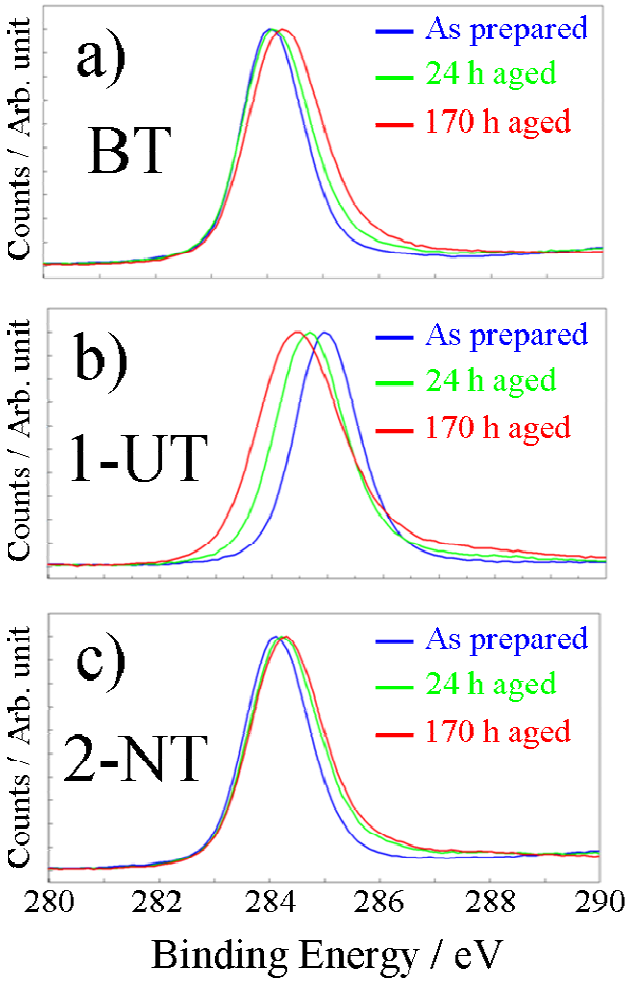

Figure 3.13: Superimposition of C1s XP spectra of: a) BT; b) 1-UT and c) 2-NT, after different ageing time.

Also the evolution of C1s spectra (Fig. 3.13) suggested a clear difference of stability between aromatic and alkylic thiols. The C1s peak of BT and 2-NT (Fig. 3.13a and c) samples appeared slightly enlarged toward higher binding energy, probably due to the adsorption of some impurities from the aerated ageing solution, as also suggested by the C/S ratio trend. Nevertheless the position of the backbone component remained almost unchanged for both the samples, indicating that no relevant changes in the aromatic rings configuration occurred. The reverse was true in the case of 1-UT (Fig 3.13b): in addition to the enlargement, another component appeared at lower binding energy with respect to the backbone signal, causing a shift of the peak maximum of about 0.5 – 0.6 eV. This behavior has been reported to be due to core-hole final state relaxation effects and is a typical

signature of the presence of large domains of alkane monolayers adsorbed with their axes oriented parallel to the metal surface[234-236] which, in our instance, is coherent with the formation of a huge amount of collapsed sites.

In figure 3.14a, b and c, the 650 – 1650 cm^{-1} region of Raman spectra relative to BT, 1-UT and 2-NT after different ageing time (spectra relative to as prepared samples have been included for comparison) is displayed. In this instance the 350 – 650 cm^{-1} region, including the broad feature due to the vibration of cuprous oxide, was cut of in order to highlight the more interesting signals arising from the grafted molecules. The temporal evolution of BT spectra (Fig. 3.14a) could not prove any specific changes both in the relative peak intensities and in the position for the bands at about 993, 1015, 1074 and 1574 cm^{-1} with aging. Conversely, a slight and progressive increase of oxide components on the copper surface was evident in the spectral range 400 – 650 cm^{-1} (data not shown). The constancy in the relative intensity could, however, indicate that the orientation of BT molecules with respect to the surface kept practically unchanged, although no direct information on the orientation of the chemisorbed molecules can be extracted from our spectra. Also in the case of 2-NT (Fig. 3.14c) no relevant changes in peak position were detected, whereas the broad feature in

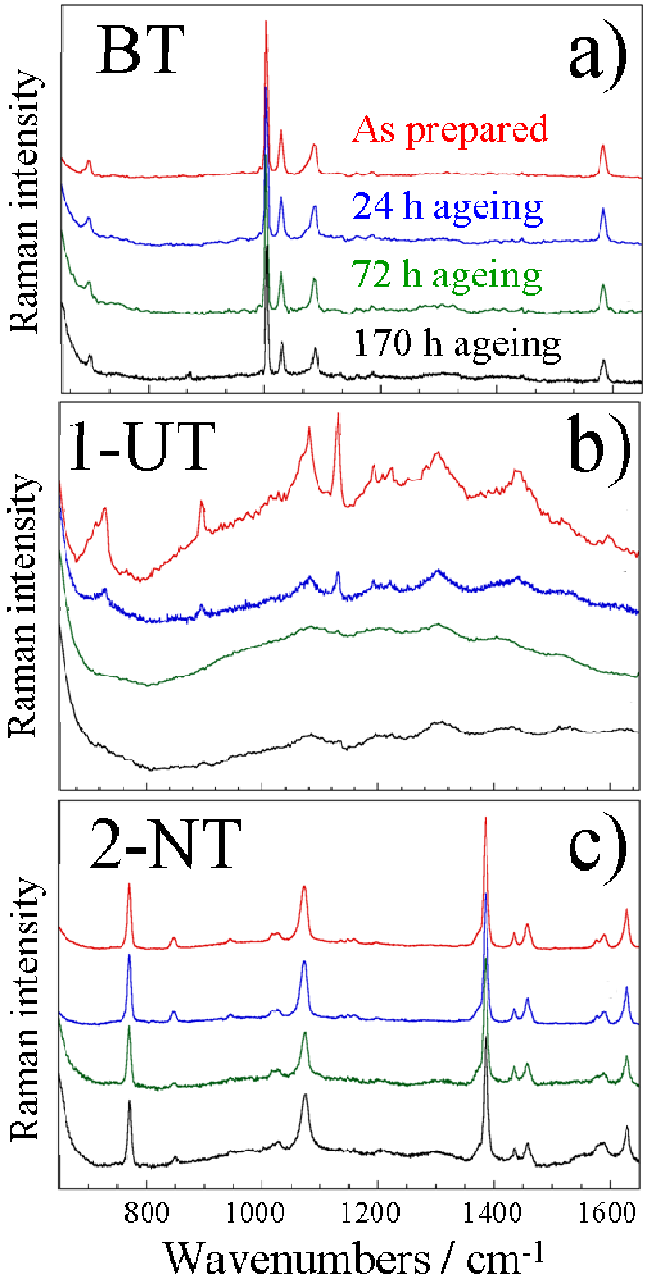

Figure 3.14: Raman spectra of: a) BT, b) 1-UT and c) 2-NT in the region 650 – 1650 cm^{-1} as a function of ageing time. Spectra are scaled and shifted for clarity.

the range 450-650 cm^{-1} (not shown) had a considerable increase in intensity indicating a higher copper surface oxidation during the air exposure. Even if the relative intensities of most of the various vibrational modes remained fairly constant with ageing time, some changes for long exposure to the acidic solution have been observed in the 1550 – 1650 cm^{-1} region. Changes in relative intensity of the 2-NT C=C ring stretching modes at 1567, 1580, and 1621 cm-1 have been used to assess the molecule orientation at the surface[223]. In fact the C=C stretching mode normal to the surface results in a band at about 1621 cm^{-1}, whereas a mode parallel to the surface gives a band at 1567 cm^{-1}. The decrease in intensity of the mode at about 1621 cm^{-1} observed after 72 h and 170 h ageing and the broadening of the bands suggested an evolution toward less ordered structures, with some molecule lying almost parallel to the surface. This behaviour could be the cause of the sudden falloff in the protective properties observed for this SAM. On the other hand, accordingly with all the other data, the evolution of the Raman spectra of 1-UT indicates a rapid degradation of this layer following the exposure to the acidic solution (Fig. 3.14b). The band at about 725 cm^{-1}, attributed to $\nu(C–S)_T$ vibration, strongly decreased in intensity with aging time of 24 h and became almost undetectable after 72 h. Also The sharp mode at about 895, 1065 and 1120 cm^{-1}, due to CH_2 rocking and C-C stretching vibrations, and at about 1375 and 1440 cm^{-1}, ascribed to C-H deformation modes, underwent a strong attenuation already after 24 h ageing. Overall, these findings suggest that the adsorption UT is labile, yielding structures becoming highly disordered after a short time, although the initial data revealed ordered structures.

Absolute Raman intensities are difficult to quantify, because of their dependence on experimental conditions. Nevertheless, keeping constant all the other parameters, it could be indicative of a higher order of the system. In a dedicated experiment, Raman spectra were recorded on small selected surface spot as function of ageing time, in order to avoid effect related to possible inhomogeneity of the samples. Comparing the spectra of as prepared BT and 2-NT SAMs with those relative to 24 h aged samples, a systematic increase in Raman absolute intensity was observed for both the samples (Fig. 3.15a and b), which has been considered as a consequence of a more regular surface morphology. It is worth noticing that

this interpretation is totally supported by the electrochemical response of 24 h aged aromatic layers

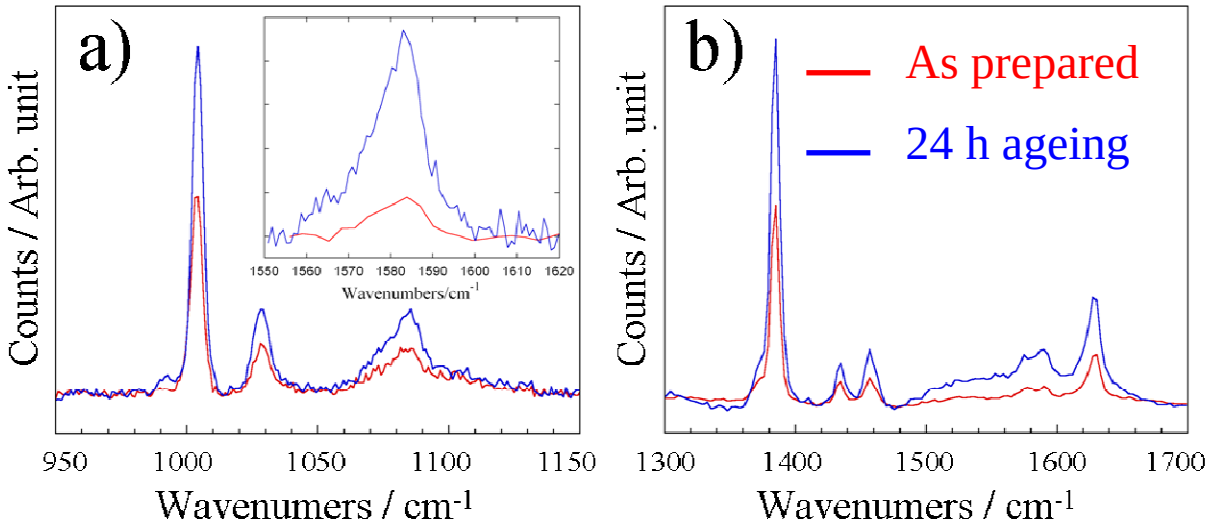

Figure 3.15: Raman spectra of: a) BT in the region 950 – 1150 cm-1 (1550 – 1620 cm-1 in the inset) and b) 2-NT in the region 1300 – 1700 cm-1 detected on the same sample spot as a function of aging time: —— freshly prepared sample; —— after 24 h ageing.

The effects of the dwelling process in H_2SO_4 on the wetting behaviour of the various samples are illustrated in Fig 3.16a and b. The 1-UT coated sample showed the minor changes and maintained its hydrophobicity, the ϑ_{adv} leveling off after 24 h at a value of 120°. The relatively small ϑ_{adv} and ϑ_{rec} decrease was assigned to the serious layer damage, partially compensated by the alkylic chain collapse on the copper surface, possibly induced by the adjacent polar water phase.

On the other hand, an unexpected dramatic increase of wettability has been recorded for BT sample, which, after an ageing period of 72 h, reached the lowest advancing contact angle (ϑ_{adv} ~ 60°) and a complete water wettability in the receding cycle (ϑ_{rec} = 0). An intermediate behavior was observed for the advancing results of 2-NT SAM and, as for BT, ϑ_{rec} = 0 after about 24 h. At a first glance, these data seem to contradict the inhibition property increase of aromatic SAMs and the highest BT stability, recorded in electrochemical and spectroscopic characterizations. As will be deeper discussed in the next section, the observed phenomena might be related to the different tendency of the chemisorbed molecules to interact with water. In fact it is well known that the aromatic

molecules, beside establish weak Van der Waals interaction, can act as a hydrogen bond acceptor for two water molecules, with their O-H bonds oriented toward the two faces of the aromatic ring[237]. The process could bring about the adsorption of water molecules on SAM surface and, thus, the overall sample wettability increase, although it is not possible to exclude other factors affecting the great variation of the recorded contact angles.

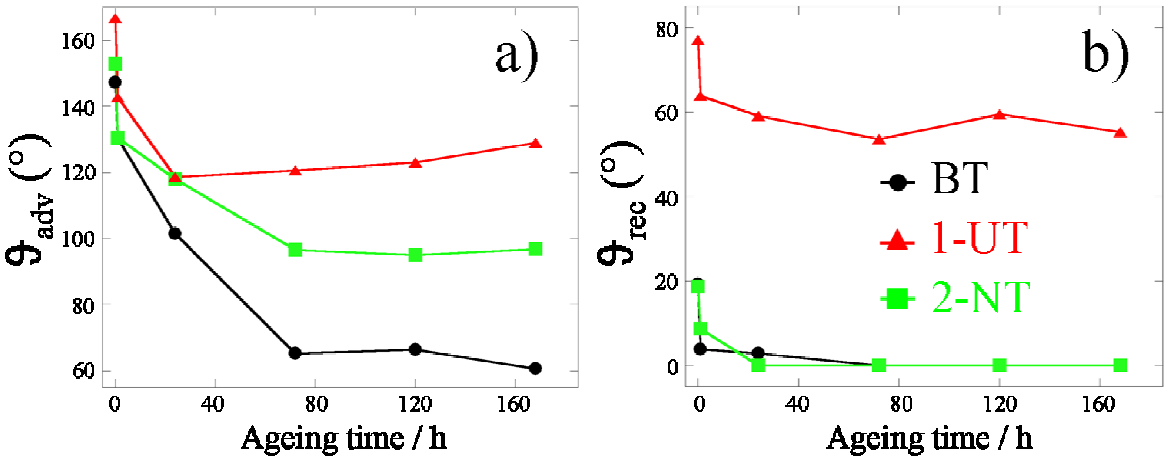

Figure 3.16: Evolution of: a) advancing contact angle and b) receding contact angle in ultra pure water as a function of the ageing time for various samples: —— BT, —— 1-UT, —— 2-NT

3.4 Discussion

The whole of information provided by the multi-technique approach adopted, allowed us to hypothesize the reasons of the surprising behaviour shown by the various SAMs with increasing ageing time. The two electrochemical techniques employed (EIS and linear polarization) have unambiguously demonstrated that the protective properties of Self-Assembled Monolayers constituted by aromatic thiols improved after exposure to acidic solutions, whereas 1-UT clearly degraded very rapidly. The accurate characterization of the as prepared samples excluded that this opposite trend could be ascribed to the poor quality of the alkylic layers. Our belief is that the dwelling of SAMs in acidic aqueous solution can lead to a reorientation of the adsorbed aromatic molecules in a sort of ordering process. The increased intensity of the Raman bands of the BT and 2-NT aged for 24 h suggests the

protection enhancement to be actually related to a reorganization of the layer structure. This hypothesis is also indirectly supported by the trend of some EIS parameters. In particular, the negative shift of the corrosion potential implies a higher overpotential in the cathodic corrosion reaction, *i.e.* the organic monolayer becomes gradually more effective in slowing down oxygen diffusion towards the metal surface. This is coherent with an enhancement in the structural order of the aromatic layers during the first hours of ageing. The remarkably different permeability to the electrolyte deduced by the capacitance trend, instead, is a possible reason for the different oxidation rates of the thiolic function to disulfide or sulfonate, which could be due to the dissolved oxygen and/or to some aggressive intermediate of corrosion reaction[238]. XPS data, and in particular the results of the curve-fitting performed on the S2p spectra, also highlighted that the degradation of alkylic SAMs is partially related to the breakage of the S-C bond. This phenomenon, which we never observed with BT and 2-NT monolayers, is consistent with the significant difference in the S-C bond strength between alkylic and aromatic thiols[186,187] already discussed in paragraph 1.4. It is worthwhile to note that the great number of damaged molecules and collapsed sites in aged 1-UT samples deduced by XP spectra is in very good agreement with electrochemical and Raman data, highlighting a dramatic loss in protective properties and structural order.

The sequence of DCA data taken at different ageing times highlighted an unexpected increase in the wettability of the aromatic SAMs, especially for BT. This result suggested us a direct role of water molecules in the reorganization process. In fact, although water and benzene are immiscible, the existence of relatively strong interaction between water and conjugated systems, which can lead even to the formation of molecular cluster[239], has been exhaustively demonstrated both theoretically[240-242] and experimentally[243,244]. The electronic binding energy between a benzene ring and a water molecule was estimated to be -3.9 kcal/mol, only 20% weaker than the water-water interaction energy[245]. Moreover, Monte Carlo simulations on liquid water-benzene system have shown that the interfacial benzene molecules lie parallel to the plane of the interface and that the interfacial water molecules are preferentially perpendicular to the interface, one of the O-H bonds pointing towards the apolar phase[246]. π-hydrogen bonding complexes were also observed when adsorbed benzene

in single-wall carbon nanohorn was exposed to water vapor or liquid. It was found that the benzene-water complex takes a stable form in high water vapor pressure condition and that the desorption process can be accomplished only at high temperature[247]. Furthermore π-hydrogen interactions were also observed between ethylene, acetylene or benzene, and ice surfaces[248], where the mobility of water molecules is dramatically limited. Also in ours aromatic monolayer the orientational degree of freedom of the aromatic ring is drastically hampered by the bond with the copper substrate. Nevertheless, during the dwelling in acidic solution, the residual mobility could promote a small but significant molecule reorientation or surface rearrangement induced by optimization of the benzene ring/water interactions.

Therefore, in our model, solvent molecules can play a double role in the surface process, depending on their ability to interact with the different monolayers. In the case of 1-UT the water molecules are not able to interact with the layer molecules but can penetrate through the defects speeding up the corrosion process and causing further damage to the protective coating (oxidation of the thiolic function, breakage of S-Cu or S-C bond), promoting in this way the penetration of further electrolyte. In the case of BT and 2-NT, on the contrary, most of the solvent molecules would interact with the aromatic rings without diffusing to the copper surface, allowing the SAM to heal its collapsed sites and to keep an ordered structure for a longer time. This reduction of the number of the defects, together with the higher strength of S-C bond, would considerably slow down the deterioration process, explaining the remarkable durability of these systems and in particular of BT. The lower effectiveness and durability of 2-NT respect of the thinner BT is probably related to the presence of small amount of sulfonate and physisorbed materials already in the freshly prepared samples, as detected by XPS, which could facilitate the formation of pinholes defects affecting the performance and the stability of the protective layer. Nevertheless, considering the relatively large size of 2-NT molecules and its rigid structure the hypothesis of a slight deficiency in the surface coverage, slight enough to be undetectable by S/Cu atomic ratio, cannot be definitively excluded.

Chapter 4: effect of different p-substituent groups on long-term performance of aromatic thiols as Cu corrosion inhibitors

4.1 Brief introduction to the chapter

As demonstrated in the previous chapter, Self-Assembled Monolayers constituted of simple aromatic thiols have, in strongly acidic environments, noticeable efficiency and exceptional durability as copper corrosion inhibitors with respect to n-alkanethiolate SAMs. Their excellent performances are due to a surprising enhancement in their charge-transfer resistance recorded during the first 24 h of exposure to the electrolytic solution, probably related to an ordering process driven by a direct interaction between the solvent molecules and the aromatic rings. The finding of this interesting behaviour opened new perspectives and raised several questions about these systems. Among many others, the effect provided by the presence of different substituent groups on the performance and the stability of the organic films represents an interesting issue. In order to answer this question SAMs constituted by several p-substituted (-F, -CH_3, -OH, -COOH, -$NHCOCH_3$) aromatic thiols have been prepared and characterized, while their protective properties and their stability up to a week in H_2SO_4 0.5 M have been checked both electrochemically and spectroscopically. The various thiols were chosen in order to relate the obtained results with several parameters directly arising from the molecular structure: the hydrophobicity of the tail group, the possibility to establish intermolecular hydrogen bond and the different polar (or electronic) effects of the substituents on the conjugated ring (electron withdrawing or electron donating groups). Toward that aim EIS and XPS were systematically performed both on freshly prepared and on aged samples with different immersion time in the acidic solution, whereas DCA measurements was used to assessed the hydrophobicity of the as prepared samples.

4.2 Characterization of freshly prepared samples

XP spectroscopy and DCA measurements allowed us to demonstrate that the adsorption of the various aromatic thiols on polycrystalline copper surface was actually successfully achieved and to certify the good quality of the obtained monolayers. Table II reports the average values of quantitative atomic ratio calculated for the freshly prepared samples.

	C/S	S/Cu	O/S	N/S	F/S
AA	7.7 (8)	0.62	1.20 (1)	1.12 (1)	/
FBT	5.5 (6)	0.47	0.06	/	1.66 (1)
MBT	7.3 (7)	0.44	0.10	/	/
MF	5.8 (6)	0.49	1.39 (1)	/	/
MBA	7.5 (7)	0.47	2.50 (2)	/	/

Table II: Average values of XPS atomic ratios for various as prepared samples. Theoretical values, where available, are reported in brackets

The S/Cu ratio values are indicative of a good surface coverage for all the samples[212]. The AA layer showed slightly higher values with respect to the other molecules; nevertheless considering the experimental error on the quantitative analysis (10 % – 15 %) is hard to say if this is indicative of an actual higher surface coverage. Furthermore, this effect could be at least partially ascribed to the larger thickness of this layer. Also the analysis of the CuLMM Auger spectra (Fig. 4.1) suggested a complete coverage of the copper substrate for all the samples, as highlighted by the high ratio between the Cu(I)-S peak at 916.1 ±

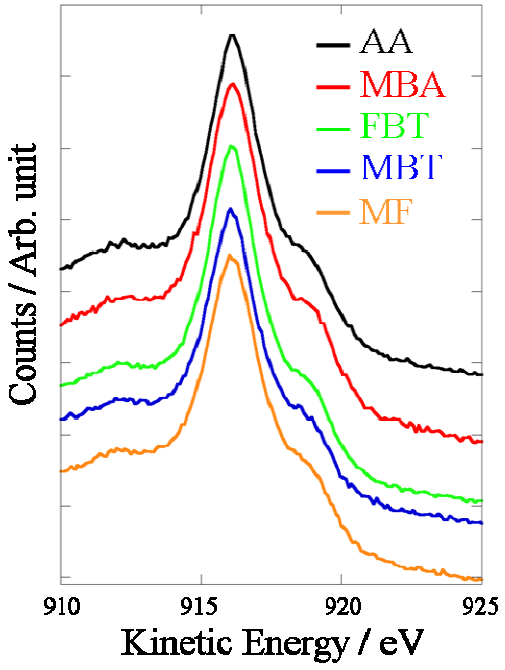

Figure 4.1: Auger CuLMM spectra relative to as prepared samples of: —— AA; —— FBT; —— MBA; —— MBT; —— MF.

0.1 eV[163] and the little shoulder ascribable to the bulk atoms lying at 918.7 ± 0.1 eV[164,216]. In this instance no appreciable differences between the various molecules have been observed.

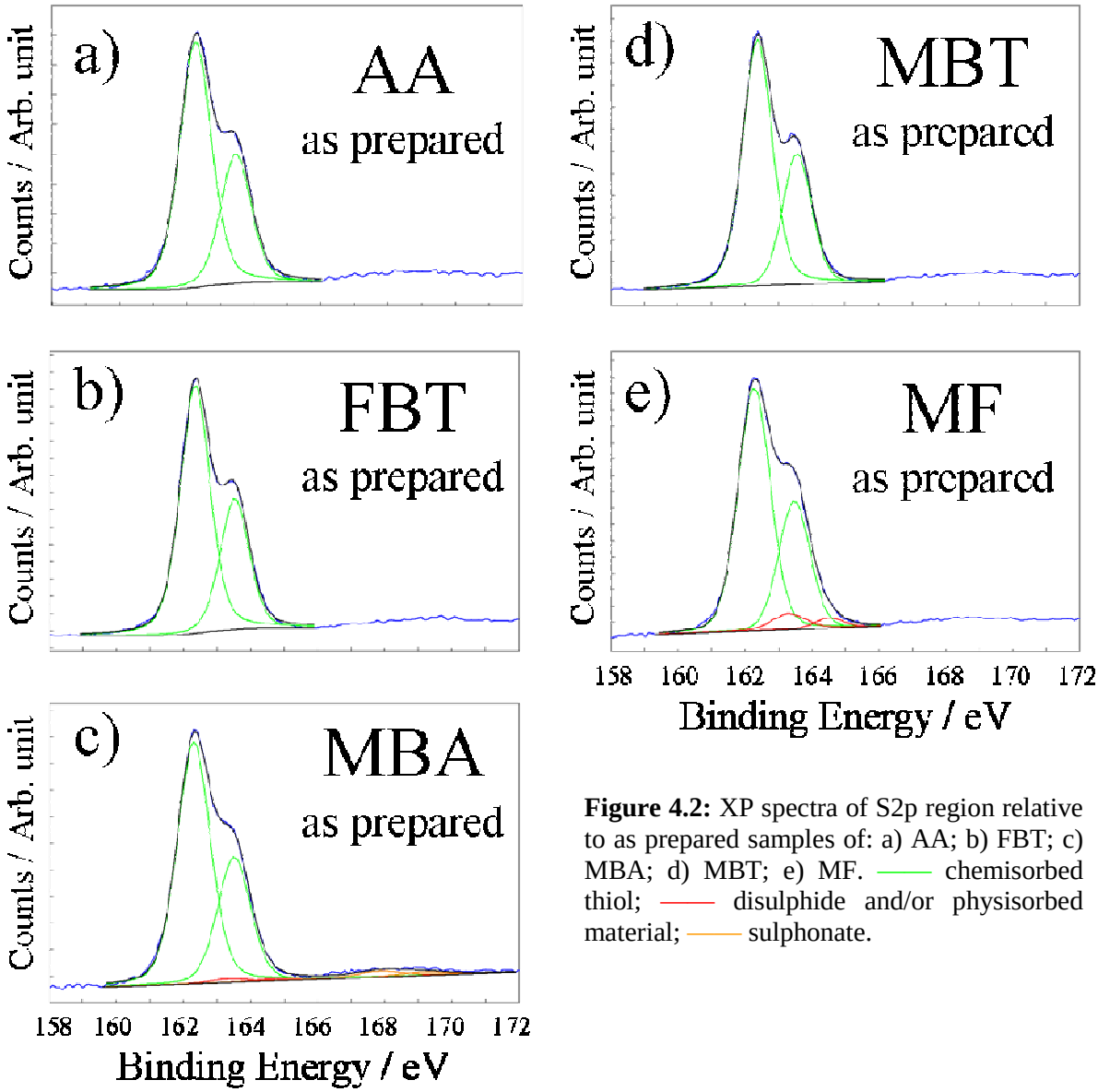

Figure 4.2: XP spectra of S2p region relative to as prepared samples of: a) AA; b) FBT; c) MBA; d) MBT; e) MF. —— chemisorbed thiol; —— disulphide and/or physisorbed material; —— sulphonate.

In figure 4.2a-e the best fits performed on the S2p spectra recorded on the various freshly prepared samples are reported. All the spectra showed a main doublet centered at 162.35 ± 0.1 eV, demonstrating that the various molecules preferentially linked the substrate through the formation of a covalent S-Cu bond[34,73,133,163,164]. The fit carried out on the MF samples revealed the presence of a little signal lying at 163.4 ± 0.1 eV (red line in the figure), attributed to a small fraction of free thiols, whereas in the case of MBA also traces of

sulfonates (167.7 ± 0.2 eV, yellow line in the figure) have been detected. The presence of some molecules not covalently chemisorbed to the copper surface as thiolate is probably related to the nature of the terminal group of MF and MBA which, having a certain affinity for the substrate, could compete with the thiolic function for the binding sites. Coherently, the spectra of FBT and MBT, whose terminal group could not covalently bind copper, showed only the component relative to the chemisorbed thiolate. The same behaviour was found in AA where the nitrogen atom of the amido group, a potential ligand for the surface, was buried too deep in the terminal chain to easily bind the copper. Nevertheless, should be noted that also for MF and MBA the component relative to the chemisorbed thiolate represent more than 95 % of the total sulfur.

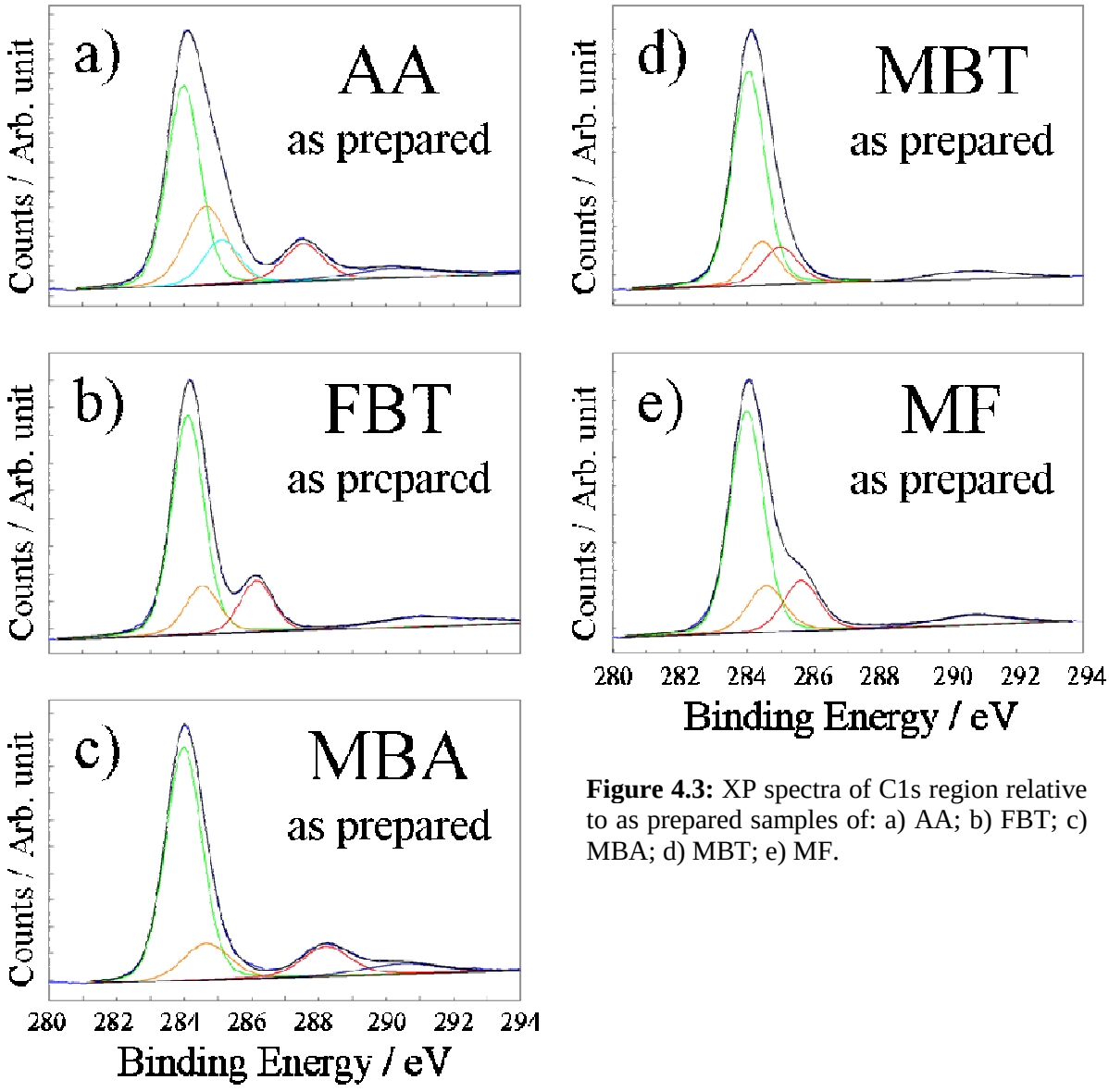

Figure 4.3: XP spectra of C1s region relative to as prepared samples of: a) AA; b) FBT; c) MBA; d) MBT; e) MF.

Another clear clue of the good quality of the prepared SAMs arose from the analysis of the C1s region. First of all, as reported in Table II, values of the C/S ratio are in very good agreement with the theoretical values (reported in brackets in the table) suggesting the absence of significant amount of contaminants. The cleanliness of the obtained SAMs was confirmed by the fit performed on C1s peaks relative to the various freshly prepared samples (Fig. 4.3a-e). As expected, all the molecules showed a main signal at 284.1 ± 0.1 eV (green line), due to the aromatic backbone [69,105], and a minor component at 284.6 ± 0.2 eV (yellow line), assigned to the carbon atom bonded to the thiolic function (in the case of AA also the carbon bonded to the amidic nitrogen fell at the same energy). The other signals lying at higher binding energies arose from the carbons belonging to the different substituents groups. Accordingly with literature reports, the signals at 287.6 ± 0.1 eV in AA spectra and 288.2 ± 0.1 eV in MBA spectra have been assigned to the amidic[249,250] and to the carboxylic[69,251] carbon respectively, whereas the peaks related to C-F in FBT and to C-OH in MF have been found at 286.2 ± 0.1 eV and 285.6 ± 0.1 eV[69,251]. The component at 285.0 ± 0.1 eV detected in AA and MBT, instead, was assigned to the alkylic terminal carbon[210,211]. Finally, the broad feature appearing at around 290.5 eV was ascribed to a well known shake-up process, due to a $\pi \rightarrow \pi^*$ transition in the aromatic ring[252,253]. It should be noted that in all the spectra the ratios between the various components exactly respect the molecular stoichiometry, demonstrating not only the absence of impurities but also that the thiols did not undergo significant chemical modification during the adsorption process. This was also suggested by the values of O/S, F/S and N/S atomic ratio, resulting in quite good agreement with the theoretical values (See Table II). In this instance, the small positive deviations from the theoretical values (quite marked for FBT SAMs) are probably related to the attenuation of the S2p signal by the overlying phenyl ring.

The conservation of the molecular structure was further confirmed by the positions of the characteristic peaks of the different tail groups. The analysis of the N1s region of AA (not shown) spectra revealed the presence of a single peak at 399.6 ± 0.1 eV, consistent with amidic nitrogen[249,254], whereas the study of the O1s region (Fig. 4.4a) revealed the presence of a large component at 531.1 ± 0.1 eV, related to the carbonyl oxygen[254,255], slightly enlarged at higher binding energy by a little signal (~ 3 % of the total oxygen) ascribable to

some kind of impurities. Equally, the single signal detected at 686.6 ± 0.1 eV for FBT samples (not shown) was attributed to the fluorine atom bonded to the ring[72]. Accordingly with the S2p spectra, the deconvolution of the O1s signal of MF adlayers (Fig 4.4b) gave rise to two distinct components. The main one, centered at 532.8 ± 0.1 eV, is characteristic of an unbound phenolic -OH group[69,251] whereas the shoulder at 531.1 ± 0.1 eV may be associated with phenoxides covalently bonded to the copper surface[256,257] and/or to the growth of cuprous sub-oxides[218,258]. The fit revealed that this minor component represents around 8 % of the total oxygen which, considering also the possible contribution of the sub-oxides, is in very good agreement with the results previously extracted by the S2p spectra. MBA layers showed a more complex O1s spectrum: the two large and almost equivalent components lying at 531.2 ± 0.1 eV and 532.9 ± 0.1 eV have been assigned to the carbonyl and the hydroxyl oxygen of the tail group, respectively[69,251,259]. Accordingly with what reported by Abelev *et al*[213], instead, the small component (~ 6 % of the total peak area) at 532.1 ± 0.1 eV was ascribed to some carboxylic groups adsorbed on the surface with a bridging bidentate coordination. Finally, the signal appearing at 534.1 ± 0.2 eV suggested the presence of some esteric oxygen atoms at the surface[260,261]. This is probably due to a collateral reaction of the carboxylic group with the ethanol of the adsorption solution. Anyway this component contributed only for less than 5 % on the total O1s peaks, confirming that also MBA molecules kept their structure essentially unchanged following

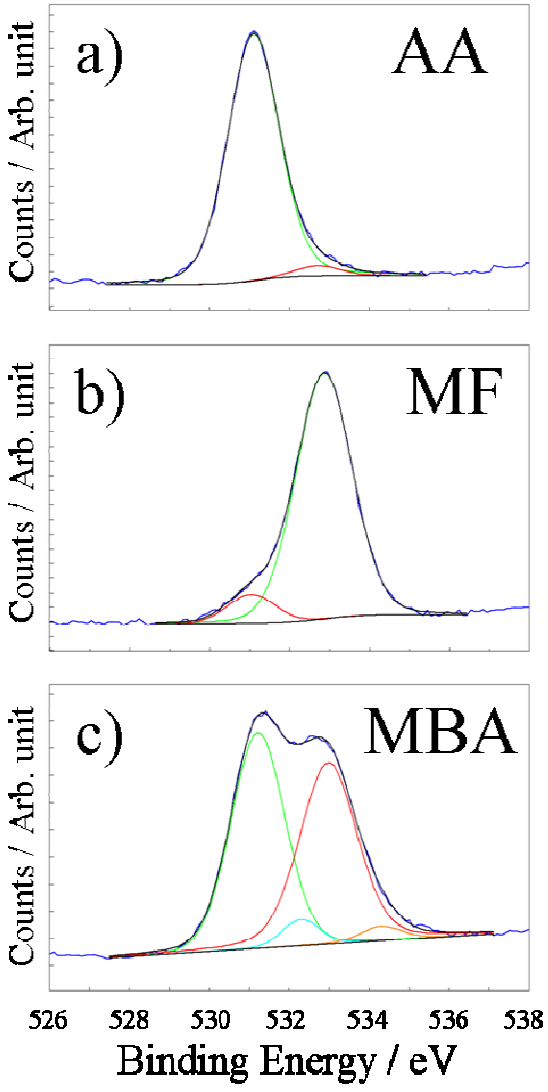

Figure 4.4: XP spectra of O1s region relative to as prepared samples of: a) AA; b) MF; c) MBA.

the adsorption process. It is worth noticing that the amount of oxygen detected in FBT and MBT samples is extremely low, indicating the almost complete displacement of the cuprous oxide from the surface during the films growth. Furthermore, a significative competitive adsorption of the solvent can be excluded.

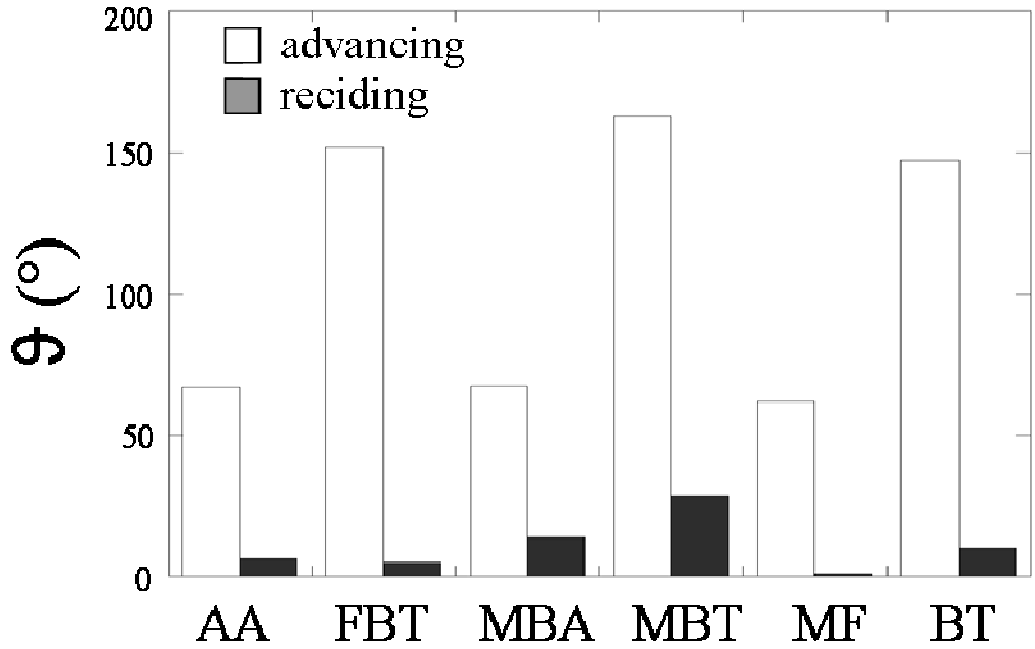

Figure 4.5: Average values obtained for advancing (white) and receding (grey) contact angle of as prepared samples. BT values were added for comparison.

The average values of advancing and receding contact angles recorded on the different freshly prepared samples are reported in figure 4.5 (values relative to BT were added for comparison). The clear differences in the advancing contact angles of the various overlayers are easily referable to the hydrophobic or hydrophilic character of the respective terminal groups. Hence FBT and MBT, having a highly hydrophobic functionality exposed, showed a very high θ_{adv}, even slightly higher than that of BT. AA, MBA and MBT, on the contrary, all exhibited advancing angles close to 65°, coherently with their wettable tail groups. It is interesting to note that the receding angles are considerably less influenced by the nature of the substituent than the advancing angles. In fact, they kept very low values (included between 0° and 13°) for all the SAMs, with the little exception of MBT which showed

slightly higher hydrophobic character. This suggests the underlying copper to have a marked influence on the θ_{rec} associated to thin aromatic SAMs.

Literature reports allowing a direct comparison with our results (same systems and similar experimental setup) were not available. On the other hand, measurements performed on the same thiols but carried out in different way and/or on different substrate showed significant deviation from our data. For example Tan *et al.*[72], measuring the wettability of aromatic layers on copper by drop shape contact angle method, did not detect marked differences between BT, FBT and AA. Barriet and coworkers, instead, studying the adsorption of different simple aromatic thiols on gold found MBA SAMs to be markedly more wettable than MF[69]. Anyway, the θ_{adv} values we obtained appeared more coherent with the various molecular structures. Again, the noticeable hysteresis observed was attributed to the surface roughness, as discussed in the previous chapter.

4.3 Ageing in aerated H_2SO_4 0.5 M

4.3.1 Electrochemical characterization

Similarly to what seen in the previous chapter, EIS was employed to estimate the integrity and the ability of the various films to protect the underlying copper. Again, the measurements were repeatedly performed on the same samples after different exposure periods to the electrolyte solution, allowing us to follow the evolution of the SAMs properties as a function of the ageing time. The equivalent circuit adopted to model our systems and to extract the EIS parameters has been already described in section 3.3.3.

The impedance spectra recorded for the various thiols at different ageing times and the corresponding average ($n \geq 3$) trend of the EIS parameters (R_{tot}, OCP, CPE_{SAM}) are collected in figures 4.6a-e and 4.7a-d respectively. In the latter case, the data relative to BT layers were added for comparison. The displayed results highlight notable differences in the electrochemical behaviour with changing the terminal group. The highly hydrophobic FBT

clearly showed at t = 0 the higher overall resistance and the lower film capacitance (R_{tot} = 5.5 ± 1.4 kΩcm^2; CPE_{SAM} Y_0 = 4.55 ± 1.05 μSs^{n}cm^{-2}). Nevertheless, contrarily to what reported by Tan *et al.*, the initial resistance values did not exactly follow the hydrophobicity degree of the molecules, although this had certainly a considerable effect.

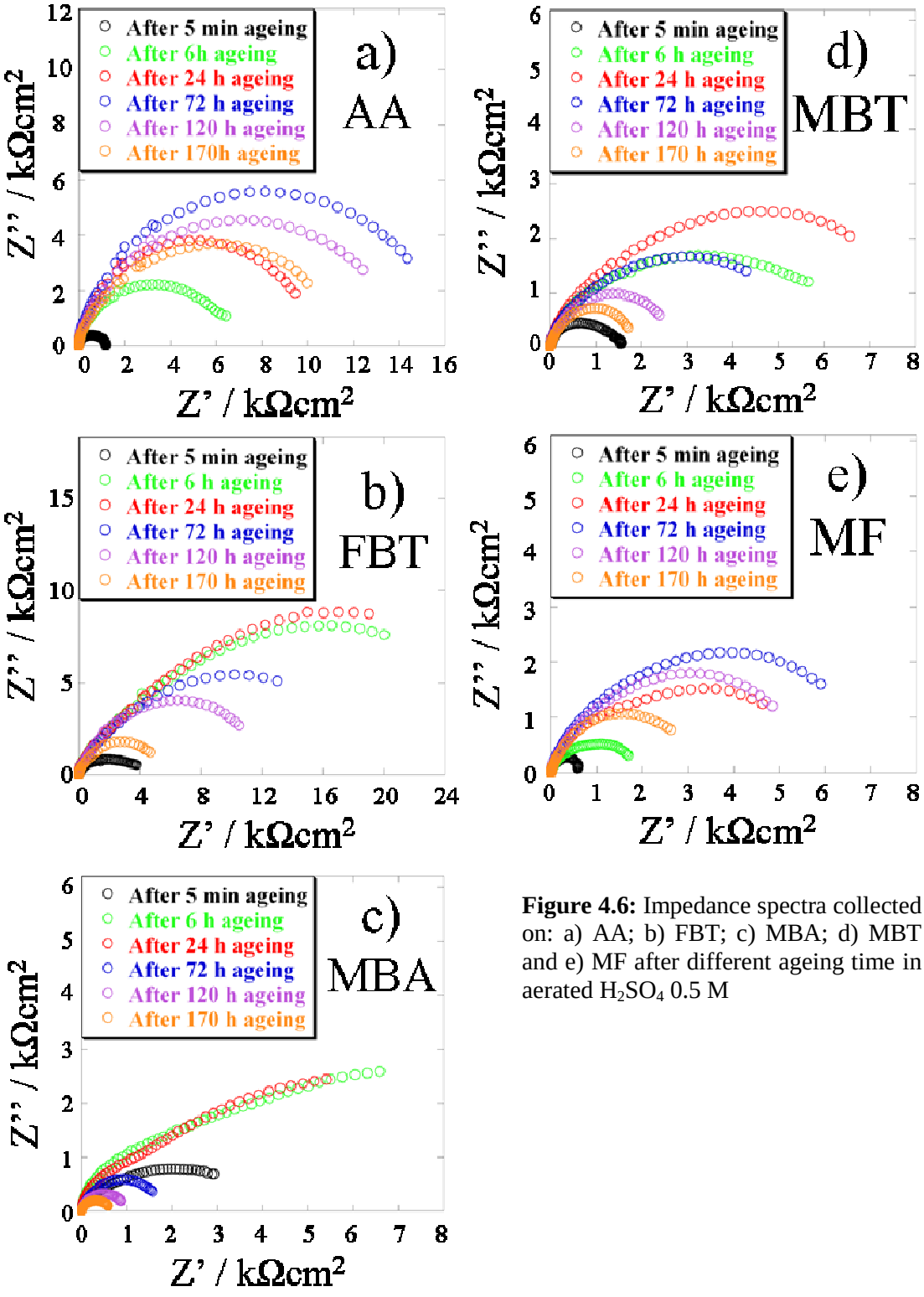

Figure 4.6: Impedance spectra collected on: a) AA; b) FBT; c) MBA; d) MBT and e) MF after different ageing time in aerated H_2SO_4 0.5 M

In fact, in spite of its hydrophilic character, freshly prepared MBA adlayers showed a charge transfer resistance of 3.58 ± 1.0 $k\Omega cm^2$, *i.e.* almost the double with respect to BT samples. Furthermore, these samples exhibited a relatively low capacitive value (CPE_{SAM} Y_0 = 21.7 ± 6.3 $\mu Ss^n cm^{-2}$), especially if compared with that recorded with that of MF films which was expected to be similar. Such data might be in part due to the partial esterification of the carboxylic group highlighted by XPS measurements. However, considering that less than 10 % of the adsorbed molecules reacted with the solvent, the MBA parameters should be considered symptomatic of a closed packed and highly ordered arrangement, plausibly related to the formation of lateral hydrogen bond. On the contrary freshly prepared MBT SAMs showed an unexpected low value of R_{tot} (1.32 ± 0.20 $k\Omega cm^2$), notwithstanding the highly hydrophobic character ascertained by DCA experiments. This is in net contrast with the results of Tan *et al.*, which reported the charge transfer resistance of MBT layers to be more than the double than that of BT, whereas in our case it resulted clearly lower. Furthermore the average value of the frequency independent element Y_0 associated with MBT layers (9.0 ± 1.8 $\mu Ss^n cm^{-2}$) was practically the same observed for BT whereas, considering the presence of the terminal methyl group, it was expected to be slightly lower. This data suggested a relatively poor structural order, which could also explain the low protective properties exhibited by these samples. However, even if it was undetectable by XPS measurements, a very little deficiency in the surface coverage for this SAMs (*i. e.* the presence of some pinholes defects) can not be definitively excluded. The parameters related to freshly prepared AA and MF, instead, showed that these molecules are not able to take advantage from intermolecular hydrogen bond as much as MBA. Anyway, the two layers exhibited markedly different properties. Taking BT values as reference, the relatively low resistance (1.43 ± 0.16 $k\Omega cm^2$) and large capacitance (30 ± 9 $\mu Ss^n cm^{-2}$) of AA could be ascribed to the higher hydrophilicity and polarizability of the molecules constituting the SAM, but are still indicative of the good quality of the layer. On the contrary, the values associated with MF (0.58 ± 0.21 $k\Omega cm^2$ and 246 ± 54 $\mu Ss^n cm^{-2}$) strongly suggest this adlayer to be highly defective and poorly defined.

Analyzing the temporal evolution of the EIS parameters it can be noted that all the layers during the first stage of ageing process experienced the enhancement of protective properties

and the sharp reduction of the OCP already observed for BT samples. Therefore, presumptively, a similar structural reorganization occurred. However, the effectiveness and the rate of this reorganization are strongly affected by the different p-substituent of the ring. The changes of R_{tot} values, displayed in figure 4.7a, followed qualitatively three different trends. Interestingly, the trend followed by a certain SAMs seems to be more related to the polar effect of its tail group than to its hydrophobicity or to the presence of intermolecular hydrogen bond. For example FBT and MBA, both containing an electron withdrawing tail group, reacted in a very similar way to the exposure to the electrolyte, even if they showed very different parameters values. Both these samples, in fact, made record a very fast improvement of their protective properties, reaching the top of their performance already after around 6 h of exposure to the acidic solution. FBT samples, in particular, showed after this ageing time an impressive inhibition efficiency, being its R_{tot} (35.0 ± 6.7 $k\Omega cm^2$) more than the double in respect to that exhibited by 1-UT freshly prepared samples (See previous chapter). Because of its hydrophilic terminal group, the best performance of MBA showed, as expected, clearly lower maximum values (14.5 ± 4.4 $k\Omega cm^2$). It should be noted, however, that this value is practically the same obtained for BT at the same ageing time and is very close to BT best performance, in spite of the higher wettability of MBA. Nevertheless, although these adlayers experienced a very fast and effective reorganization, both exhibited a relatively low stability. After the initial remarkable growth, in fact, the overall charge transfer resistance of FBT SAMs decreased linearly, similarly to what observed for BT but with a considerably larger slope. Thus, after 96 h ageing its protective properties became lower than that of AA and after a week went down to the BT level, while maintaining better performance than the freshly prepared samples. MBA, despite the lateral interaction, revealed to be even less stable showing a dramatic drop of R_{tot} already after 72 h ageing, so that its long-term performance resulted worst than all the other samples. In addition it was the only sample whose R_{tot}, during the ageing period, went down under the initial value. The trends of the others EIS parameters traced out quite well the resistive one. As can be appreciate in the enlargement in figure 4.7d, both FBT and MBA showed, during the first hour ageing, the more pronounced drop of the rest potential among the other molecules.

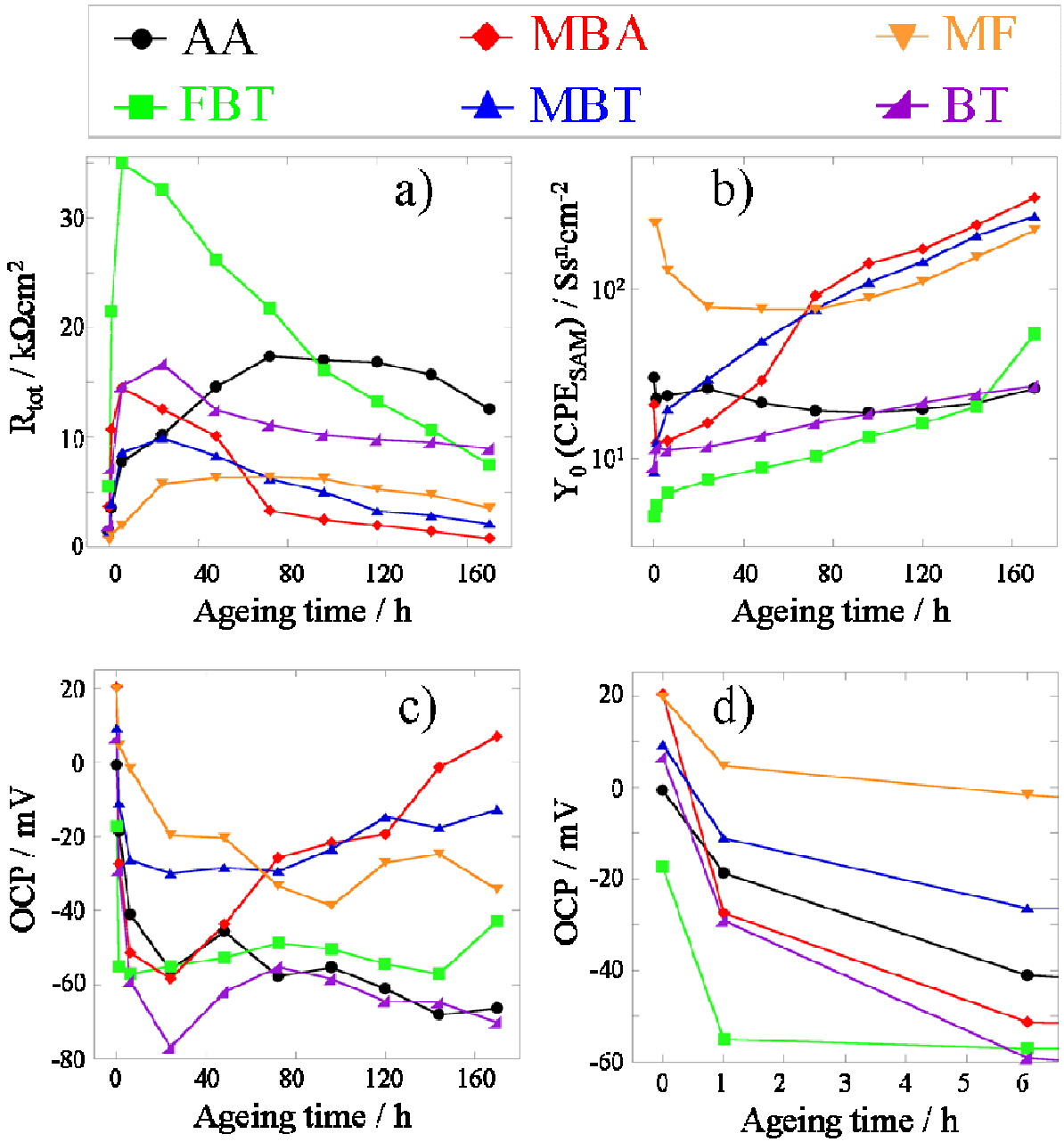

Figure 4.7: average trend (n≥3) of the parameters extracted from the EIS measurements as a function of the ageing time. A maximum error of 25% was found

Also the capacitance values confirmed the initial rapid improvement of the layer structure, showing even a noticeable decrease for MBA during the first hour of exposure to the acid (Fig 4.7b). After 72 h, in correspondence to the drop of R_{tot}, MBA samples made record a marked increase of both OCP and capacitance, confirming the breakdown of the ordered structure of the monolayer. FBT, on the other hand, was able to keep a quite low OCP whereas its capacitance increased constantly and linearly, with a slope slightly larger in respect to BT. This indicates that, despite the progressive formation of defects was relatively

fast, this layer conserved a good structural organization during the exposure to H_2SO_4, even if the sudden steep rise of both the parameters after 170 h ageing seems to anticipate an imminent collapse of the SAM.

Compared to FBT and MBA, SAMs having an electron donating terminal group, *i. e.* AA and MF, showed a total different response to the exposure to the acidic solution. In fact, while the presence of the fluorine atom or the carboxylic group in para to the thiolic function caused a very rapid enhancement in the protective properties following the exposure to the electrolyte, the presence of the amidic and hydroxylic groups led to a slower but more durable structural reorganization. In fact, as highlighted in figure 4.7a, the increase in R_{tot} values in this case occurred with a relative low rate, leading to the achievement of the best performance after 72 h – 96 h of ageing. Subsequently the samples underwent a slight and constant loss of inhibition efficiency but, at the end of the week of ageing, still showed resistance values higher by almost and order of magnitude than the initial ones. AA layers, in particular, starting by the fourth day of exposure to the electrolyte constantly displayed the best protective properties, with R_{tot} values almost double than BT. Although it did not reach such performances also MF, despite it was initially poorly defined, denoted a remarkable durability. In fact, from the third day of ageing, it overcame by far the inhibition efficiency of MBA and MBT. The OCP evolution (Fig. 4.7c-d) of AA and MF faithfully reproduced their resistive trend, with the potential value decreasing relatively slowly until to a final value of ~ – 60 mV and ~ – 35 mV respectively. It should be noted that already for freshly prepared samples AA exhibited corrosion potential considerably lower than MF (See Fig. 4.7d). The marked difference in the OCP values seems to reflect the difference of effectiveness between the two layers, which is mainly ascribable to their molecular structure. In this instance no increases which could indicate an imminent breakdown of the layers have been observed. Also the trends of the frequency independent parameter Y_0 associated with CPE_{SAM} suggested AA and MF to experience an effective and durable structural reorganization (Fig 4.7b). Both the samples during the first 72 h – 96 h of ageing showed a noticeable decrease in the capacitance value, attributed to an improvement in the packing arrangement. This was particularly true for MF which, exhibiting initially a quite disordered structure, made record a clear drop in the capacitance value (from ~ 246 $\mu Ss^n cm^{-2}$ of the as

prepared samples, to ~ 75 $\mu Ss^n cm^{-2}$ after 96 h ageing), so that after 72 h it resulted constantly lower than those of MBA and MBT. Moreover, should be noted that AA and MF were the only samples whose capacitance, after a week of ageing, resulted lower than the respective initial values. Despite its larger polarizability, after 5 – 6 days the AA capacitance value was even lower than that of BT and FBT. This feature confirmed the exceptional durability of these SAMs.

Finally, as highlighted in figure 4.7a, MBT layers showed an intermediate behaviour, reaching the maximum performance after around 24 h, similarly to BT. Again, can be mainly ascribed to the polar effect of its tail group. In fact, although the methyl group is generally considered an electron donating group, the absence of a lone pair to share with the aromatic ring limits this behaviour to a little inductive effect, making it weaker compared to that of hydroxylic or amidic functionalities. Nevertheless, despite its highly hydrophobic character, this SAMs continued to exhibit relatively disappointing protective properties. In fact, even if a noteworthy increase in the inhibition efficiency occurred, the maximum value of R_{tot} resulted just over half than that obtained for BT, and lower than all the other SAMs with the little exception of the highly hydrophilic MF. After the first 24 h of immersion, MBT resistance decreased linearly, without indicate sudden breakdown of the layer but denoting a progressive and relatively fast formation of defects. Anyway, at the end of the ageing time, it was still almost the double than the initial value. The trends of the others EIS parameters confirmed that of the resistance: OCP decreased quite rapidly to a relative high value (~ -30 mV) and then slightly increased whereas the capacitance of the layer raised constantly and rapidly overcoming already after 72 h that of MF. On the whole, these data suggested MBT layers to be relatively poor protective and rather permeable to the electrolyte.

4.3.2 Spectroscopic characterization[1]

As in the previous chapter, XPS was systematically applied also on aged samples in order to assess the chemical stability of the layers as a function of the ageing time. First of all the quantitative analysis, and in particular the evolution of the S/Cu ratio (Fig 4.8a), clearly demonstrated that none of the molecules desorbed from the surface in a significant extent during the ageing process. Also in this case the slight increasing trend observed has been attributed to an attenuation of the $Cu2p_{3/2}$ signal caused by the adsorption of some contaminants, as also suggested by the C/S ratio trend (Fig 4.8b). Both the quantitative trends suggested FBT layers to be more prone to the adsorption of such impurities with respect to the other samples. The evolution of O/S atomic ratios denoted some meaningful difference between the various samples. Both AA and MF showed just a little increase in the oxygen amount with respect to that observed for FBT and MBT. This data apparently reflect the higher long-term stability of AA and MF highlighted by the electrochemical characterization. In the first 72 h ageing, instead, MBA samples exhibited an intermediate behaviour. However, considering the EIS results, a relatively steep increase of the oxygen quantity is expected for longer ageing time. No significant changes in the shape of Cu2p and CuLMM signal have been

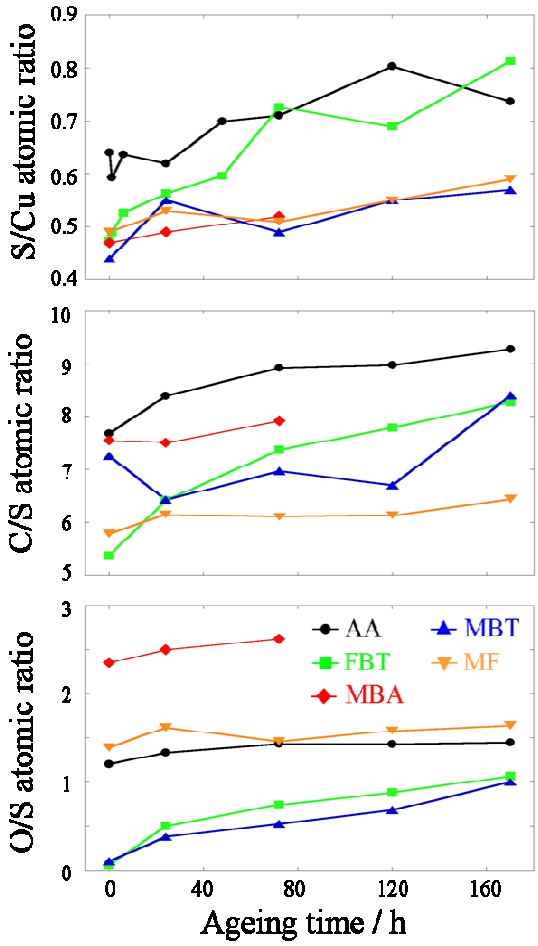

Figure 4.8: Average trend (n≥3) of atomic ratios obtained by XPS measurements for various samples. An error of 10% should be considered.

[1] Unfortunately, at the time of writing this thesis, XPS data relative to MBA samples are available only until 72 h of ageing, because of some technical problems of the instrument.

observed in none of the samples (data not shown), which demonstrated the absence of Cu(II) compounds on the surface.

Furthermore, in spite of the strongly acidic environment, none of the molecules underwent any chemical modification of the terminal group. In fact, the little changes observed in the O1s spectra of AA, MF and MBA (data not shown) can be ascribed to the presence of sulphonate, copper suboxide and some water molecules adsorbed to the copper surface, whereas the presence of the components characteristic of the respective substituent groups clearly indicated that no meaningful chemical modification occurred. On the other hand, both N1s signal in AA and F1s signal in FBT (data not shown) kept their shape and the position practically unchanged during all the ageing period.

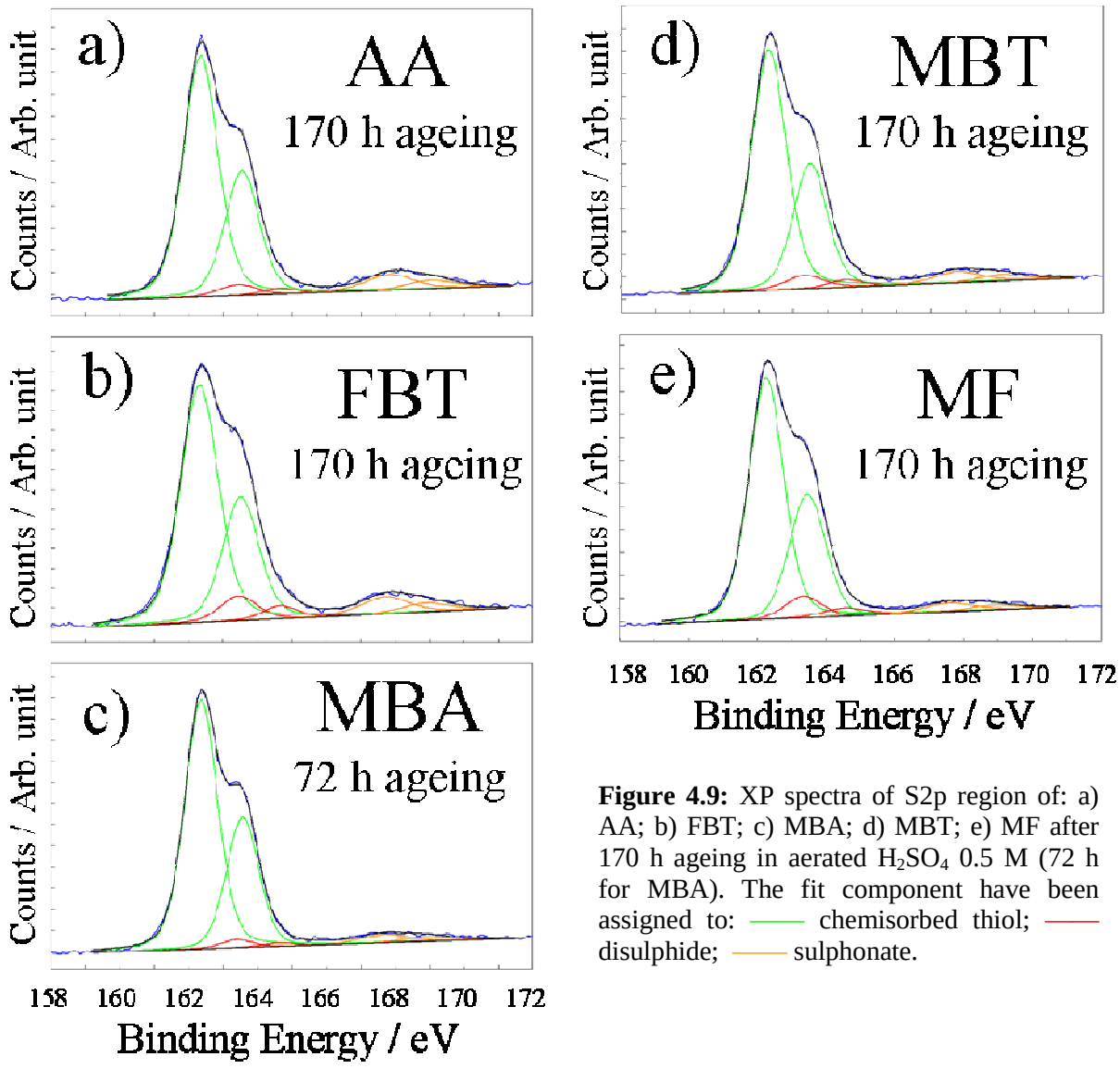

Figure 4.9: XP spectra of S2p region of: a) AA; b) FBT; c) MBA; d) MBT; e) MF after 170 h ageing in aerated H_2SO_4 0.5 M (72 h for MBA). The fit component have been assigned to: —— chemisorbed thiol; —— disulphide; —— sulphonate.

The evolution of the S2p spectra (Fig. 4.9a-e) following the immersion in the acidic solution did not showed appreciable difference between the different layers. All the molecules, even in these harsh conditions, revealed a remarkable chemical stability comparable to that observed for BT layers, regardless the p-substituent group. This was true even for MF and MBA, although they initially had some molecules linked to the surface in a "wrong" way (*i.e.* through the terminal group). In fact, as shown in figure 4.10, all the samples at the end of the ageing period still exhibit a percentage of chemisorbed thiolate included between 84 % and 89 %. The remaining part of the signal was roughly equally divided between molecules oxidized to disulfide and sulfonate. In fact, similarly to BT and 2-NT layers, none of the samples exhibited any evidence of S-C bond breakage. Finally, also the effect of the ageing on the C1s spectra (data not shown) appeared very similar to that observed for BT and 2-NT, regardless the tail group. All the samples exhibited a slight enlargement of the signal toward higher binding energy, ascribable to the adsorption of some contaminants in the layer whereas the main component, relative to the aromatic backbone, did not show any appreciable shift suggesting that all the molecules essentially preserved their up-right configuration.

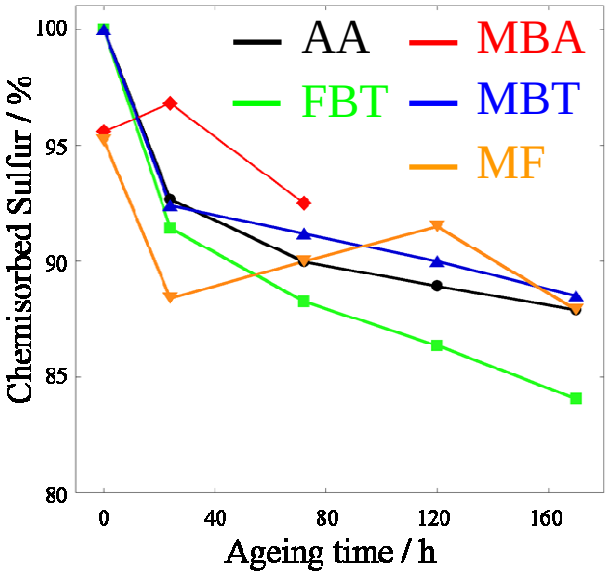

Figure 4.10: Ratio between chemisorbed thiol and total sulfur as a function of the ageing time for various samples. Values were obtained from the best fit performed on S2p spectra

4.4 Discussion

The electrochemical and spectroscopic data set previously illustrated, traced a rather complex picture of our systems where the behaviour of the various layers does not depend by a single parameter but is determined by the combination of several effects. First of all, the

characterization of the as prepared samples indicated that a good quality layer was achieved for all the molecules, without significant difference in surface coverage and cleanliness. Therefore, the different behaviour of the various SAMs seems not to be related to initial deficiencies. Furthermore the trends of S/Cu ratio ascertained that following the ageing the thiols, regardless the tail group, did not desorbed from the surface in an appreciable extent (although the data relative to MBA are still partial).

Although EIS measurements clearly pointed out marked difference in terms of protective properties and durability with changing the terminal group, it is worth noticing that, similarly to BT and 2-NT samples, all the aromatic SAMs experienced an enhancement in charge-transfer resistance following the exposure to the electrolyte, providing a more durable corrosion inhibition than 1-UT (see Chapter 3). Coherently, XP spectra suggested for all samples a similar chemical stability, resulting remarkable with respect to the alkylic thiols as demonstrated by the evolution of the S2p spectra.

The electrochemical data pointed out that hydrophobicity, as expected, clearly affects the passivating properties of the SAMs. Nevertheless, both the initial effectiveness and the long-term stability of our systems seem to be mainly related, although in a different way, to the polar effect of the terminal group. As suggested in literature[72], in fact, the excellent protective properties initially displayed by FBT and MBA SAMs can be related to the presence of an electron-withdrawing group which, facilitating the deprotonation of the sulfur atom, promotes a faster chemisorption of the thiols favouring the formation of a highly ordered layer. Furthermore, the surprisingly good initial performance of MBA suggests a possible effect due to the presence of intermolecular hydrogen bond. Conversely, the presence of an electron-donor group on the ring is expected to slightly inhibit the deprotonation of the sulfur, leading to a slower adsorption of the thiols. Thus MF molecules, having an electron donor substituent, seem to form relatively poorly defined SAMs even if they can establish strong lateral interaction too. Also AA samples, although they showed considerably better performance than MF, appear initially clearly less effective than MBA even if the samples showed almost the same wettability.

As previously discussed in paragraph 4.3.1, although all the SAMs in contact with the acidic solution showed a clear improvement of their protective properties, the rate of this

enhancement and the long-term stability of the various layer are strongly affected by the nature of the tail group. SAMs having an electron-withdrawing group experienced a very steep increase in their efficiency but resulted relatively poor stable whereas AA and MF, having an electron donor group, required at least 72 h ageing to reach their maximum performances and appeared very stable on the long run. The way the nature of the tail group influences the durability of the various layers, appears coherent with the hypothesis, discussed in Chapter 3, of a direct involvement of the water molecules in the reorganization process observed in the aromatic layers. In fact, as known, conjugated systems interact with the water molecules establishing relatively strong electrostatic π-hydrogen bond[237,239]. Therefore, it is reasonable to expect that water molecules establish stronger and more durable interaction with an electron-rich ring, such as AA and MF, than with an electron-poor ring like FBT or MBA, in accordance with our data. It is worth noticing that the different electrochemical behaviour between molecules having the same polar effect (*i.e.* FBT vs MBA and AA vs MF) was mainly determined by the hydrophobicity of their terminal group and, in the case of AA and MF, probably also by the different thickness. The particularly high degradation rate observed MBA could suggest the poor stability of this SAMs to be partially related to the presence of some molecules that are not bonded to the surface through the thiolic function. Anyway, the covalent bond between copper and the carboxylic group is expected to be quite strong, thus the presence of free thiol signal in the S2p spectra is not related to weakly physisorbed molecules, like in the case of 2-NT. Furthermore MF samples, which equally have some molecules bonded to the surface by the "wrong side", showed a remarkable durability. Therefore seems unlikely that this issue can seriously affect the stability of MBA samples.

On the other hand MBT samples, which were expected to be highly passivant because of their marked hydrophobic character, displayed someway disappointing performance both in terms of maximum efficiency and durability. As can be seen in Table II, freshly prepared MBT layers displayed the lower S/Cu ratio among the investigated molecules. Anyway, the difference with the values obtained for other SAMs was very small and likely ascribable to the experimental error. Moreover several other XPS data such as the shape of the CuLMM Auger spectra, the initial very small amount of oxygen and the absence of physisorbed

material, strongly suggested for this layer a high surface coverage. Nevertheless, the electrochemical characterization of as prepared samples showed for MBT a surprisingly small charge-transfer resistance, not only lower than that of freshly prepared BT but also than the more hydrophilic AA layers. During the ageing process, as previously discussed, these samples kept an intermediate behaviour between “electron-rich” (AA and MF) and “electron-poor” (FBT and MBA) aromatic SAMs. This behaviour is coherent with the nature of its alkylic substituent, which is expected to have electron-donor character but with a weaker effect with respect to the hydroxylic or the amidic group. Also in the long run the performance of this SAMs resulted lower than expected. In fact, it displayed relatively weak protective properties, with a maximum charge-transfer resistance notably lower than BT, and relatively poor stability if compared with the SAMs having an electron-donor substituent. The reasons of this disappointing behaviour are still not clear. The electrochemical data suggest that already the freshly prepared samples suffer of some little deficiency, such as a relatively high number of local pinholes defects, resulting undetectable by XPS measurements. This could be related to the “electron-donor effect” during the adsorption process, causing a decrease in the adsorption rate, which in this case would not be mitigated by the presence of intermolecular hydrogen bond, conversely to what happen with AA and MF. Anyway, our current data do not allow to support this hypothesis.

Chapter 5: electrochemical response of BT and 1-UT SAMs on gold following exposure to ultrapure water

5.1 Brief introduction to the chapter

As exhaustively discussed in the introductive chapter, gold is by far the widest employed substrate for the deposition of thiolate overlayers. In fact, its inert nature and its good affinity for the sulfur make it the most suitable support in the majority of SAMs applications. Long chain n-alkanethiolate thiols have been extensively used to modify gold electrodes[55,97,230,262-264]. Their closed packed arrangement and their quasi crystalline structure together with the neglectable conductivity of the alkylic backbone confer them a highly blocking behaviour, so that a gold electrode coated by a monolayer of 1-Dodecanethiol acts as an Ideal Polarizable Electrode (IPE) in a wide range of potential[140]. In the last ten years, several studies have been performed to assess both the structural order and the electrochemical response of SAMs constituted by simple aromatic molecules adsorbed on gold surfaces. The structural investigations on BT adlayers and its derivates pointed out a relatively poorly defined structure characterized by a pretty high tilt angle (~ 50°)[103,105,106] in contrast with what reported for copper, where the simple aromatic thiols adsorbs in a highly ordered closed packed arrangement and a total up-right configuration (tilt angle ~ 20°)[81,114,115]. This lack in the structural order, together with their lower thickness, translates in poorly blocking properties of these systems[108,265 -267] in comparison with the corresponding alkylic films.

The unexpected results we obtained with copper substrates prompted us to investigate the response of simple aromatic SAMs on gold to the exposure to aqueous solutions. Toward that aim monolayers of BT and 1-UT were prepared on polycrystalline gold and the evolution of their blocking behaviour as a function of the ageing time was checked by EIS

and CV in presence of a redox couple (*i. e.* $[Fe(CN)_6]^{3-/4-}$). The inert nature of the substrate, which does not undergo oxidation in ambient conditions, allowed us to perform the ageing process directly in ultrapure water. On the contrary, working on copper we were forced to use acidic solutions to avoid the formation of insoluble oxides, which could hamper the correct molecular packing. In this way the possible effects related to the low pH and/or to the ionic force have been excluded, allowing us to evaluate directly the effects of the aqueous solvent on the monolayers. Thus, a further observation of the enhancement in the protective properties of the aromatic SAMs would indirectly confirm our hypothesis of an active role of the water molecules in the reorganization process. In addition, for BT samples, the effect of a second immersion in the preparation solution following the ageing process has been checked, in attempt to further improve the film quality and minimize the defects.

The utility of this study not only resides in the more general attempt to develop strategies to improve the stability of thiolate layers. In fact highly unsaturated phenyl terminated SAMs are increasingly used as wires in molecular electronic[194,195], and several investigations pointed out a strict relationship between their packing arrangement and their electronic properties[109,198,199]. Therefore, the comprehension of the structural changes occurring in an aromatic SAMs during the exposure to aqueous solutions and/or the optimization of a new simple method to obtain high quality phenyl-terminated monolayers could be very useful also in that emerging field.

5.2 Characterization of the as prepared samples

EIS and CV measurements performed on bare Au and as prepared BT and UT SAMs are displayed in figure 5.1. Both the techniques adopted to characterize the samples clearly highlighted, as expected, that the adsorption of thiols strongly affect the properties of gold electrodes and that the two molecules employed behave very differently between each other. The equivalent circuits employed to model naked and coated gold are those showed in figure 3.6a and 3.6b respectively, and have been already described in section 3.3.3. The EIS spectra

of the bare gold (Fig 5.1a) electrode were dominated by a diffusive component appearing at low frequency, whereas a little resistive/capacitive loop attributable to the electron transfer reaction between the redox probe and the electrode appeared in high frequency domain. The resistance and the capacitance values (R_{ct} = 8.88 ± 2.1 Ωcm^2 and Y_0 = 43.5 ± 9.4 μSs^{n}cm^{-2} with n ~ 0.9) extracted by the data fitting are in good agreement with those reported in literature[265,268,269] for analogous systems and indicated a fast and reversible electron transfer as expected considering the experimental setup. This behaviour was totally confirmed by the CV experiments, which showed for the bare electrode two large symmetric redox peaks centered around to ~ 0.2 V.

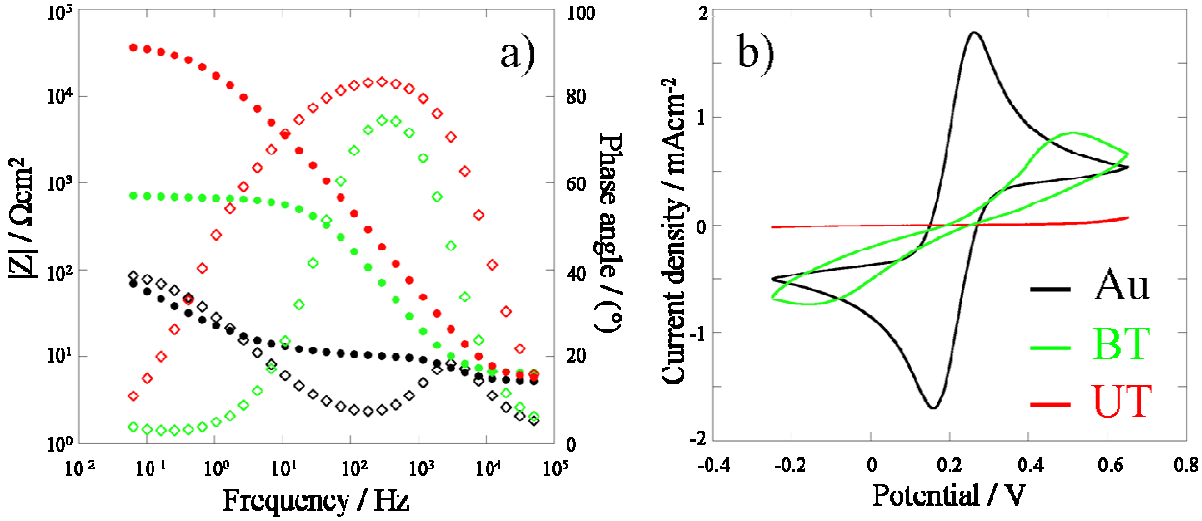

Figure 5.1: a) Bode plot representation of EIS measurements and b) CV measurements performed on freshly prepared —— bare Au; —— BT and —— 1-UT. Experiment were conducted in presence of 5 mM $[Fe(CN)_6]^{3-/4-}$ and 0.1 M $NaClO_4$ as supporting electrolyte.

The adsorption of BT molecules on the electrode surface led to a significant inhibition of the redox reaction. As can be seen in figure 5.1a, the EIS measurements pointed out a noticeable increase in the overall charge transfer resistance, whose value (R_{tot} = 537 ± 167 Ωcm^2) resulted in good agreement with the reported literature[266,269]. Coherently, the marked decrease in intensity and the larger separation observed for the current peaks in CV measurements indicated that BT layer significantly inhibits the redox reaction. However the shape of the voltammetric curve pointed out that BT adlayers are not able to quench the electron transfer at all, thus confirming their poor blocking behaviour[108,265-267]. On the contrary, as expected, UT SAMs showed very pronounced blocking properties. The overall

charge transfer resistance assessed by EIS, in fact, resulted to be more than 60 times larger with respect to that of BT. Furthermore, the absence of detectable signals during the CV measurements confirmed that on electrodes modified by UT molecules the redox reaction practically did not occurred, suggesting this film to have a densely packed and highly ordered arrangement. It is worth noticing that the difference observed between the performance of BT and 1-UT on gold is considerably larger with respect to what seen in chapter 3. This can be probably related to the poorly packed arrangement of BT on gold, which has been already discussed in sections 1.2.3.1 and 5.1.

5.3 Effect of the ageing in ultrapure water

Similarly to what observed for copper surfaces, also when adsorbed on gold SAMs constituted by aromatic and alkylic thiols reacted very differently to the exposure to aqueous solutions. In figure 5.2a-d are plotted the EIS and CV measurements performed for both the samples after different immersion time in ultrapure water. As can be clearly seen in figure 5.2a, BT layers on gold surfaces behave likewise to those on copper: during the ageing period, in fact, they made record a noticeable increase of the overall charge-transfer resistance which, after 24 h, resulted more than five times with respect to the initial value. Moreover, also the CV measurements clearly pointed out a progressive enhancement of the blocking behaviour of BT SAMs, demonstrated by the almost complete disappearance of the current peak associated with the ferro/ferricyanide redox reaction The fact that the phenomenon previously observed for aromatic SAMs on copper exposed to acidic solution was repeated also in these ageing conditions (*i. e.* neutral pH, absence of electrolytes) indirectly support our hypothesis of a direct involvement of the water molecules in the enhancement of the structural order of the layer. On the other hand, SAMs constituted by long-chain n-alkylic thiols confirmed to be relatively poor stable in aqueous media. Although UT samples kept a good blocking behaviour even after 24 h ageing, EIS measurements show that these layers underwent a progressive and rather quick decrease of

their charge-transfer resistance. Already after one hour of exposure to the electrolyte, in fact, it resulted around the half than the initial value whereas at the end of the ageing period it was reduced of almost an order of magnitude. Furthermore, also the CV experiments were totally coherent with the hypothesis of quite rapid transition of these layers toward less ordered configurations.

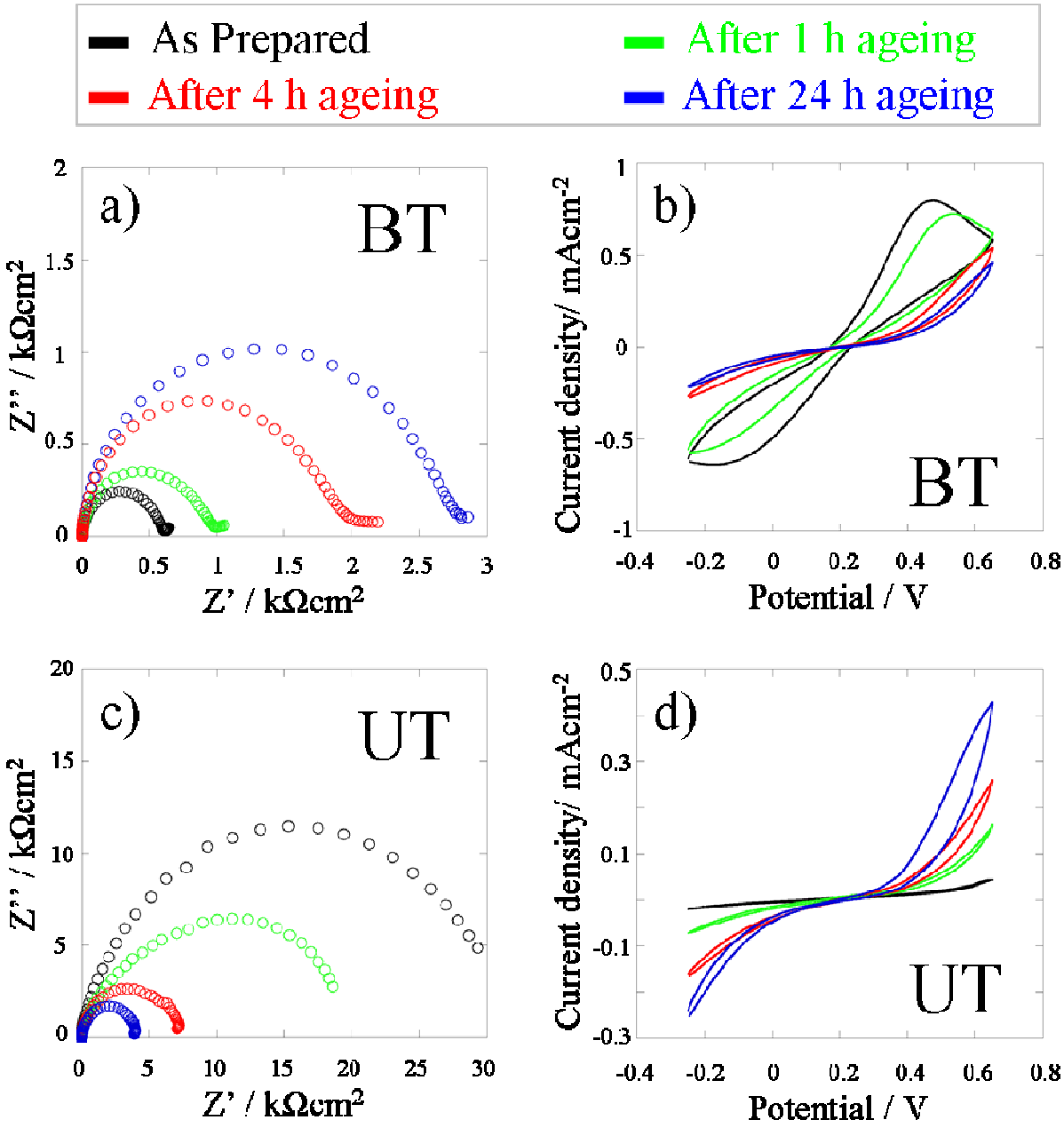

Figure 5.2: a) and c) Nyquist plot representation of EIS measurements performed respectively on BT samples and 1-UT samples after different ageing time. b) and d) CV measurements performed respectively on BT samples and 1-UT samples after different ageing time Experiment were conducted in presence of 5 mM $[Fe(CN)_6]^{3-/4-}$ and 0.1 M $NaClO_4$ as supporting electrolyte.

It is worth noticing that both the employed techniques indicated that, at the end of the ageing process, the blocking properties of BT SAMs resulted very close to those of UT, in spite of the large difference observed for the as prepared samples.

Figure 5.3 displays the evolution of the capacitive values extracted from the EIS data fitting. Consistently with the structures of the two molecules, UT layers exhibited considerably lower values for both CPE_{SAM} and CPE_{def}. The latter, in particular, showed a large difference between the two samples, which might be at least partially correlated to the better structural organization expected for the alkylic overlayers. The capacitance associated with the BT organic layers showed during the exposure to the aqueous media a slight decrease, shifting from 8.16 ± 0.53 $\mu Ss^n cm^{-2}$ to 6.33 ± 0.61 $\mu Ss^n cm^{-2}$. This data could be coherent with a diminution of the average tilt angle of the aromatic molecules following the exposure to the ultrapure water, but further spectroscopic and/or microscopic investigation are absolutely required to verify this hypothesis. On the other hand, the temporal evolution of CPE_{def} did not seem to have a well defined trend, with the final value resulting very close to the initial one.

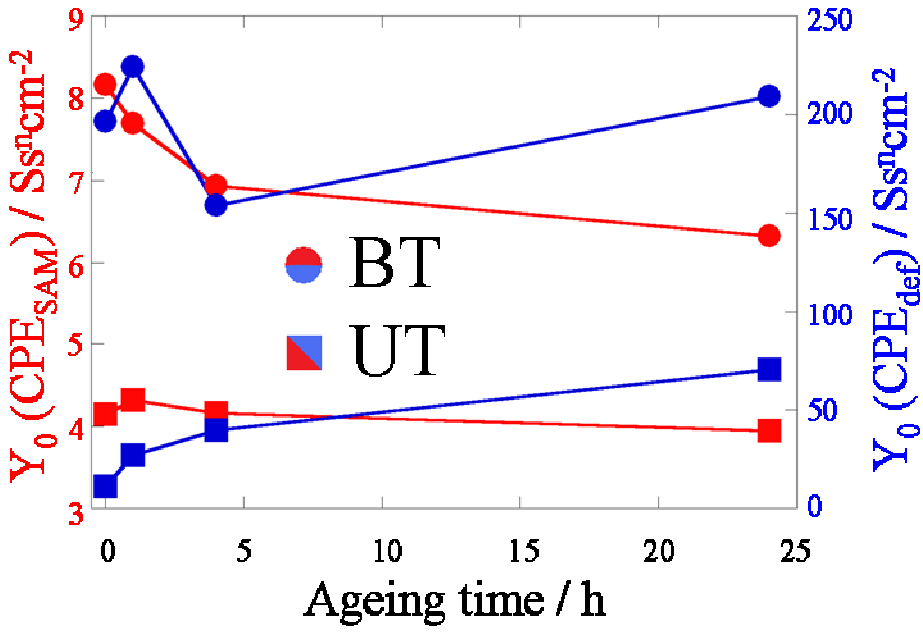

Figure 5.3: Trend of the values of frequency indipendent parameters Y_0 associated with the elements —— CPE_{SAM} and —— CPE_{def} as a function of ageing time in ultrapure water of BT (circle) and 1-UT (square)

UT samples showed for both the capacitance a rather different trend. Contrarily to what observed in acidic solution, UT showed very small variation of the capacitance value associated with the organic layers which at the end of the 24 h ageing can be considered practically constant. On the contrary, Y_0 value associated to CPE_{def} element made record a significant increase (from 11.3 ± 1.8 $\mu Ss^n cm^{-2}$ to 70.5 ± 22.3 $\mu Ss^n cm^{-2}$) whereas no meaningful changes in n values, which constantly resulted included between 0.61 and 0.64, were detected. This trend, coherently with that of the overall resistance, suggests for UT adlayers exposed to aqueous media a progressive evolution towards less ordered structures.
It is worth noticing that the evolution of the two capacitance denoted marked difference with that observed for aged SAMs on copper where a constant increase of the Y_0 values, very rapid in the case of UT samples, was pointed out. This is mainly ascribable to the different ageing conditions experienced by the SAMs. In fact, the exposition to a harsh environment such as H_2SO_4 0.5 M caused chemical damages to the organic layers, and in particular UT, leading to a sharp increase of their capacitance. The data collected on gold, on the contrary, clearly indicated UT to assume a less ordered structure following the exposure to ultrapure water, allowing for an easier electron transfer, but also suggested the layer to resist essentially intact to the ageing process.

5.4 Preparation of high quality BT SAMs

As demonstrated in the previous section, the exposure to aqueous media positively affect SAMs constituted by simple aromatic thiols on gold, conferring them a more ordered and less defective structure. In principle, the healing of collapsed sites and/or the assumption of a more vertical configuration might free some binding sites of the surfaces which were not available before the exposure to H_2O. Thus a second exposure to a thiolic solution performed after the ageing process could allow to fill these “holes”, leading to the formation of an even more densely packed layer. Although the electrochemical characterization performed on aged BT does not allow to establish if a change in molecules orientation actually happened,

it clearly indicated a reduction of the number of defects and/or collapsed sites. Hence we decided to investigate the effects of a new dip of aged BT samples in their preparation solution up to 24 h, in order to optimize a simple method to obtain high quality aromatic SAMs. Once again, the quality of the layer was checked by EIS and CV. The results obtained for different immersion time are displayed in figure 5.4a-b. The EIS measurements actually showed a constant and rather impressive increase in the charge transfer resistance, becoming after 24 h around 6 times larger with respect to that of the simply aged samples. The EIS data were totally confirmed by the CV measurements, showing how, at the end of the second adsorption procedure, the reaction of the redox couple at the modified gold electrode was practically completely inhibited. It is worth noticing that, on the whole, all the treatments experienced by BT layers led, on average, to a relative enhancement of their blocking behaviour of around 30 times, so that it resulted more than the half with respect to freshly prepared UT samples.

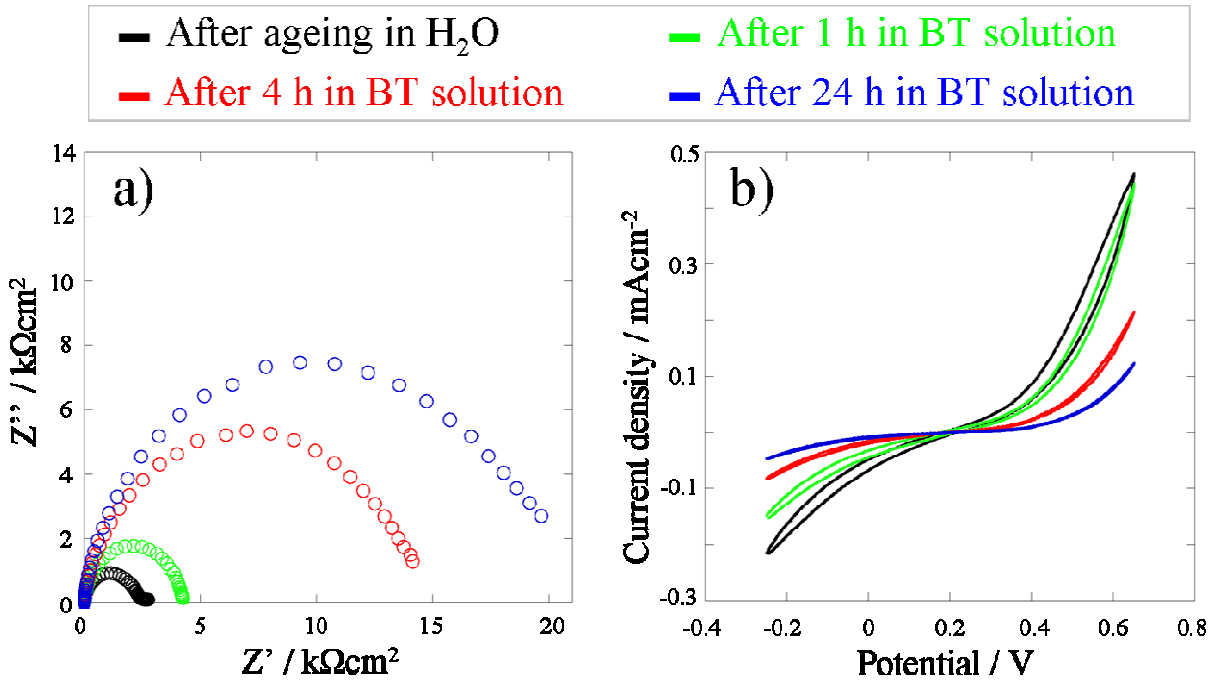

Figure 5.4: a) EIS and b) CV measurements performed on BT samples previously aged for 24 h in ultrapure water and than newly immersed in the adsorption solution for different times. Experiment were conducted in presence of 5 mM $[Fe(CN)_6]^{3-/4-}$ and 0.1 M $NaClO_4$ as supporting electrolyte.

Also the trend of the capacitance values, and in particular the temporal evolution of CPE_{def}, revealed the second immersion in the thiolic solution to have a strong impact on the

structural order of the SAMs (Fig 5.5). In fact, while the capacitance related to the organic coat only showed very small deviations, with an initial increase followed by a slight diminution, the capacitance associated to the layer defects exhibit a marked decreasing trend. As highlighted in figure 5.5, already after the first hour the Y_0 CPE_{def} parameter fell from 209 ± 66 $\mu Ss^n cm^{-2}$ to 40.2 ± 11.0 $\mu Ss^n cm^{-2}$ and then continued to slightly go down to the final value of 24.4 ± 7.9 $\mu Ss^n cm^{-2}$, with a n value always included between 0.60 and 0.75. Although it is quite difficult furnish a precise interpretation of this data, the clear trend detected, together with the resistance results, strongly suggest that the followed preparation protocol provided notably less defective and less permeable BT SAMs. Another evidence of the enhanced stability of BT layers prepared following the new procedure arose from the electrochemical desorption performed in basic solution.

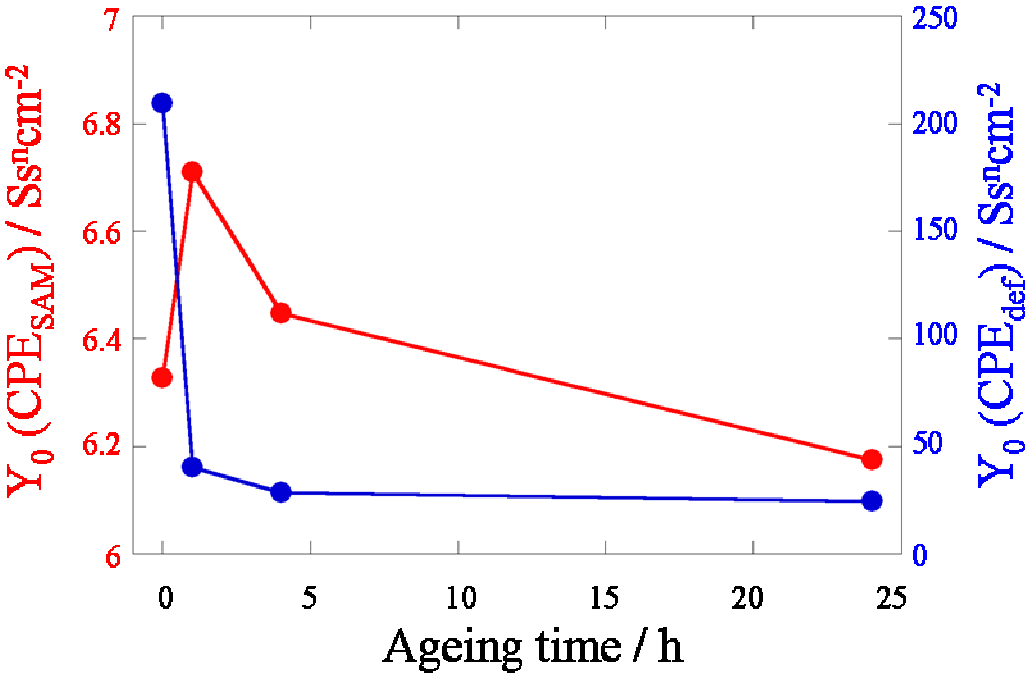

Figure 5.5: Trend of the values of frequency indipendent parameters Y_0 associated with the elements —— CPE_{SAM} and —— CPE_{def} for BT samples previously aged for 24 h in ultrapure water and then newly immersed in the adsorption solution for different times.

As known[202,203], thiolate SAMs can be electrochemically removed by gold surfaces applying to the electrode, in alkaline environments, a potential negative enough to promote the reaction:

$$RS - Au(I) + e^- \rightarrow RS^- + Au(0)$$

The desorption potential, depending by the adsorbed molecules, is generally included between -0.8 V and -1.2 V and can be used to assess the stability of the layer[124]. In fact, a shift of the cathodic desorption peak toward more negative potentials means that more energy is needed to remove thiols from the substrate. As evidenced in figure 5.6, samples which, after the adsorption process, experienced 24 h immersion in ultrapure water and then other 24 h immersion in the thiolic solution, systematically showed a negative shift of about 50 mV (from - 0.98 V to - 1.03 V) with respect to as prepared BT layers, thus confirming that this preparation procedure gave rise to more stable overlayers.

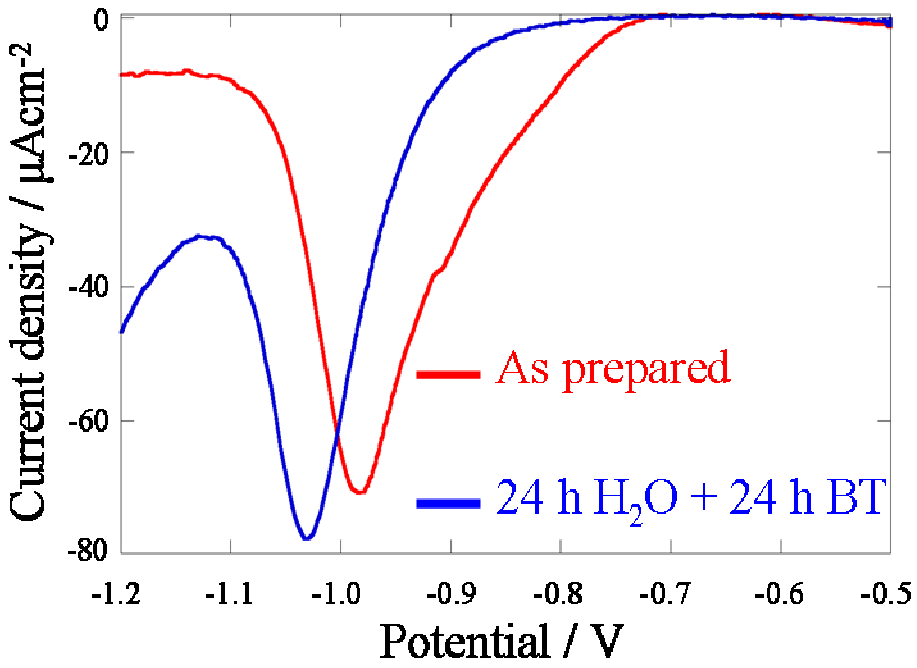

Figure 5.6: Voltammogram representing the cathodic desorption of: —— as prepared BT and —— BT aged 24 h in ultrapure water and then kept other 24 h in the adsorption solution. The measurements were performed in deareated NaOH 1 M at the scan rate of 0.1 Vs^{-1}

Finally, in order to further demonstrate that the obtained results are due to the ageing in ultrapure water and do not arise simply by a longer exposure to the thiolic solutions, gold electrodes were modified by a continuative 72 h immersion into BT adsorption solution and their performance were compared with those just commented. The data displayed in figure

5.7a-b clearly demonstrated that the immersion in aqueous media before the second adsorption process was decisive in order to achieve high quality BT layers.

In fact, both EIS and CV measurements did not shown any substantial difference between samples prepared by 24 h and 72 h of immersion in the thiolic solution. Thus, also the latter exhibited rather poor blocking behaviour, with an overall charge transfer resistance lower by almost 30 times with respect to the high quality BT SAMs.

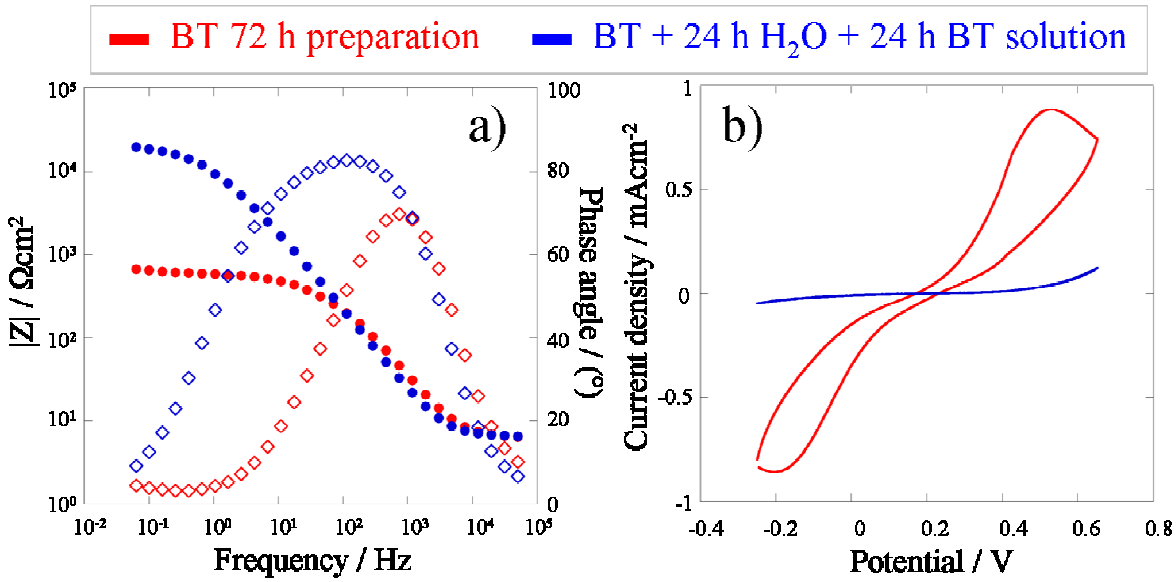

Figure 5.7: a) EIS and b) CV measurements performed on —— BT samples prepared by continuative 72 h immersion in the adsorption solution and —— BT aged 24 h in ultrapure water and then kept other 24 h in the adsorption solution. Experiment were conducted in presence of 5 mM [Fe(CN)6]3-/4- and 0.1 M NaClO4 as supporting electrolyte.

Chapter 6: conclusions and perspectives

This PhD work aimed to a deep characterization of thiolate SAMs constituted by simple aromatic thiols adsorbed on copper and gold polycrystalline surfaces, giving particular emphasis to their behaviour in aqueous media, which have been never accurately investigated before. In particular, we believed that the relatively strong intermolecular ring interaction could provide a higher stability of these systems in aqueous environments, a very topical issue for most of applications of the SAMs, both on gold and copper. The obtained results were in some way surprising. In Chapter 3 the adsorption on polycrystalline copper of two aromatic thiols, namely Benzenethiol and 2-Naphthalenethiol, and of one long-chain n-alkylic thiol, *i.e.* 1-Undecanethiol, was deeply investigated, comparing the stability of the respective SAMs and their ability to inhibit the corrosion process up to a week in a strongly acidic solution such as H_2SO_4 0.5 M. All the employed characterization methods agreed showing the adlayers constituted by aromatic thiols to be notably more stable and, on the long run, more effective than UT layers in spite of their lower thickness, which is reported in literature to be a crucial parameter to determine the protective properties of SAMs on copper. The electrochemical characterization, in particular, revealed that both BT and NT in contact with the electrolyte solution show an unexpected enhancement of their protective properties, an effect always lasting for several days. On the contrary, as expected, the inhibition efficiency of UT samples decreased quite fast, suggesting a rapid degradation of the layer. The spectroscopic characterization confirmed the markedly higher stability of the aromatic layers. XPS measurements, in particular, allowed to clarify the degradation mechanism of thiolate layers on copper which, to the best of our knowledge, has never been deeply investigated so far. Raman spectroscopy, on the other hand, not only highlighted the different stability of the various layers, but also suggested the aromatic SAMs to experience a sort of ordering process during the first 24 h immersion, accordingly with the electrochemical data. The evolution of the wetting behaviour of BT and NT with the ageing time suggested the water molecules to be directly involved in the enhancement of the structural order of these SAMs.

This interesting results led us to investigate the effects of the presence of various (-F, -CH_3, -OH, -COOH, -$NHCOCH_3$) p-substituent groups on the aromatic ring. The data revealed that the terminal group has a considerable influence on the layer properties. According to what suggested in literature, the presence of an electron withdrawing group, such as -F or -COOH, may to promote a faster and more effective adsorption of the aromatic molecules, probably facilitating the deprotonation of the thiolic function and thus the link with the substrate. The evolution of the protective properties as a function of the ageing time showed an increase of the charge transfer resistance for all the samples during the first hours of ageing, confirming the previous data. The passivity of the various samples was in good accordance with the grade of hydrophobicity of the overlayer; nevertheless the interaction with the ageing solution and even more the stability of the SAMs seemed to be mainly related to the polar effect of the tail group. Rings relatively poor of electrons, in fact, showed a very sharp enhancement of the protective properties but a relatively low stability whereas rings rich of electrons showed a relatively slow ordering process but an exceptional stability. This is consistent with the hypothesis of a direct involvement of water molecules, which are expected to establish stronger interaction with rings having high electronic density. The obtained results provided useful information about the relationship between the molecular structures and the properties of the aromatic SAMs, which could be precious to design more complex systems for several applications.

Finally, in Chapter 5 preliminary results concerning the electrochemical response of aromatic SAMs on gold when exposed to ultrapure water are reported. Also in this ageing environment BT layers clearly showed a noticeable improvement of their blocking behaviour, indicating the evolution toward more ordered structures. The confirmation of this behaviour even in absence of electrolytes indirectly supported the hypothesis of a role of the water molecules in the ordering process. In addition, the effect of a second immersion in the thiolic solution after the ageing process was investigated. The EIS and CV results demonstrated that this procedure led to the formation of high quality BT layers, exhibiting blocking properties up to 30 times larger than those obtained in the traditional way. Further spectroscopic and/or microscopic characterization would be necessary to unveil the phenomena leading to these results.

On the whole, our results demonstrated SAMs of simple aromatic thiols to be extremely interesting systems, particularly suitable for those applications requiring the exposure to the aqueous media. Their unexpected performance and their notable stability seem to be mainly related to two features: the high strength of C-S bond, preventing its breakage even in harsh conditions, and, apparently, the ability of the aromatic ring to interact with the water molecules promoting an evolution toward more ordered structures. These findings open new attractive perspective. In fact molecules combining the interesting features pointed out for simple aromatic SAMs with other characteristic could be easily designed. For example, polyphenyl thiols or molecules containing two rings separated by an alkyl chain should, in principle, combine both the SAM durability arising from their aromatic character with a higher layer thickness which could be very useful in many applications such as the corrosion inhibition. Finally, although the work is far to be concluded, the new preparation protocol illustrated in Chapter 5, allowing to the formation of extremely ordered SAMs on gold, appears of particular interest. In fact, if such procedure proves to be generally effective for all phenyl terminated layers, it could represent a very useful tool to improve the quality and the stability of these layers with important repercussion on molecular electronic as well as on many other fields.

List of publications

- F. Caprioli*, M. Beccari, A. Martinelli, V. Di Castro, F. Decker “A multi-technique approach to the analysis of SAMs of aromatic thiols on copper” *Phys. Chem. Chem. Phys* **2009**, *11*, 11624

- M. Liberatore*, A. Petrocco, F. Caprioli, C. La Mesa, F. Decker, C. A. Bignozzi “Mass transport and charge transfer rates for $Co^{(III)}/Co^{(II)}$ redox couple in a thin-layer cell” *Electrochim. Acta* **2010**, *55*, 4025

- F. Caprioli*, F. Decker, A. G. Marrani, M. Beccari, V. Di Castro “Copper protection by self-assembled monolayers of aromatic thiols in alkaline solutions” *Phys. Chem. Chem. Phys* **2010**, *12*, 9230

- V. Di Castro*, M. Beccari, F. Bruni, F. Caprioli, F.Decker “Comparison of the protective effect of aromatic thiols adsorbed on copper” *Surf. Interface Anal.* **2010**, *42*, 601

- F. Caprioli*, F. Decker, V. Di Castro “Durable Cu corrosion inhibition in acidic solution by SAMs of Benzenethiol” *J. Electroanal. Chem.* **2011**, *657*, 192

- F. Caprioli, A. Martinelli, D. Gazzoli, V. Di Castro, F. Decker “Enhanced protective properties and structural order of Self-Assembled Monolayers of aromatic thiols on copper in contact with acidic aqueous solution” *Submitted*

- F. Caprioli, A. Martinelli, V. Di Castro, F. Decker “effect of different p-substituent groups on long-term performance of aromatic thiols as Cu corrosion inhibitors in acidic solution” *In preparation*

- F. Caprioli, P. Bucci, F. Decker “A new simple protocol to prepare high quality aromatic SAMs on gold” *In preparation*

References

[1] K. S. Birdi; *"Handbook of Surface and Colloid Chemistry"*, Third Edition, CRC Press, Boca Raton, **2009**

[2] G. A. Samorjal, Y. Li; *"Introduction to Surface Chemistry and Catalysis"*, Second Edition, John Wiley & Sons, Hoboken, **2010**

[3] A. W. Adamson, A. P. Gast; *"Physical Chemistry of Surfaces"*, Sixth Edition, John Wiley & Sons, New York, **1997**

[4] J. C. Love, L. A. Estroff, J. K. Kriebel, R. G. Nuzzo, G. M. Whitesides; *Chem. Rev.* **2005**, *105*, 1103

[5] F. Schreiber; *Prog. Surf. Sci.* **2000**, *65*, 151

[6] A. Pockels; *Nature* **1891**, *43*, 437

[7] A. Pockels; *Nature* **1892**, *46*, 418

[8] A. Pockels; *Nature* **1893**, *48*, 152

[9] A. Pockels; *Nature* **1894**, *50*, 223

[10] I. Langmuir; *J. Am. Chem. Soc.* **1917**, *39*, 1848

[11] I. Langmuir; *Trans. Faraday Soc.* **1920**, *15*, 62

[12] K. Blodgett; *J. Am. Chem. Soc.* **1935**, *57*, 1077

[13] K. Blodgett; *Phys. Rev.* **1937**, *51*, 964

[14] W.C. Bigelow, D. L. Pickett, W.A.J. Zisman; *Colloid Interface Sci.* **1946**, *1*, 513

[15] J. Sagiv; *J. Am. Chem. Soc.* **1980**, 102, 92

[16] L. Netzer, J. Sagiv; *J. Am. Chem. Soc* **1983**, *105*, 674

[17] J. Gun, J. Sagiv; *J. Phys. Chem.* **1986**, *90*, 3054

[18] M. Pomerantz, A. Segmueller; L. Netzer, J. Sagiv, *Thin Solid Films* **1985**, *132*, 153

[19] R. G. Nuzzo; D. L. Allara; *J. Am. Chem. Soc.* **1983**, *105*, 4481

[20] R. G. Nuzzo, F. A. Fusco, D. L. Allara; *J. Am. Chem. Soc.* **1987**, *109*, 2358

[21] G. L. Gaines, "Insoluble Monolayers at Liquid-Gas Interfaces"; Interscience, New York, **1966**

[22] C. D. Bain, G. M. Whitesides; *Angewandte Chemie* **1989**, *101*, 522

[23] G. M. Whitesides, P. E. Laibinis; *Langmuir* **1990**, *6*, 87

[24] P. E. Laibinis, J. J. Hickman, M. S. Wrighton, G. M. Whitesides; *Science (Washighton, DC, U. S.)* **1989**, *245*, 845

[25] C. D. Bain, H. A. Biebuyck, G. M. Whitesides; *Langmuir* **1989**, *5*, 723

[26] C. D. Bain, G. M. Whitesides; *J. Phys. Chem.* **1989**, *93*, 1670

[27] C. D. Bain, E. B. Troughton, Y. T. Tao, J. Evall, G. M. Whitesides, R. G. Nuzzo; *J. Am. Chem. Soc.* **1989**, *111*, 321

[28] C. D. Bain, G. M. Whitesides; *Science (Washighton, DC, U. S.)* **1988**, *240*, 62

[29] L. Strong, G. M. Whitesides; *Langmuir* **1988**, *4*, 546

[30] C. D. Bain, G. M. Whitesides; *J. Am. Chem. Soc.* **1988**, *110*, 3665

[31] C. D. Bain, G. M. Whitesides; *J. Am. Chem. Soc*. **1989**, *111*, 7164

[32] P. E. Laibinis, G. M. Whitesides, D. L. Allara, Y. T. Tao, A. N. Parikh, R. G. Nuzzo; *J. Am. Chem. Soc.* **1991**, *113*, 7152

[33] M. A. Bryant, J. E. Pemberton; *J. Am. Chem. Soc.* **1991**, *113*, 8284

[34] P. E. Laibinis, G. M. Whitesides; *J. Am. Chem. Soc.* **1992**, *114*, 9022

[35] Z. Li, S.-C. Chang, R. S. Williams; *Langmuir* **2003**, *19*, 6744

[36] J. C. Love, D. B. Wolfe, R. Haasch, M. L. Chabiniyc, K. E. Paul, G. M. Whitesides, R. G. Nuzzo; *J. Am. Chem. Soc.* **2003**, *125*, 2597

[37] K. Mitsuo, I. Masaki; *J. Phys. Chem. B* **2006**, *110*, 21124

[38] M. J. Stevens; *Langmuir* **1999**, *15*, 2773

[39] S. Onclin, B. J. Ravoo, D. N. Rainhoudt; *Angew. Chem. Int. Ed. Engl.* **2005**, *44*, 6282

[40] T. L. Niederhauser, Y.-Y. Lua, G. Jiang, S. D. Davis, R. Matheson, D. A. Hess, I. A. Mowat, M. R. Linford; *Angew. Chem. Int. Ed. Engl.* **2002**, *41*, 3353

[41] C. E. Taylor, D. K. Schwartz; *Langmuir* **2003**, *19*, 2665

[42] D. L. Allara, R. G. Nuzzo; *Langmuir* **1985**, *1*, 45

[43] D. L. Allara, R. G. Nuzzo; *Langmuir* **1985**, *1*, 52

[44] M. G. Samant, C. A. Brown, J. G. Gordon II; *Langmuir* **1993**, *9*, 1082

[45] G. Haehner, R. Hofer, I. Klingenfuss; *Langmuir* **2001**, *17*, 7047

[46] T. L. Breen, P. M. Fryer, R. W. Nunes, M. E. Rothwell; *Langmuir* **2002**, *18*, 194

[47] M. K. Chaudhury; *Biosens. Bioelectron.* **1995**, *10*, 785

[48] O. M. Magnussen, B. M. Ocko, M. Duetsch, M. J. Regan, P. S. Pershan, D. Abernathy, G. Gurebel, J.- F. Legrand; *Nature (London)* **1996**, *384*, 250

[49] R. Wiesendanger, G. Tarrach, D. Buergler, T. Jung, L. Eng, H. J. Guentherodt; *Vacuum* **1990**, *41*, 386

[50] G. E. Poirier, M. J. Tarlov; *Langmuir* **1994**, *10*, 2853

[51] S. Kramer, R. R. Fuierer, C. B. Gorman; *Chem. Rev.* **2003**, *103*, 4367

[52] M.-C. Daniel, D. Astruc; *Chem. Rev.* **2004**, *104*, 293

[53] A. Cossaro, R. Mazzarello, R. Rousseau, L. Casalis, A. Verdini, A. Kohlmeyer, L. Floreano, S. Scandolo, A. Morgante, , M. L. Klein, G. Scoles; *Science (Washighton, DC, U. S.)* **2008**, *321*, 943

[54] C. Vericat, M. E. Vela, G. Benitez, P. Carro, R. C. Salvarezza; *Chem. Soc. Rev.* **2009**, *39*, 1805

[55] M. D. Porter, T. B. Bright, D. L. Allara, C. E. D. Chidsey; *J. Am. Chem. Soc.* **1987**, *109*, 3559

[56] C. Miller, P. Cuendet, M. Graetzel, *J. Phys. Chem.* **1991**, *95*, 877

[57] C. E. D. Chidsey, C. R. Bertozzi, T. M. Putvinski, M. Mujsce; *J. Am. Chem. Soc.* **1990**, *112*, 4301

[58] P. L. Schilardi, P. Dip, P. C. Dos Santos Claro, G. A. Benitez, M. H. Fonticelli, O. Azzaroni, R. C. Salvarezza; *Chem.–Eur. J.*; **2006**, *12*, 38

[59] D. Burshtain and D. Mandler, *Phys. Chem. Chem. Phys.*; **2006**, *8*, 158

[60] X. D. Cui, A. Primak, X. Zarate, J. Tomfohr, O. F. Sankey, A. L. Moore, T. A. Moore, D. Gust, G. Harris, S. M. Lindsay; *Science (Washighton, DC, U. S.)* **2001,** *294*, 571.

[61] R. P. Andres, T. Bein, M. Dorogi, S. Feng, J. I. Henderson, C. P. Kubiak, W. Mahoney, R. G. Osifchin, R. Reifenberger; *Science (Washighton, DC, U. S.)* **1996**, *272*, 1323

[62] M. A. Reed, C. Zhou, C. J. Muller, T. P. Burgin, J. M. Tour; *Science (Washighton, DC, U. S.)* **1997**, *278*, 252

[63] R. S. Clegg, S. M. Reed, J. E. Hutchinson; *J. Am. Chem. Soc.* **1998**, *120*, 2486

[64] E. Cooper, G. J. Leggett; *Langmuir* **1999**, *15*, 1024

[65] H. O. Finklea; *J. Electroanal. Chem.*, **1996**, *19*, 109

[66] H. Klein, W. Blanc, R. Pierrisnard, C. Fauquet, P. Dumas; *Eur. Phys. J., B: Condens. Matter. Phys.*

[67] J. A. Veneables; *Introduction to Surface and Thin Film Processes;* Cambridge University Press: Cambridge, U.K., **2000**

[68] M. Schlesinger, M. Paunovic; *Modern Electroplating;* John Wiley & Sons: New York, **2000**

[69] D. Barriet, C. M. Yam, O. E. Shmakova, A. C. Jamison, T. R. Lee; *Langmuir* **2007**, *23*, 8866

[70] J. Tkac, J. J. Davis; *J. Electroanal. Chem.* **2008**, *621*, 117

[71] Y. Feng, W.-K. Teo, K.-S. Siow, Z. Gao, K.-L. Tan, A.-K. Hsieh; *J. Electrochem. Soc.* **1997**, *144*, 55

[72] Y. S. Tan, M. P. Srinivasan, S. O. Pehkonen, S. Y. M. Chooi; *Corros. Sci.* **2006,** *48*, 840

[73] P. Wang, C. Yang, B. Wu, N. Huang, J. Li; *Electrochim. Acta* **2010**, *55*, 878

[74] G. Li, H. Ma, Y. Jiao, S. Chen; *J. Serb.Chem. Soc.* **2004**, *69*, 791

[75] P.G. Ganesan, A. Kumar, G. Ramaneth, *Appl. Phys. Lett.*, **2005**, *87*, 011905

[76] M. M. Sung. K. Sung, C. G. Kim, S. S. Lee, Y. Kim; *J. Phys. Chem. B* **2000**, *104*, 2273

[77] D. K. Schwartz; *Annu. Rev. Phys. Chem.* **2001**, *52*, 107

[78] H. Kondoh, C. Kodama, H. Sumida, H. Nozoye; *J. Chem. Phys* **1999**, *111*, 1175

[79] P. Fenter, A. Eberhardt, P. Eisenberger; *Science (Washighton, DC, U. S.)* **1994**, *266*, 1216

[80] H. Kondoh, N. Saito, F. Matsui, T. Yokohama, T. Ohta, H. Kuroda; *J. Phys. Chem. B* **2001**, *105*, 12870

[81] C. Schmidt, J. Götzen, G. Witte; *Langmuir* **2011**, *27*, 1025

[82] O. Dannenberger, M. Buck, M. Grunze; *J. Phys. Chem. B* **1999**, *103*, 2202

[83] K. A. Peterlinz, R. Georgiadis; *Langmuir* **1996**, *12*, 4731

[84] C. Fruböse, K. Doblhofer; *J. Chem. Soc. Faraday Trans.* **1995**, *91*, 1949

[85] R. F. DeBono, G. D. Loucks, D. D. Manna, U. J. Krull; *Can. J. Chem.* **1996**, *74*, 677

[86] A. Ulman; *Chem. Rev.* **1996**, *96*, 1533

[87] G. E. Poirier; *Chem. Rev.* **1997**, *97*, 1117

[88] W. K. Paik, S. Eu, K. Lee, S. Chon, M. Kim; *Langmuir* **2000**, *16*, 10198

[89] H. Ron, H. Cohen, S. Matlis, M. Rappaport, I. Rubinstein; *J. Phys. Chem. B* **1998**, *102*, 9861

[90] F. Bensebaa, R. Voicu, L. Huron, T.H. Ellis, E. Kruus, *Langmuir* **1997**, *13*, 5335

[91] M. Buck, M. Grunze, F. Eisert, J. Fischer, F. Träger; *J. Vac. Sci. Technol. A* **1992**, *10*, 926

[92]J. G. Vos, R. J. Forster, T. E. Keyes, *Interfacial Supramolecular Assemblies*; Wiley, New York **2003**

[93] O. Dannenberger, J. J. Wolff, M. Buck; *Langmuir* **1998**, *14*, 4679

[94] R. Yamada, H. Sakai, K. Uosaki; *Chem. Lett.* **1999**, *28*, 667

[95] T. W. Schneider, D. A. Buttry, *J. Am. Chem. Soc.* **1993**, *115*, 12391

[96] T. Ishida, W. Mizutani, H. Azehara, F. Sato, N. Choi, U. Akiba, M. Fujihira, H.Tokumoto; *Langmuir* **2001**, *17*, 7459

[97] J. Dai, Z. Li, J. Jin, J. Cheng, J. Kong, S. Bi; *J. Electroanal. Chem.* **2008**, *624*, 315

[98] M. Kawasaki, T. Sato, T. Tanaka, K. Takao; *Langmuir* **2000**, *16*, 1719.

[99] R. Yamada, H. Wano, K. Uosaki; *Langmuir* **2000**, *16*, 5523

[100] D. P. Woodruff; *Phys. Chem. Chem. Phys.* **2008**, *10*, 7211

[101] G. Hähner, Ch. Wöll, M. Buck, M. Grunze; *Langmuir* **1993**, *9*, 1955

[102] R. G. Nuzzo, L. H. Dubois, D. L. Allara; *J. Am. Chem. Soc.* **1990**, *112*, 558

[103] A. Shaporenko, A. Terfort, M. Grunze, M. Zharnikov; *J. Electron Spectrosc. Relat. Phenom.* **2006**, *151*, 45

[104] S. Frey, V. Stadler, K. Heister, W. Eck, M. Zharnikov, M. Grunze, B. Zeysing, A. Terfort; *Langmuir* **2001**, *17*, 2408

[105] M. Zharnikov, M. Grunze; *J. Phys.: Condens. Matter* 2**001**, *13*, 11333

[106] D. Käfer, A. Bashir, G. Witte; *J. Phys. Chem. C* **2007**, *111*, 10546

[107] W. Geyer, V. Stadler, W. Eck, M. Zharnikov, A. Golzhauser, M. Grunze; *Appl. Phys. Lett.* **1999**, *75*, 2401

[108] V. Ganesh, V. Lakshminarayanan; *J. Chem. Phys. B* **2005**, *109*, 16372

[109] D. Käfer, G. Witte, P. Cyganik, A. Terfort, C. Wöll; *J. Am. Chem. Soc.* **2006**, *128*,1723

[110] J. F. Kang, A. Ulman,, S. Liao, R. Jordan, G. Yang, G.-Y. Liu; *Langmuir* **2001**, *17*, 95

[111] A. Imanishi, K. Isawa, F. Matsui, T. Tsuduki, T. Yokohama, H. Kondoh, Y. Kitajima, T. Ohta; *Surf. Sci.* **1998**, *407*, 282

[112] H. Rieley, G. K. Kendall; *Langmuir* **1999**, *15*, 8867

[113] A. Nemetz, T. Fischer, A. Ulman, W. Knoll; *J. Chem. Phys.* **1993**, *98*, 5912

[114] M. Beccari, A. Kanjilal, M. G. Betti, C. Mariani, L. Floreano, A. Cossaro, V. Di Castro, *J. Electron Spectrosc. Relat. Phenom.* **2009**, *172*, 64

[115] V. Di Castro, F. Bussolotti, C. Mariani; *Surf. Sci.* **2005**, *598*, 218

[116] L. Carbonell, C. M. Whelan, M. Kinsella, K. Maex; *Superlattice Microstruct.* **2004**, *36*, 149

[117] S. Xu, S. Cruchon-Dupeyrat, J.C. Garno, G.-Y. Liu, G.K. Jennings, T.-H. Yong, P.E. Laibinis; *J. Chem. Phys.* **1998**, *108*, 5002.

[118] J. A. M. Sondag-Huethorst, C. Schonenberger, L. G. J. Fokkink; *J. Phys. Chem.* **1994**, *98*, 6826

[119] H. O. Finklea, S. Avery, M. Lynch; *Langmuir* **1987**, *3*, 409

[120] P. Diao, M. Guo, D. Jiang, Z. Jia, X. Cui, D. Gu , R. Tong, B. Zhong; *J. Electroanal. Chem.* **2000**, *480*, 59

[121] M. H. Schoenfisch, J. E. Pemberton; *J. Am. Chem. Soc.* **1998**, *120*, 4502

[122] N. Prathima, M. Harini, N. Rai, R. H. Chandrashekara, K. G. Ayappa, S. Sampath, S. K. Biswas; *Langmuir* **2005**, *21*, 2364

[123] M.T. Lee, C. C. Hsueh, M.S. Freund, G. S. Ferguson; *Langmuir* **1998**, *14*, 6419

[124] C. Vericat, G. A. Benitez, D. E. Grumelli, M. E. Vela, R. C. Salvarezza; *J. Phys.: Condens. Matter* **2008**, *20*, 184004

[125] R. Valiokas, M. Östblom, S. Svedhem, S. C. T. Svensson, B. Liedberg; *J. Phys. Chem. B* **2002**, *106*, 10401

[126] J. B. Schlenoff, M. Li, H. Ly; *J. Am. Chem. Soc.* **1995,** *117*, 12528

[127] G. Yang, N. A. Amro, Z. B. Starkewolfe, G.-Y. Liu; *Langmuir* **2004**, *20*, 3995

[128] N. T. Flynn, T. N. T. Tran, M. J. Cima, R. Langer; *Langmuir* **2003**, *19*, 10909

[129] G. Mani, D. M. Johnson, D. Marton, V. L. Dougherty, M. D. Feldman, D. Patel, A. A. Ayon, C. M. Agrawal; *Langmuir* **2008**, *24*, 6774

[130] B. Kong, Y. Kim, I. S. Choi; *Bull. Korean Chem. Soc.* **2008**, *29*, 1843

[131] H.Y. Ma, C. Yang, S. H. Chen, Y. L. Jiao, S. X. Huang, D.G. Li, J. L. Luo; *Electrochim. Acta* **2003**, *48*, 4277

[132] G. K. Jennings, P. E. Laibinis; *Colloids Surf., A* **1996**, *116*, 105

[133] C. M. Whelan, M. Kinsella, L. Carbonell, H. M. Ho, K. Maex; *Microelectron. Eng.* **2003**, *70*, 551

[134] I.-H. Sung, D.-E. Kim; *Tribol. Lett.* **2004**, *17*, 835

[135] R., Jr. Colorado, T. R. Lee; *Langmuir* **2003**, *19*, 3288

[136] J. E. Houston, H. I. Kim; *Acc. Chem. Res.* **2002**, *35*, 547

[137] G. J. Leggett; *Anal. Chim. Acta* **2003**, *479*, 17

[138] R. K. Smith, P. A. Lewis, P. S. Weiss; *Prog. Surf. Sci.* **2004**, *75*, 1

[139] D. M. Adams, L. Brus, C. E. D. Chidsey, S. Creager, C. Creutz, C. R. Kagan, P. V. Kamat, M. Lieberman, S. Lindsay, R. A. Marcus, R. M. Metzger, M. E. Michel-Beyerle, J. R. Miller, M. D. Newton, D. R. Rolison, O. Sankey, K. S. Schanze, J. Yardley, X. Zhu; *J. Phys. Chem. B* **2003**, *107*, 6668

[140] A. J. Bard, L. R. Faulkner; *Electrochemical Methods: Fundamentals and Applications*, Second Edition, John Wiley & Sons, New York, **2001**

[141] C. E. D. Chidsey; *Science (Washington, D.C.)* **1991**, *251*, 919

[142] E. Tran, M. A. Rampi, G. M. Whitesides; *Angew. Chem., Int. Ed. Engl.* **2004**, *43*, 3835

[143] M. S. Ravenscroft, H. O. Finklea; *J. Phys. Chem.* **1994**, *98*, 3843

[144] J. F. Smalley, S. W. Feldberg, C. E. D. Chidsey, M. R. Linford, M. D. Newton, Y.-P. Liu; *J. Phys. Chem.* **1995**, *99*, 13141

[145] F.-R. F. Fan, J. Yang, S. M. Dirk, D. W. Price, D. Kosynkin, J. M. Tour, A. J. Bard, *J. Am. Chem. Soc.* **2001**, *123*, 2454

[146] R. M. Haddox, H. O. J. Finklea; *Phys. Chem. B* **2004**, *108*, 1694

[147] C. Cannes, F. Kanoufi, A. J. Bard; *Langmuir* **2002**, *18*, 8134

[148] K. Hu, Z. Chai, J. K. Whitesell, A. J. Bard; *Langmuir* **1999**, *15*, 3343

[149] A. Salomon, D. Cahen, S. Lindsay, J. Tomfohr, V. B. Engelkes, C. D. Frisbie; *Adv. Mater.* **2003**, *15*, 1881

[150] I. Willner, E. Katz; *Angew. Chem., Int. Ed. Engl.* **2000**, *39*, 1180.

[151] Y.-D. Zhao, D.-W. Pang, S. Hu, Z.-L. Wang, J.-K. Cheng, H.-P. Dai; *Talanta* **1999**, *49*,751

[152] A. E. Kasmi, J. M. Wallace, E. F. Bowden, S. M. Binet, R. J. Linderman; *J. Am. Chem. Soc.* **1998**, *120*, 225

[153] B. Bonanni, A. R. Bizzarri, S. Cannistraro; *J. Phys. Chem. B* **2006**, *110*, 14574

[154] J. Lahiri, P. Kalal, A. G. Frutos, S. J. Jonas, R. Schaeffler; *Langmuir* **2000**, *16*, 7805

[155] S. K. Aryaa, P. R. Solankia, M. Datta, B. D. Malhotra; *Biosens. Bioelectron.* **2009**, *24*, 2810

[156] D. D. Schlereth; *Comprehensive Analytical Chemistry* **2005**, *44*, 1

[157] G. F. Paciotti, L. Myer, D. Weinreich, D. Goia, N. Pavel, R. E. McLaughlin, L. Tamarkin; *Drug Delivery* **2004**, *11*, 169

[158] K. J. C. van Bommel, A. Friggeri, D. Mateman, F. A. J. Geurts, K. G. C. van Leerdam, W. Verboom, F. C. J. M. van Veggel, D. N. Reinhoudt; *Adv. Funct. Mater.* **2001**, *11*, 140

[159] T. Pham, D. Lai, D. Ji, W. Tuntiwechapikul, J. M. Friedman, T. R. Lee; *Colloids Surf., B* **2004**, *34*, 191

[160] Y.-J. Han, J. Aizenberg; *Angew. Chem., Int. Ed. Engl.* **2003**, *42*, 3668

[161] D. A. Jones, *Principles and Prevention of Corrosion*, 2nd ed.; Prentice Hall: Upper Saddle River, NJ, **1996**

[162] J. Scherer, M. R. Vogt, O. M. Magnussen, R. J. Behm; *Langmuir* **1997,** *13*, 7045

[163] F. Sinapi, I. Lejeune, J. Delhalle, Z. Mekhalif; *Electrochim. Acta* **2007**, *52*, 5182

[164] Z. Mekhalif, F. Sinapi, F. Laffineur, J. Delhalle; *J. Electron Spectrosc. Relat. Phenom.* **2001**, *121*, 149

[165] F. Sinapi, S. Julien, D. Auguste, L. Hevesi, J. Delhalle, Z. Mekhalif; *Electrochim. Acta* **2008**, *53*, 4228

[166] M. Metikoš-Huković, R. Babić, Ž. Petrović, D. Posavec; *J. Electrochem. Soc.* **2007**, *154*, C138

[167] Ž. Petrović, M. Metikoš-Huković, R. Babić; *Prog. Org. Coat.* **2008**, *61*, 1

[168] Y. Yamamoto, H. Nishiara, K. Aramaki; *J. Electrochem. Soc.* **1993**, *140*, 436

[169] M. Ishibashi, M. Itoh, H. Nishihara, K. Aramaki; *Electrochim. Acta* **1996**, *41*, 241

[170] G. K. Jennings, J. C. Munro, P. E. Laibinis; *Adv. Mater.* **1999**, *11*, 1000

[171] H. Y. Ma, C. Yang, B. S. Yin, G.Y. Li, S. H. Chen, J. L. Luo; *Appl. Surf. Sci.* **2003**, *218*, 143

[172] Y. S. Tan, M. P. Srinivasan, S. O. Pehkonen, S. Y. M. Chooi; *J. Vac. Sci. Technol., A* **2004**, *22*, 1917

[173] G. K. Jennings, J. C. Munro, T.-H. Yong, P. E. Laibinis; *Langmuir* **1998**, *14*, 6130

[174] P. Srivastava, W. G. Chapman, P. E. Laibinis; *J. Phys. Chem. B* **2009**, *113*, 456

[175] M. Itoh, H. Nishiara, K. Aramaki; *J. Electrochem. Soc.* **1994**, *141*, 2018

[176] M. Itoh, H. Nishiara, K. Aramaki; *J. Electrochem. Soc.* **1995**, *142*, 3696

[177] M. Itoh, H. Nishiara, K. Aramaki; *J. Electrochem. Soc.* **1995**, *142*, 1839

[178] R. Haneda, H. Nishiara, K. Aramaki; *J. Electrochem. Soc.* **1997**, *144*, 1215

[179] R. Haneda, K. Aramaki; *J. Electrochem. Soc.* **1998**, *145*, 1856

[180] R. Haneda, K. Aramaki; *J. Electrochem. Soc.* **1998**, *145*, 2786

[181] G. K. Jennings, T.-H. Yong, J. C. Munro, P. E. Laibinis; *J. Am. Chem. Soc* **2003**, *125*, 2950

[182] P. Srivastava, W. G. Chapman, P. E. Laibinis; *Langmuir* **2009**, *25*, 2689

[183] F. Laffineur, J. Delhalle, S. Guittard, S. Géribaldi, Z. Mekhalif; *Colloids Surf., A* **2002**, *198-200*, 817

[184] T. Patois, A. E. Taouil, F. Lallemand, L. Carpentier, X. Roizard, J.-Y. Hihn, V. Bondeau-Patissier, Z. Mekhalif; *Surf. Coat. Technol.* **2010**, *205*, 2511

[185] R.-F. Dou, X.-C. Ma, L. Xi, H. L. Yip, K. Y. Wong, W. M. Lau, J.-F. Jia, Q.-K. Xue, W.-S. Yang, H. Ma, A. K-Y. Jen; *Langmuir* **2006**, *22*, 3049

[186] J. Zhao, D. Xu, K. Zhang, X. Cheng; *J. Mol. Struct.: THEOCHEM* **2009**, *909*, 9

[187] Y.R. Luo, *Handbook of Bond Dissociation Energies in Organic Compounds*, CRC Press, **2003**

[188] N. Garg, E. Carrasquillo-Molina, T. R. Lee; *Langmuir* **2002**, *18*, 2717

[189] A. Turchanin, M. Schnietz, M. El-Desawy, H. H. Solak, C. David, A. Gölzhäuser; *Small* **2007**, *3*, 2114

[190] A. Gölzhäuser, W. Geyer, V. Stadler, W. Eck, M. Grunze, K. Edinger, T. Weimann, P. Hinze; *J. Vac. Sci. Technol. B* **2000**, *18*, 3414

[191] A. Turchanin, M. El-Desawy, A. Gölzhäuser; *Appl. Phys. Lett.* **2007**, *90*, 053102

[192] W. Eck, A. Küller, M. Grunze, B. Völkel, A. Gölzhäuser; *Adv. Mater.* **2005**, *17*, 2583

[193] A. Turchanin, D. Käfer, M. El-Desawy, C. Wöll, G. Witte, A. Gölzhäuser; *Langmuir* **2009**, *25*, 7342

[194] M. H. Zareie, H. Ma, B. W. Reed, A. K. Y. Jen, M. Sarikaya; *Nano Lett.* **2003**, *3*, 139

[195] J. M. Tour; *Acc. Chem. Res.* **2000**, *33*, 791

[196] J. Chen, M. A. Reed, A. M. Rawlett, J. M. Tour; *Science* **1999**, *286*, 1550

[197] C. R. Kagan, A. Afzali, R. Martek, L. M. Gignac, P. M. Solomon, A. G. Schrott, B. Ek; *Nano Lett.* **2003**, *3*, 119

[198] P. Cyganik, M. Buck, W. Azzam, C. Wöll, *J. Phys. Chem. B* **2004**, *108*, 4989

[199] H. Valkenier, E. H. Huisman, P. A. van Hal, D. M. de Leeuw, R. C. Chiechi, J. C. Hummelen; *J. Am. Chem. Soc.* **2011**, *133*, 4930

[200] K. Wong, K.-Y. Know, B.V. Rao, A. Liu, L. Bartels; *J. Am. Chem. Soc.* **2004**, *126*, 7762

[201] F. P. Zamborini, J. K. Campbell, R. M. Crooks; *Langmuir* **1998**, *14*, 640

[202] C. A. Widrig, C. Chung, M. D. Porter; *J. Electroanal. Chem.* **1991**, *310*, 335

[203] C.-J. Zhong, J. Zak, M. D. Porter; *J. Electroanal. Chem.* **1997**, *421*, 9

[204] H. Ron, S. Matlis, I. Rubinstein; *Langmuir* **1998**, *14*, 1116

[205] S. Trasatti, O. A. Petrii; *Pure Appl. Chem.* **1991**, *63*, 711

[206] J. H. Scofield; *J. Electron Spectrosc. Relat. Phenom.* **1976**, *8*, 129

[207] J. C. Vickerman; *Surface Analysis – The principal techniques* Wiley & Sons, Chicester, **1997**

[208] D. G. Castner; *Langmuir* **1996**, *12*, 5083

[209] O. Cavalleri, L. Oliveri, A. Daccà, R. Parodi, R.Rolandi; *Appl. Surf. Sci.* **2001**, *175-176*, 357

[210] A. Kühnle, S. Vollmer, T. R. Linderoth, G. Witte, C. Wöll, F. Besenbacher; *Langmuir* **2002**, *18*, 5558

[211] T. M. Willey, A. L. Vance, T. van Buuren, C. Bostedt, L. J. Terminello, C. S. Fadley, *Surf. Sci.* **2005**, *576*, 188

[212] A. Boccia, V. Lanzillotto, V. Di Castro, R. Zanoni, L. Pescatori, A. Arduini, A. Secchi, *Phys. Chem. Chem. Phys.* **2011**, *13*, 4452

[213] E. Abelev, D. Starosvetsky, Y. Ein-Eli; *Langmuir* **2007**, *23*, 11281

[214] H. H. Strehblow, B. Titze; *Electrochim. Acta* **1980**, *25*, 839

[215] N. S. McIntyre, M. G. Cook; *Anal. Chem.* **1975**, *47*, 2208

[216] B. Timmermans, F. Renier, A. Hubin, C. Buess-Herman; *Appl. Surf. Sci.* **1999**, *144-145*, 54

[217] A. Galtayries , J.-P. Bonnelle; *Surf. Interface Anal.* **1995**, *23*, 171

[218] I. Platzman, R. Brener, H. Haick, R. Tannenbaum; *J. Phys. Chem C* **2008**, *112*, 1101

[219] S. L. Harmer, W. M. Skinner, A. N. Buckley, L.-J. Fan; *Surf. Sci.* **2009**, *603*, 537

[220] A. Kudelski; *Vib. Spectros.* **2005**, *39*, 200

[221] S. Li, D. Wu, X. Xu, R. Gu; *J. Raman Spectrosc.* **2007**, *38*, 1436

[222] C. A. Szafranski, W. Tanner, P. E. Laibinis, R. L. Garrell; *Langmuir* **1998**, *14*, 3570

[223] R. A. Alvarez-Puebla, D. S. Dos Santos Jr., R. F. Aroca; *Analyst (Cambridge U. K.)* **2004**, *129*, 1251

[224] R. E. Johnson, R. H. Dettre; *Adv. Chem. Ser.* **1963**, *43*, 112

[225] S. Lee, A. Puck, M. Graupe, R. Colorado, Y.-S. Shon, T. R. Lee, S. S. Perry; *Langmuir* **2001**, *17*, 7364

[226] S. Wang, L. Feng, H. Liu, T. Sun, X. Zhang, L. Jiang, D. Zhu; *Chem. Phys. Chem.* **2005**, *6*, 1475

[227] K. Abe, H. Takiguchi, K. Tamada; *Langmuir* **2000**, *16*, 2394

[228] J. Yang, J. Han, K. Isaacson, D. Y. Kwok; *Langmuir* **2003**, *19*, 9231

[229] J. M. Miller, N. L. Abbott; *Langmuir* **1997**, *13*, 7106

[230] E. Bobour, R. B. Lennox; *J. Phys. Chem. B* **2000**, *104*, 9004

[231] D.-Q. Zhang, X.-M. He, Q.-R. Cai, L.-X. Gao, G. S. Kim; *Thin Solid Films* **2010**, *518*, 2745

[232] K. M. Ismail; *Electrochim. Acta* **2007**, *52*, 7811

[233] G. Contini, K. Laajalehto, E. Suoninen, M. Marabini; *J. Electron Spectrosc. Relat. Phenom.* **1995**, *171*, 234

[234] G. Witte, C. Wöll; *J. Chem. Phys.* **1995**, *103*, 5860

[235] H.-J. Himmel, C. Wöll, R Gerlach, G. Polanski, H. G. Rubahn; *Langmuir* **1997**, *13*, 602

[236] X. Xiao, B. Wang, C. Zhang, Z. Yang, M. M. T. Loy; *Surf. Sci.* **2001**, *472*, 41

[237] G. Graziano, B. Lee; *J. Phys. Chem. B* **2001**, *105*, 10367

[238] H. Leidheiser, Jr. ed., *Corrosion Control by Organic Coatings*, NACE, Houston, **1981**

[239] K. S. Kim, P. Tarakeshwar, J. Y. Lee; *Chem. Rev.* **2000**, *100*, 4145

[240] G. Karlström, P. Linse, A. Wallquist, B. Jönsson, *J. Am. Chem. Soc.* **1983**, *105*, 3777

[241] S. Suzuki, P. G. Green, R. E. Bumgamer, S. Dasgupta, W. A. Goddard III, G. A. Blake; *Science*, **1992**, *275*, 942

[242] S. Y. Fredericks, K. D. Jordan, T. S. Zwier; *J. Phys. Chem.* **1996**, *100*, 7810

[243] A. J. Gotch, T. S. Zwier; *J. Chem. Phys.* **1992**, *96*, 3388

[244] R. N. Pribble, A. W. Garret, K. Haber, T. S. Zwier; *J. Chem. Phys.* **1995**, *103*, 531

[245] D. Feller; *J. Phys. Chem. A* **1999**, *103*, 7558

[246] A. Kereszturi, P. Jedlovszky; *J. Phys. Chem. B* **2005**, *109*, 16782

[247] J. Fun , M. Yudasaka, Y. Kasuya, D. Kasuya, S. Iijima, *Chem. Phys. Lett.* **2004**, *397*, 5

[248] S. C. Silva, J. P. Devlin, *J. Phys. Chem.* **1994**, *98*, 10847

Langmuir **2006**, *22*, 6102

[249] A. Gölzhäuser, S. Panov, M. Mast, A. Schertel, M. Grunze, C. Wöll; *Surf . Sci.* **1995**, *334*, 235

[250] C.-Y. Lee, G. M.Harbers, D. W.Grainger, L. J. Gamble, D.G. Castner; *J. Am. Chem. Soc.* **2007**, *129*, 9429

[251] D. A. Hutt, G. J. Leggett; *Langmuir* **1997**, *13*, 2740

[252] Beecher J.F.; *Surf. Interface Anal.* **1991**, *17*, 245

[253] B.I. Rosario-Castro, E.R. Fachini, J. Hernández, M.E. Pérez-Davis, C.R. Cabrera; *Langmuir* **2006**, *22*, 6102

[254] R. S. Clegg, S. M. Reed, R. K. Smith, B. L. Barron, J. A. Rear, J. E. Hutchison; *Langmuir* **1999**, *15*, 8876

[255] Y. Cho, A. Ivanisevic; *J. Phys. Chem. B* **2005**, *109*, 12731

[256] X. Xu, C. M. Friend; *J. Phys. Chem.* **1989**, *93*, 8072

[257] J. G. Serafin, C. M. Friend; *Surf. Sci.* **1989**, *209*, L163

[258] J.-B. He, D.-Y. Lu, G.-P. Jin; *Appl. Surf. Sci.* **2006**, *253*, 689

[259] R. Arnold, W. Azzam, A. Terfort, C. Wöll; *Langmuir* **2002**, *18*, 3980

[260] J. P. Labukas, T. J. H. Drake, G. S. Ferguson; *Langmuir* **2010**, *26*, 9497

[261] O. M. Cabarcos, A. Shaporenko, T.Weidner, S. Uppili, L. S. Dake, M. Zharnikov, D. L. Allara; *J. Phys. Chem. C* **2008**, *112*, 10842

[262] H. O. Finklea, D. A. Snider, J. Fedyk, E. Sabatini, Y. Gafni, I. Rubinstein; *Langmuir* **1993**, *9*, 3660

[263] F. P. Zamborini, R. M. Crooks; *Langmuir* **1998**, *14*, 3279

[264] R. P. Janek, W. R. Fawcett, A. Ulman; *Langmuir* **1998**, *14*, 3011

[265] K. Bandyopadhyay, K. Vijayamohanan; *Langmuir* **1999**, *15*, 5314

[266] V. Ganesh, R. R. Pandey, B. D. Malhotra, V. Lakshminarayanan; *J. Electroanal. Chem.* **2008**, *619-620*, 87

[267] E. Sabatini, J. Cohen-Boulakia, M. Bruening, I. Rubinstein; *Langmuir* **1993**, *9*, 2974

[268] L. V. Protsailo, W. R. Fawcett; *Langmuir* **2002**, 18, 8933

[269] R. K. Pandey, K. A. Suresh, V. Lakshminarayanan; *J. Colloid Interface Sci.* **2007**, *315*, 528